



UNIVERSITÀ DEL PIEMONTE ORIENTALE

DEPARTMENT OF HEALTH SCIENCES

Università del Piemonte Orientale, Italy

SMALL CALIBER ARTERIAL PROSTHESIS:
PROTOTYPE AND PRE-INDUSTRIALIZATION

Ph.D Thesis in Medical Science and Biotechnologies

Academic Year:

2019 – 2020

Student:

Marta CALVO CATOIRA

Supervisor:

Francesca BOCCAFOSCHI **Ph.D**

Abstract

Cardiovascular diseases represent the leading cause of death in developed countries. Modern surgical methods show poor efficiency in the substitution of small-diameter arteries (< 6 mm). Due to the mismatch in mechanical properties between the native artery and the substitute, the behavior of the vessel wall remains a major cause of inefficient substitutions an unsolved complication in surgery since 1970. The potential of decellularized scaffolds has raised major hope in several applications for regenerative medicine. The purpose of this work was to obtain polylysine-enriched vascular substitutes, derived from decellularized porcine femoral and carotid arteries. Polylysine was selected as a matrix cross-linker, increasing the mechanical resistance of the scaffold with respect to decellularized vessels, without altering the native biocompatibility and haemocompatibility properties.

The biological characterization showed excellent biological performances, while mechanical tests displayed that the Young's modulus of the polylysine-enriched matrix was comparable to that of the native vessel. Burst pressure test demonstrated strengthening of the polylysine-enriched matrix, which resists at higher pressures with respect to the native vessel. Mechanical analyses also show that polylysine-enriched vessels presented minimal degradation compared to native.

Concerning haemocompatibility, the performed analyses show that polylysine-enriched matrices increase coagulation time, with respect to commercial Dacron[®] vascular substitutes. Based on these findings, polylysine-enriched decellularized vessels resulted in a promising approach for vascular substitution.

In order to consider the industrial phase, a business plan (BP) and the pre-engineering of the production reactor were developed in the present project. Is crucial to consider the scale-up process of the project from the initial stages to increase the chances of its success. In this way, the feasibility study will contemplate the viability of the project from an economic point of view thus, the BP is the most important document of the study. From an engineering point of view, the industrial production reactor is the heart of the plant, so designing it from the outset will allow considering costs and performing the necessary experiments for its final design.

Riassunto

Le malattie cardiovascolari rappresentano la principale causa di morte nei paesi sviluppati. I moderni metodi chirurgici mostrano poca efficacia nella sostituzione di arterie di piccolo calibro (< 6 mm), a causa della mancata corrispondenza delle proprietà meccaniche tra le arterie native ed i sostituti vascolari. L'utilizzo dei materiali decellularizzati ha costituito un'innovazione nella medicina rigenerativa. Lo scopo di questo progetto è quello di ottenere sostituti vascolari arricchiti con polilisina, derivati da arterie femorali e carotidi porcine decellularizzate. La polilisina è stata selezionata come reticolante per la matrice, in modo da aumentare la resistenza meccanica dello scaffold rispetto a quella del vaso decellularizzato, senza tuttavia alterarne le proprietà naturali di biocompatibilità e di emocompatibilità.

La caratterizzazione biologica mostra un'eccellente biocompatibilità, ed i test meccanici dimostrano che il modulo di Young delle matrici arricchite con polilisina è simile a quello dei vasi nativi. I test sulla burst pressure mostrano che la matrice arricchita con polilisina resiste a più alte pressioni rispetto ai vasi nativi. I test di resistenza dinamica dimostrano anche che i vasi arricchiti con polilisina presentano una degradazione minore rispetto a quella dei vasi nativi.

Riguardo l'emocompatibilità, le analisi svolte mostrano che le matrici arricchite con polilisina aumentano il tempo di coagulazione rispetto ai sostituti vascolari in Dacron[®] commercializzati. In base a queste scoperte, i vasi decellularizzati ed arricchiti con polilisina risultano essere un promettente sostituto biologico per l'utilizzo in chirurgia vascolare.

Con il fine di considerare nel progetto anche la fase di industrializzazione del prodotto, sono stati sviluppati un business plan (BP) ed una pre-ingegneria del reattore di produzione. Per incrementare le possibilità di successo del progetto è cruciale che fin dall'inizio venga realizzato lo studio di fattibilità. Il BP è il documento più importante di tale studio, che infatti comprende la valutazione della sostenibilità economica e finanziaria del progetto e ne stima la redditività. Da un punto di vista ingegneristico, il reattore per la produzione industriale è il cuore dell'impianto, e la progettazione del reattore fin dalle fasi iniziali permetterà di considerare i costi e gli eventuali esperimenti necessari per la realizzazione finale.

Contents

List of Figures	6
List of Tables	7
Statement of original authorship	8
Acknowledgements	9
1 Introduction	10
1.1 General considerations. Outlook and clinical evaluation of peripheral arterial disease. General overview	12
1.2 Vascular replacements: clinical need for small diameter replacements .	14
1.3 Current biological options: perspectives in vascular tissue engineering and peripheral substitutions	18
1.3.1 Synthetic materials	20
1.3.2 Scaffolds from natural polymeric materials for vascular tissue engineering	23
1.3.3 Hybrid scaffolds from synthetic and natural polymers	31
1.4 Decellularized vascular substitutes	33
1.4.1 Decellularization agents and techniques	34
1.4.2 Physical methods	35
1.4.3 Chemical agents	37
1.4.4 Techniques for agent's application	41
1.5 Clinical trials of vascular tissue engineering	47
1.6 Industrialization process	48
1.6.1 Clinical products	49
1.6.2 Regulation aspects	53
1.7 Thesis outline	56
2 Materials and methods	57
2.1 Decellularization process	57
2.1.1 Functionalization of the decellularized biologic tissue (sueGraft® process)	57

2.1.2	Evaluation of the decellularization procedure	57
2.2	Enrichment process assessment and morphological analysis	58
2.2.1	X-ray Photoelectron Spectroscopy (XPS)	58
2.2.2	Attenuated Total Reflectance Infra-red spectroscopy (ATR-IR) .	59
2.2.3	Confocal microscopy	59
2.2.4	Micro Computed Tomography (Micro-CT)	60
2.3	Mechanical test	61
2.4	Cell viability assay	61
2.5	Haemocompatibility	62
2.6	Industrialization	63
2.6.1	Business plan	63
2.6.2	Reactor design	64
2.7	Ethics	66
3	Results	68
3.1	Decellularization process efficiency	68
3.2	Enrichment process assesment and morphological analysis	69
3.3	Mechanical test	71
3.3.1	Young’s modulus, tensile strength and burst pressure results: static conditions	71
3.3.2	Young’s modulus, tensile strength and burst pressure results: dy- namic conditions	72
3.4	Cell viability assay: static and dynamic conditions	74
3.5	Haemocompatibility test	76
3.6	Industrialization	77
3.6.1	Business plan	77
3.6.2	Reactor design	78
4	Discussion	82
	References	97
	Appendixes	i
	Appendix A: Blood vessel simulation reactor prototype	i

Appendix B: Business plan iii
Appendix C: Blood vessel decellularization reactor prototype v

List of Figures

1	Arteries layers and its different cell population.	11
2	Overview of small caliber peripheral diseases.	12
3	Progressive stages of vascular disease and the corresponding surgical strategies (Seifu et al. 2013).	13
4	Dacron [®] straight prosthesis implanted in the abdominal aorta.	16
5	Scheme of origin material of arterial scaffold. Modified from Tara et al. (2014).	19
6	MiniBreath [®] commercial bioreactor.	65
7	Decellularization of porcine artery test	68
8	XPS and AT-IR spectra	70
9	Confocal microscopy and micro-CT analysis of materials	71
10	Mechanical testing results under static conditions	73
11	Photographs of the 3D printed bioreactor.	74
12	Endothelial cells viability assays and histology test	75
13	Haemocompatibility test	76
14	Hydraulic conditions and their H&E staining results for the three different settings of the dynamic decellularization test.	78
15	H&E histology of the blood vessel obtained using the selected protocol.	79
16	Schematic representation of Re for the inner (Re_{in}) and outer (Re_{out}) perfusion circuits over time on the optimized MiniBreath [®] protocol.	80
17	Photograph of the surgical intervention to implant the vascular polylysine graft in the left carotid artery.	84

List of Tables

1	Biological vascular grafts in clinical use (Boccafoschi et al. 2017b). . . .	15
2	Vascular substitutes in clinical use according to the body region (Boccafoschi et al. 2017b).	17
3	Biodegradable polymers for tissue engineered vascular grafts (Tara et al. 2014)	22
4	TEVGs made using hybrid scaffolds (Catto et al. 2014).	32
5	Summary of the different decellularization agents and techniques (Boccafoschi et al. 2017a; Crapo et al. 2011; Kawecki et al. 2018)	45
6	Influence of different decellularizing methods on blood vessel substitutes mechanical properties (Boccafoschi et al. 2017b).	45
7	Selected crosslinking agents and their influence on properties of biomaterials (Kawecki et al. 2018).	46
8	Summary of <i>in vivo</i> performance of variant decellularized vascular grafts since 2001 (Lin et al. 2018).	47
9	Available commercial decellularized products.	52
10	Technical data of confocal images.	60
11	Surface composition of tested samples	69
12	Final decellularization protocol selected for the three treating and washing phases	79

Statement of original authorship

The work contained in this thesis has not been previously submitted to meet requirements for an award at this or any other higher education institution. To the best of my knowledge and belief, the thesis contains no material previously published or written by another person except where due reference is made.

Signature:

A handwritten signature in black ink, appearing to read 'Marta Calvo Catoira', written in a cursive style.

Chemical Eng. Marta Calvo Catoira

Date: *February, 5th, 2020*

Acknowledgements

Some results of this thesis were obtained thanks to the cooperation and networking of different institutions. In this context, I would like to acknowledge Central Laser Facility, Rutherford Appleton Laboratory, Didcot, Oxfordshire, OX11 0QX. UK for providing the facilities to obtain the confocal images and the Engineering and Physical Science Research Council (EPSRC) for funding the Henry Moseley X-ray Imaging Facility which has been made available through the Royce Institute for Advanced Materials through grants (EP/F007906/1, EP/F001452/1, EP/I02249X, EP/M010619/1, EP/F028431/1, EP/M022498/1, EP/R00661X/1).

I also would like to thank Life and Device S.r.l. for its contributions to this work providing the native arteries.

My doctorate would have never happened if one day, more than three years ago, I had not accidentally found Professor Boccafoschi who trusted me from the beginning and taught me everything I know about the regenerative medicine field, that until that day I did not know. That is the reason why I thank her, for the possibility she gave me and the three fantastic years that I have spent in her laboratory.

I want to thank Luca for his patience with my Italian and my useless efforts to improve my Neapolitan. I thank Martina for sharing sad and joyful moments together. To all the students who have passed through the Anatomy laboratory in these years, especially Dalila, Fabio, Alessia and Alessandro because although I sometimes get angry with them, the “spañolita” loves them.

I want to thank all the people who have been by my side during this time, especially Cristiano and Javier for their love.

Finally, thanks to my parents for always being there.



1 Introduction

Arteries are a fundamental part of the human body since, not only do they transport nutrients, but also oxygenated blood, metabolites, and waste products, they serve as a conduit for hormonal communication between distant tissues and facilitate rapid deployment of immune responses to distal sites within the body.

The aorta is the artery with a largest diameter (20 mm), which progressively divides and decreases in diameter until reaching arteries with a diameter < 5 mm, they are considered small. In turn, small arteries divide in arterioles (< 1 mm), which branch further to become capillaries ($< 100 \mu\text{m}$), through which only single cells can pass. Circulatory system is close due to capillaries joining together to form venules and the diameter then increases in small veins, and then in larger veins which connect with lungs and heart (Kottke-Marchant and Larsen 2006).

The structure of normal arteries is divided in three layers: the internal intima, the middle media, and the external adventitia.

From the point of view of chemical composition, collagen is the most abundant protein in the elastic arterial (> 5 mm diameter) extracellular matrix (ECM). Among the different collagen types, collagen I and II represent the 30% and 60% of the total collagen while collagen V, XII, and XIV represent the remaining 10% (Xu and Shi 2014). The collagen role is retaining tensile strength, while the elastin fibers preserve the elastic properties of the scaffold and GAGs provide it viscoelasticity (Wagenseil and Mechem 2009). Other components present in the structure are elastin, fibronectin, fibrillin, and laminin (Nair and Thottappillil 2015). Cell functions such as growth, differentiation, and apoptosis are regulated by glycosaminoglycans (GAGs), proteoglycans, growth factors, cytokines, and matrix-degrading enzymes and their inhibitors contained as well in the ECM (Ruoslahti and Engvall 1997).

Equally important, cell composition defines the mechanical properties and the function of the different layers. In this regard, cells in the intima and tunica media are endothelial cells (ECs) and smooth muscle cells (SMCs), respectively. The most important function of the endothelium, formed by the monolayer of ECs, is the prevention of thrombosis but it is also responsible for the maintenance and alterations in the vascular

tone, which control blood flow. The intima layer is delimited by the internal elastic lamina formed by type IV collagen and laminin like ECM proteins (Pankajakshan and Agrawal 2010).

Regardless of SMCs function, their circumferentially disposition along with collagen and elastin fibers, provide mechanical support in the medial layer of the vessels. Due to the SMCs contractile properties, they induce and produce not only the artery wall expansion and contraction according with the blood flow cycle, but also they replenish the ECM degraded fibers.

To contribute mechanical support, fibroblast, located primarily in the adventitia layer, along with large bundles of collagen fibers, are responsible of the longitudinal direction mechanical support (Lin et al. 2018). Adventitia layer function is to supply nutrients to the cells in the blood vessel itself. For this purpose, it contains a small arterioles and capillaries network which conform the vasa vasorum. Medial smooth muscle cells contraction or relaxation is stimulated by a nerve also integrated in the vasa vasorum layer. Adventitia thickness decreases progressively as the vessel diameter decreases. Arterioles and capillaries lack an adventitia completely (Tucker and Mahajan 2019). Figure 1 shows the different layers and cells compositions.

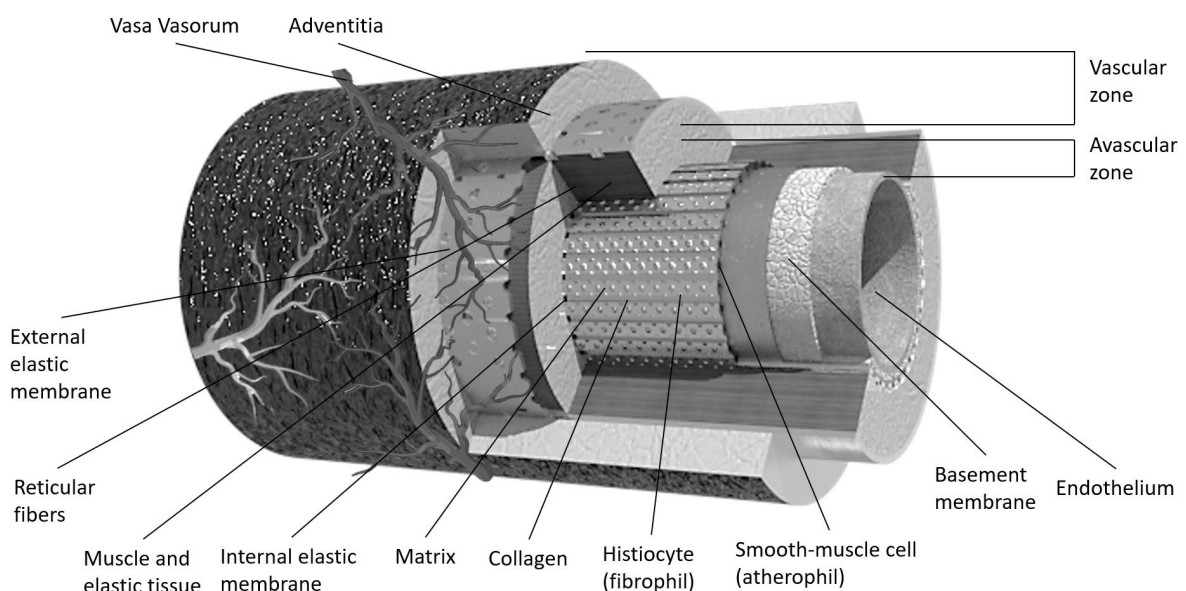


Figure 1: Arteries layers and its different cell population.

1.1 General considerations. Outlook and clinical evaluation of peripheral arterial disease. General overview

Non-communicable diseases (NCDs), which include cancers, cardiovascular diseases, chronic respiratory diseases, and diabetes, are the leading cause of death in 70% of the total world population (Bennett et al. 2018). Among the NCDs, cardiovascular diseases are on top of the mortality ranking. Indeed, the World Health Organization (WHO) estimated 17,7 million people died in 2015 from cardiovascular diseases but the tendency predicts a rise to 23 million worldwide by 2030 (Mathers and Loncar 2006; Rodrigues et al. 2018). The commonest cardiovascular diseases are coronary heart disease (CHD), cerebrovascular disease, peripheral arterial disease (PAD), and deep vein thrombosis. All of them are mostly due to atherosclerosis, whose non-modifiable risk factors are age, gender and genetic predisposition to hypercholesterolemia, hypertension, diabetes and systemic inflammation. Concerning the modifiable risk factors cigarette-smoking, diet rich in saturated fats and sedentary lifestyle can be identified (Settembrini et al. 2017).

Atherosclerotic cardiovascular disease may give rise to coronary artery disease (CAD), myocardial infarction, stroke, and peripheral occlusive artery disease (PAOD). Atherosclerosis is a multifactorial disorder of the arterial system, characterized by vascular lipidic accumulation and calcification, with the development of lipid-laden deposits, or “plaques” in the vessel wall. Figure 2 shows the connections between the diseases. This eventually leads to stenosis of the vascular lumen caused by lipid dysregulation and vascular inflammation that leads to endothelial injury (Kannan et al. 2005).

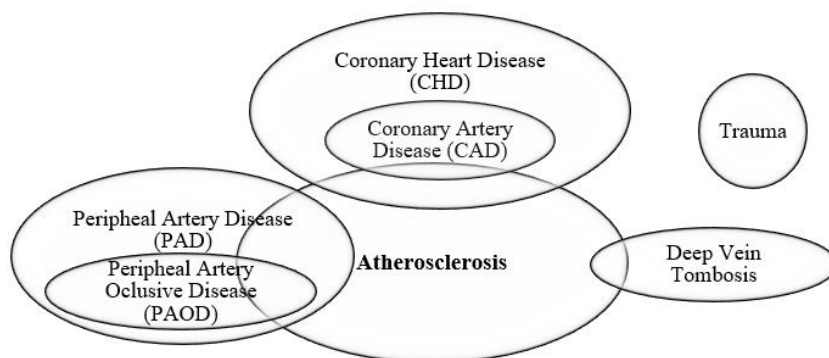


Figure 2: Overview of small caliber peripheral diseases.

The normal blood flow is compromised through the artery as a consequence of the stenosis and plaque formation, with subsequent thrombosis and this can lead to the occlusion of the vessel and, depending on the artery location, it can result in an end organ dysfunction.

Among the PAD, the occlusion of the lower extremities is predominant, and its prevalence is estimated between 10% and 25% in < 55 years old population, but this percentage increases up to 40% in > 80 years of age.

According with the American College of Cardiology/American Heart Association Practice Guidelines, the PAOD can be categorized in asymptomatic, claudication, critical limb ischemia (CLI), and acute limb ischemia (ALI) depending on the stage of plaque deposition in the lumen, which compromises the blood flow. Figure 3 represents the different stages of the vascular diseases and their treatment modalities.

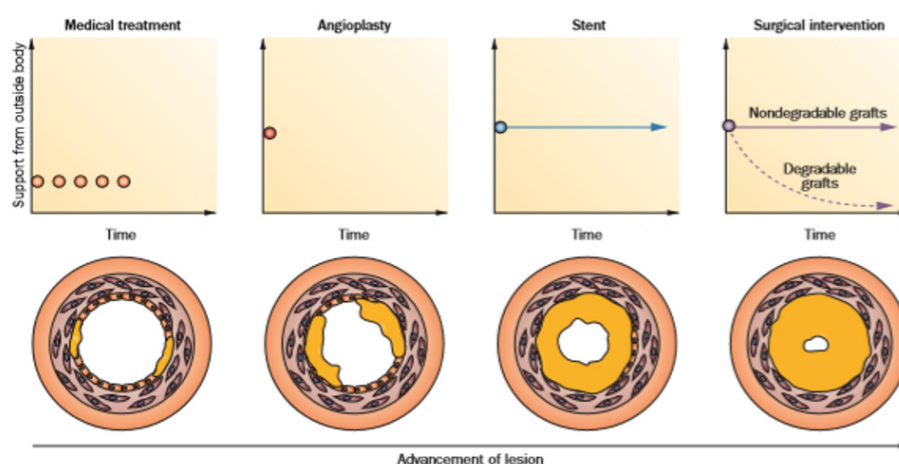


Figure 3: Progressive stages of vascular disease and the corresponding surgical strategies (Seifu et al. 2013).

In severe vascular trauma cases, laceration or transection of blood vessels can occur and replacement is necessary if the vessel wall cannot be surgically repaired (Voorhees et al. 1952).

1.2 Vascular replacements: clinical need for small diameter replacements

Pharmacological and endovascular atherosclerosis therapies are improving their efficiency continuously, even so a surgical bypass of blood vessels on a lower extremity remains the procedure of choice in several patients. This traditional treatment allows the patient to keep his limb as an alternative to amputation. Cost-effective ratio of this approach is also significantly better than other therapies (Olin et al. 2016).

Currently, the gold standard for the surgical treatment of diseased small-diameter vessels are autologous arteries or veins due to their adequate physiological properties. Saphenous veins (vena saphena magna) are the most commonly used autografts in case of lower limb or peripheral bypass surgery. It has an easy access but due to the mechanical mismatch, they often present aneurysm, intimal hyperplasia, and accelerated atherosclerosis when exposed to high-pressure arterial sites (Akowuah et al. 2003; Owens et al. 2009; Schmitto et al. 2010). Indeed, saphenous vein graft displays failure rates of around 50% at 10 years (Harskamp et al. 2013; Klinkert et al. 2004). For this reason, internal mammary arteries and radial arteries are also used because of their superior patency (Athanasίου et al. 2011; Cho et al. 2006; Goldman et al. 2004; Masden et al. 2012).

For example, in aorto-iliac bifurcation atherosclerosis, vessel substitution is the best option if the occlusion is severe but, in 15% of patients, the saphenous vein is not available due to its prior use for coronary artery bypass surgery (Desai et al. 2004). On the other side, autologous vessels present a limited availability, may be of poor quality, and their extraction causes donor site morbidity (Chew et al. 2002; Conte 2013; Klinkert et al. 2004; Taylor et al. 1987).

Mismatch in compliance and elasticity between the autologous graft and the native vessel often leads to re-occlusion, due to atherosclerotic progression and cellular infiltration. Furthermore, previous phlebitis, vessel removal, varicosities, hypoplasia, or anatomical unsuitability are presented in almost 30–40% of the patients, this causes the absence of a viable saphenous vein (Kannan et al. 2005).

A summary of biological vascular conduit materials is presented in Table 1.

Biological vascular grafts				
Autografts			Allografts (homografts)	
Arterial		Venous	Arterial	Venous
Advantages	Closest approximation, less diameter mismatch, internal mammary artery anatomically nearby, excellent function		Durable and versatile, good results, infection resistance, relative availability	
Disadvantages	Availability, vasospasm (radial artery), donor site morbidity		Antigenicity, graft deterioration, early occlusions, chronic rejection, intake of drugs, infection risk	
First use	Jaboulay et al. (1896)	Goyannes (1906)	Gross et al. (1948)	Dardik et al. (1979)

Table 1: Biological vascular grafts in clinical use (Boccafoschi et al. 2017b).

An alternative approach proposes to use the human umbilical vein as vascular graft for peripheral substitutions, it is named Dardik Biograft. Currently it is the best option when the saphenous vein is not available. In the graft preparation, the umbilical vein is treated with dialdehyde starch or glutaraldehyde and is reinforced with an outer polyester fiber mesh. In this way, the native basement membrane in the luminal side of the vessel guarantees the thromboresistance. Nevertheless, Dardik Biograft presents complications such as infections, thrombosis and aneurysm, usually due to the surgical method (Eskandari 2015).

During the last 50 years regenerative medicine tried to obtain a satisfactory alternative in that case. Early 1960s, fresh or cryopreserved homografts (i.e., human allografts from cadaver donors) was abandoned owing to difficulties in preserving them, late graft deterioration and aneurysm formation. As an alternative, synthetic prosthesis were introduced due to the anticipated availability. Currently homografts are not routinely used, but they have been reintroduced to treat aortic prosthetic graft infection, lower extremity primary revascularization, and simultaneous or sequential revascularization surgery in solid organ transplant recipients (Boccafoschi et al. 2017b).

Currently, the available alternatives to autologous vessel are different according to the vessel diameter (Table 2). Arteries with a diameter greater than 8 mm are consid-

ered large-caliber arteries. In this case prosthesis made with synthetic material obtain a good result from the critical thrombogenicity point of view. Dacron[®] (INVISTA Technologies S.r.l., Saint Gallen, Switzerland) prosthesis is the commercial product in these cases (Figure 4).

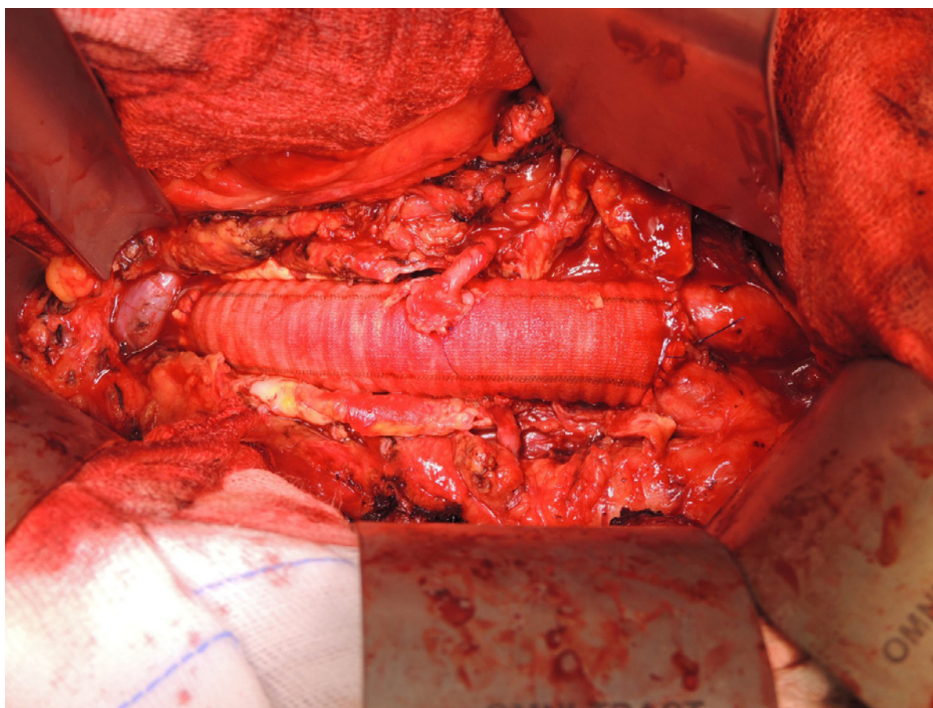


Figure 4: Dacron[®] straight prosthesis implanted in the abdominal aorta.

There is not a clear preference between natural and synthetic grafts in medium caliber replacements, diameter between 6 and 8 mm, typically carotid and femoral arteries. The results are controversial, but the solution exists.

The alternative to autologous transplant for small-caliber vessels (< 6 mm), such as coronary arteries (heart), infrainguinal arteries (below the inguinal ligament), and particularly in low-flow infrageniculate arteries (below the knee joint), is not currently up to standard and the statistics prove that 5-years patency falls to 15%–30%. In this context, almost 1.200.000 small-caliber grafts are used every year.

Vascular regions			
Vascular substitute choice	Large-caliber arteries (≥ 8 mm). Aorta, arch vessels, and common femoral arteries	Medium-caliber arteries (6-8 mm). Carotid, subclavian, common femoral, visceral, and above-the-knee arteries	Small-caliber arteries (≤ 6 mm). Coronary, below-the-knee, tibial, and peroneal arteries
First choice	Prosthesis (Dracon [®] , ePTFE)	Prosthesis or autograft (equal)	Arterial venous autograft
Second choice	Allograft, deep venous autograft	Prosthesis or autograft	Composite graft, vein interposition, prosthesis (ePTFE, Dracon [®]), allograft, biosynthetic

Table 2: Vascular substitutes in clinical use according to the body region (Boccafoschi et al. 2017b).

As reported by Couet et al. (2007), vascular tissue engineering “aims to apply the principles of engineering and life sciences towards the development of a vascular construction that demonstrates biological and mechanical properties as close as possible to those of a native vessel”.

Tissue engineering offers two main alternatives to autologous vessel, prosthesis made with natural or synthetic materials. Independently of the material origin, the prosthesis must achieve multiple requirements. First of all, the material should be biocompatible. That is to say, it must satisfy characteristics such as: nontoxicity, nonimmunogenicity, resistance to *in vivo* thrombosis, ability to withstand infection, complete incorporation into the host tissue with satisfactory graft healing and ability to grow when placed in children, maintenance of functional endothelium and in general functional vascular cells. In particular, in vascular substitutions, dysfunctional endothelium becomes adhesive to inflammatory cells, exposes thrombogenic surfaces and, thus, promotes inflammation, atherosclerosis and thromboembolism.

Secondly, a vascular graft should possess adequate mechanical properties related to the anatomical replacement needed, this means that the vascular substitute needs to possess compliance and burst pressure similar to that of native vessels in order to withstand long-term hemodynamic stresses. These characteristics guarantee no modi-

fications in the hemodynamic environment, therefore, avoiding the induction of inflammatory and clotting response which may lead to lumen stenosis after the implant. In the peripheral regions, the vascular substitute may also resist to kink and compression forces without undergoing any structural modification. Good operative suturability and simplicity of surgical handling are essential qualities for a suitable surgical device (Meyer et al. 2009).

Regarding the prosthesis processability, low manufacturing cost, readily availability with a large variety of lengths and diameters, serializability and easy storage requirements are mandatory to obtain a good industrial product. This aspects will be considered in the industrialization chapter in order to obtain an optimal technology transfer process (Catto et al. 2014).

1.3 Current biological options: perspectives in vascular tissue engineering and peripheral substitutions

Scaffold biomaterials are classified into two broad categories based on their origin which can be natural and/or synthetic (Figure 5).

Synthetic polymers are manufactured, and they allow stricter control over physical and mechanical properties in order to mimic the natural matrix by chemically tailoring polymers. However, they lack the natural capacity of bidirectional communication with cells. In order to minimize this restriction, soft, porous materials such as hydrogels can incorporate cells, adhesive ligands, and proteolytically degradable peptides. The standard production method and the easy sterilization phase are the reasons for the use of synthetic polymeric biomaterials in tissue engineering.

By contrast, natural biomaterials are derived from both plant and animal sources and intrinsically contain biological cues, such as growth factors, or sites that promote cell adhesion and/or degradation. Most natural materials used as biologically derived matrices are composed by proteins and polysaccharides. Collagen, gelatin, fibrin and silk are widely used in tissue engineering applications due to the intrinsic non-immunogenic properties and the ability to tune the mechanical properties by tailoring the amount of crosslinking within the gel. However, their mechanical properties

performance are not acceptable. In order to fix this main problem, cross-linking agents and copolymers such as collagen, fibrinogen, chitosan, alginate or hyaluronic acid with poly lactic-co-glycolic acid are used to improve the mechanical strength and minimize the degradation predisposition. Another approach is nanoscale fibers electrospinning, in this context, fibrin is usually used and it can form scaffolds exhibiting high structural integrity while retaining biological activity (Taylor et al. 2018).

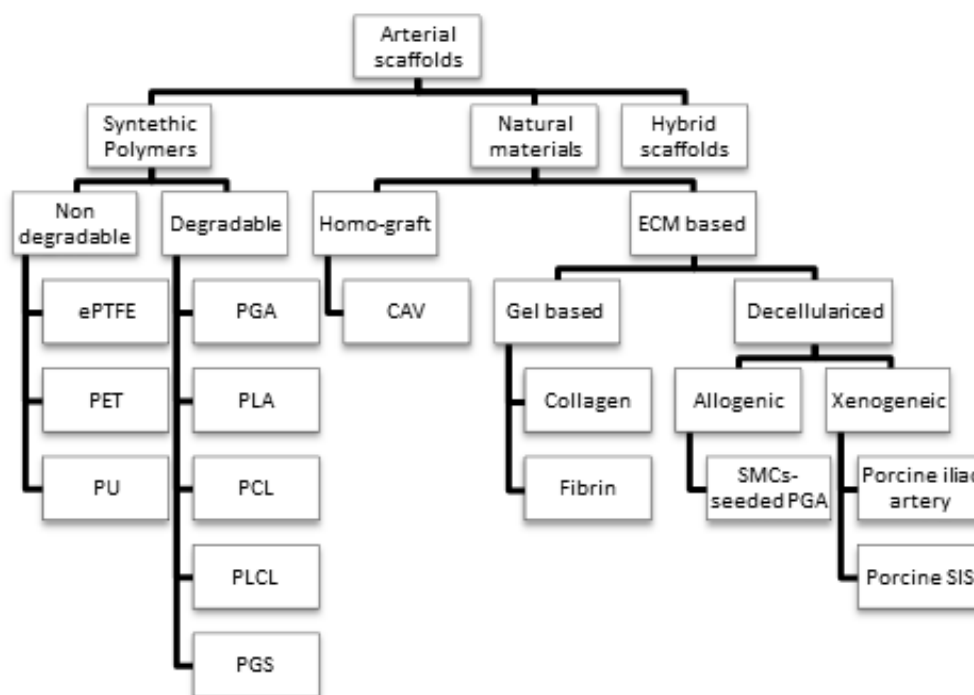


Figure 5: Scheme of origin material of arterial scaffold. Modified from Tara et al. (2014).

In vitro vascular graft recellularization using autologous patient cells is a promising approach in order to avoid thrombosis and a host immunogenic response, but it presents a lot of problems in terms of the subsequent implementation. One of these problems is given by the time necessary to obtain the needed cells from the patient. Another issue is the assuring of the isolated cell line from the patient remains stable during its *in vitro* amplification time. All this has an important impact on the cost effectiveness process (Nair and Thottappillil 2015).

1.3.1 Synthetic materials

Synthetic scaffolds are composed of polymers whose properties can be tailored to the target tissue, that are easy to process, have high reproducibility between batches and, compared to natural polymers can be produced in large amounts under asepsis conditions. By contrast, they exhibit some negative features like low biocompatibility and cell adhesion, fistula formation, gradual degradation into byproducts that may be toxic and chronic inflammation that results in serious dysfunctional and mechanical degradation of the transplant which may be, inter alia, the reason of clinical failure.

The two main categories of synthetic materials are non-biodegradable and biodegradable.

Non degradable

Initial vascular prosthesis utilized non-degradable polymers like polyethylene terephthalate (PET, Dacron[®]) and expanded-polytetrafluoroethylene or Teflon (ePTFE, Gortex[®]) and they still dominates the market for large and medium diameter vessel due to the fact that they require grafts greater than 6 mm in diameter in a high-flow, low-resistance circulation (Tara et al. 2014).

Electronegative luminal surface and porosity properties allow a 5 years patency of 91% in the ePTFE case. Also, flexibility, elasticity and kinking resistance of PET confers an excellent performance in terms of platelet adhesion and leukocyte aggregation when compared with ePTFE. Unfortunately, for small-diameter vessels (< 6mm) its use is limited due to poor patency rates related to thrombosis and stenosis (Nair and Thottappillil 2015).

Despite the low thrombogenicity and exceptional physical and mechanical properties, the first generation of polyurethanes (PU) was unstable and failed in clinical trials but, the second generation, materials based on PU combined with different materials, such as urea, fibronectin, collagen, and elastin obtained promising results in terms of endothelialization and platelet adhesion when compared to the unmodified PU scaffolds. On the contrary, the involvement of toxic precursors like toluene diisocyanates in PU synthesis is the major limitation of this synthetic polymer in the biomedical field (Pankajakshan and Agrawal 2010).

PET and ePTFE prosthesis used for small caliber vessels fail due to the insufficient functional endothelium regeneration and the differences between the mechanical properties of tissue-engineered vascular graft (TEVG) and natural blood vessels (Catto et al. 2014).

Degradable

Biodegradable polymers can be used as provisional structures for blood vessels before the ingrowing tissue replaces them. Their degradation produces chemical sub products of smaller molecular weight when metabolism, via hydrolytic cleavage at the ester bond, occurs. These products may alter the local cellular environment and could affect the cell functions. After this process, the materials suffer a loss of mechanical properties followed by a reduction of mass and/or volume, and the speed depends on different parameters such as the initial molecular weight, the exposed surface area and the crystallinity (Tara et al. 2014).

One of the most used biodegradable polymers in tissue engineering is poly glycolic acid (PGA). It is a semicrystalline thermoplastic of aliphatic polyester and it is produced by the ring-opening polymerization of glycolide. It completely degrades *in vivo* within 6 months and is a material approved for human clinical use (Couet et al. 2007; Pankajakshan and Agrawal 2010).

Typically, PGA is combined with polylactic acid (PLA) in different ratios to synthesize it, poly lactic-co-glycolic acid (PLGAs). PLA is a thermoplastic aliphatic polyester synthesized by ring-opening polymerization of lactic acid. PLA degrades slower than PGA and usually its degradation rate is controlled by mixing it with PGA. PLA L-chiral molecule poly-L-lactide (PLLA) can take months or even years to degrade, because it is more hydrophobic, and its biocompatibility is good (Chen et al. 2002).

Although PGA presents a good biocompatibility, *in vitro* studies suggest that its breakdown products may induce inflammatory response (Higgins et al. 2003). In addition, low differentiation ratio and cell proliferation support the fact that, PGA doesn't represents an optimal vascular scaffold for tissue engineering (Pankajakshan and Agrawal 2010).

Due to their hydrophobic properties, poly ϵ -caprolactone (PCL) and PLA present

a successful option for different clinical applications. PCL is a semicrystalline aliphatic polyester and among other advantages it presents a very slow degradation rate producing degradation products that don't interfere with cell proliferation, easy fabrication, optimum porosity and viscoelastic properties.

As a consequence, they are commonly used like arterial scaffold materials. Since, PCL and PLA used alone cannot reach the mechanical performances for small artery pressure and high flow conditions, they are used combined with additional synthetic polymers to create copolymers such as poly(lactide-co- ϵ -caprolactone) (PLCL), with fine tuning of mechanical properties and degradation rates by controlling the composition ratio and molecular weights. Even though the mechanical scaffold properties feasibility of the *in vivo* studies are demonstrated (Tara et al. 2014) these studies also show a delayed tissue remodeling. Hence, mechanical properties of biodegradable scaffolds are important for their clinical success, Table 3 shows different parameters in order to compare it with native vessel parameters.

Polymer	Tm	Tg	Initial tensile strength (MPa)	Elastic modulus (GPa)	Elongation at break (%)	Degradation period
PGA	230	36	890	8,4	30	2-3 weeks
PLA	170	56	900	8,5	25	6-12 months
PCL	60	-60	50	0,3	70	12 weeks
PLCL ($LA/CL = 75/25$)	140	22	500	4,8	70	8-10 weeks
PLCL ($LA/CL = 50/50$)	105	-17	12	0,9	600	4-6 weeks

Table 3: Biodegradable polymers for tissue engineered vascular grafts (Tara et al. 2014). Tm, melting temperature; Tg, glass-forming temperature.

Focusing on improving PLA cell affinity and haemocompatibility, many authors synthesized synthetic copolymers such as poly lactideco-b-malic acid (PLMA) with minimum platelets attraction and enhanced cell proliferation (Wang et al. 2009) or in combination with biological materials like gelatin, elastin, collagen I (Li et al. 2006; Stitzel et al. 2006).

Poly glycerol sebacate (PGS) is a bioelastomer created specifically to fulfill the requirements of a dynamic mechanical environment such as the cardiovascular system. It degrades *in vivo* by hydrolysis in 2 months and is Food and Drug Administration (FDA) approved for medical applications (Catto et al. 2014).

These poor mechanics, combined with the lack of endothelialization and the thrombogenic nature of the synthetic surface, leading to thrombosis and luminal narrowing, due to intimal hyperplasia, are reflected in their poor long-term patency (Kannan et al. 2005; Lemson et al. 2000).

1.3.2 Scaffolds from natural polymeric materials for vascular tissue engineering

Collagen

Collagen is the main ECM protein in the body and its function is to provide mechanical support to contrast action forces and, at the same time the collagen type and fiber orientation define the different kind of cells and their disposition in the tissue.

Until now 29 types of collagen were individuated, but collagen I and II represent 30% and 60%, respectively, of vascular wall composition. Collagen I primary structure is formed by 3α helix and each chain has about 1.014 amino acids. The amino acids sequence along the entire chain is composed by the tripeptide sequence of $-(\text{Gly-X-Y})_n-$, where glycine (Gly) constitutes about 30% of the total amino acid content in collagen and generally, X is a proline and Y is an hydroxyproline (Liu et al. 2019).

Collagen presents low antigenicity, low inflammatory response, biocompatibility, biodegradability, and excellent biological properties (Couet et al. 2007; Marelli et al. 2012; Pankajakshan and Agrawal 2010). As a result, it was the first material used in attempt to develop a blood vessel scaffold using a biological material.

In 1986, Weinberg and Bell created a blood vessel cocultured of ECs and SMC cells in a collagen tube. Unfortunately, this scaffold had poor mechanical strength and years after a Dacron[®] support was integrated into the structure, between the media and adventitial layers, to reinforce the vessel. Regrettably, synthetic material caused complications, such as immune rejection and compliance mismatch (Seifu et al. 2013) and the conduit were unable to reach adequate burst strengths for *in vivo* applications (Pankajakshan and Agrawal 2010).

Different techniques that utilize collagen as a scaffold were used over the years. Notably, bioreactors were used to endothelialize collagen constructs and stimulate the rate

of matrix remodeling through pulsatile circumferential stretch action on SMCs metalloproteinase-2 production. Combination of collagen with other synthetic polymers, for example poly-(glycolic acid), poly-(lactic acid) and poly-(L-lactide-co- ϵ -caprolactone) (Boccafoschi et al. 2017a), and use of cross linking agents, like ultraviolet radiation (Achilli et al. 2010; Haisch et al. 2000; Rajan et al. 2008), attempted to increase the mechanical performances.

However, the reason why collagen is not the best option to use in the matrix is that the degradation product of collagen results in the production of amino acids that have thrombogenic potential and activate the coagulation cascade. In addition, high cost of pure collagen also curtails its use as a cost effective approach to vascular graft construction (Nair and Thottappillil 2015).

Elastin

Elastin is a protein that can be found in some mammalian tissues and it is produced until puberty. In particular, it plays an important role in the blood vessel ECM because it provides enough elasticity to ensure the correct blood flow (Couet et al. 2007). This protein confers elastic recoil, resilience, and durability to the arterial wall and the reason can be found in its microstructure.

Elastin is made of its soluble precursor tropoelastin, this results in an insoluble polymer. The elastic fiber is composed of amorphous elastin and microfibrils which act as a scaffold on which elastin is deposited. An important property of tropoelastin and elastin-like peptides is their potential to self-assemble under physiological conditions. As collagen, cross-linking fibers are mediated by lysil-oxidase and take to sequential reactions leading to the functional and insoluble form of elastin (van Eldijk et al. 2012). Collagen contains 1–4 cross links per unit, whereas elastin has 15–20 cross-links which cause the different mechanical behavior. Indeed, these characteristics are palpable when the compliance is measured, due to the fact that elastin stores elastic energy and high strain to ensure smooth blood flow (Nair and Thottappillil 2015).

The addition of elastin to create a scaffold has been proved very useful for inducing cell activity, elastic recoil to collagen fibers in the case of strain, and at the same time reducing the rigidity in collagen-elastin for vascular scaffolds application (Boland et al. 2004). Recent works study different techniques to add elastin to scaffolds, collecting

data about the resulting mechanical properties (Williams et al. 2009; Buijtenhuijs et al. 2004), or the process of electrospinning which makes it able to control the composition, the structure, and the mechanical properties of biomaterials.

In conclusion elastin, considered as a biomaterial, has a very high potential for VTE due to its favorable properties such as resistance to degradation, easy purification, and low thrombogenic potential (Hinds et al. 2006), but it is still limited due to the problems represented by the task of mixing, solubilizing, and processing elastin with other materials to obtain a scaffold with a well-organized microstructure (Couet et al. 2007). The main reason why it is not used as often as other natural protein-based material, is because during the purification process, contaminations often take place which can then lead to immune responses by the body.

Furthermore elastin has a tendency to calcify (Bobryshev 2005; Khavandgar et al. 2014-02; Pai et al. 2011-02). In recent years more successful elastin purification methods have been developed (Daamen et al. 2001), however since elastin is highly insoluble, its soluble forms are often used, like tropoelastin, alpha-elastin, elastin like polypeptides (ELPS) and a type of genetic-recombined elastin (ELRs).

Fibrin

Fibrin is a natural fibrillar protein which can form three-dimensional structures. It is naturally involved in wound healing and tissue repair due to the fibrin clots providing structural scaffolding for adhesion, proliferation, and migration of cells involved in the repairing process. The goal of using fibrinogen precursors of polymeric fibrin isolated from the patient's own blood to build the scaffold is to eliminate immunological concerns of human or cross-species donor incompatibility. Cells which grow on fibrin scaffolds seem to produce more collagen and elastin than cells entrapped in a collagen gel but this is not enough to increase the weak mechanical strength. To increase the elastin fibers and collagen amount from SMCs, the initial fibrin scaffold was enriched with TGF- β and insulin. Also, incorporation of angiogenic and platelet growth factors can improve the synthesis of elastin and collagen by the vascular cells. In order to improve the cell adhesion, specific adhesion receptors can be cross-linked into the fibrin matrix. Moreover, several studies support the incorporation of specific biochemical factors, like fibroblast growth factor 1 and heparin, into fibrin matrices. There

are a variety of other ECM proteins (fibronectin, hyaluronan, and laminin) that upon incorporation to fibrin may further enhance the properties and functions of engineered tissues. However, fibrin localization poses a problem of initiation of the coagulation cascade and the degradation profile of fibrin requires a detailed investigation.

Fibrin is a protein particularly involved in the natural repairing process of tissues and in the coagulation cascade. Fibrinogen is the inactive form of fibrin and when activated it plays a key role in wounded tissue regeneration by forming an extensive fiber network. In this context, fibrillar gel composed of fibrin clots provides support forming a scaffold which is involved in the final healing process.

Fibrinogen can be obtained from blood and it can be used as an autologous source for the scaffold, mitigating or eliminating the risk of immunological incompatibility (Catto et al. 2014). These materials are considered an alternative solution to collagen due to the fact that they are easily obtained from the patient's blood (Seifu et al. 2013).

Fibrin based hydrogels are commonly used in cardiac tissue engineering, however the main obstacle is their low mechanical strength. Nevertheless, some studies report that cells grown into a fibrin gel produce more collagen and elastin than cells seeded into a collagen gel (Grassl et al. 2002). For example, Seifu et al. (2013) shows that cell-seeded fibrin gels implanted in a vein of chronically heparinized lambs improved the mechanical properties and the elasticity of the graft after 12 weeks.

Several studies probed the techniques for improving the healing process. Among these studies we can remark: incorporation of vascular endothelial growth factor (VEGF) in fibrin that promotes the endothelial proliferation and maturation (Santhosh Kumar and Krishnan 2002) and binds specifically and saturable to both fibrinogen and fibrin (Sahni and Francis 2000); the incorporation of specific factors like fibroblast growth factor 1 and heparin in fibrin (Zarge et al. 1997); and the incorporation of fibrin into biodegradable polymers that can be used to combine the biological properties of fibrin with the mechanical properties of the polymer to define an approach to improve the mechanical strength of the scaffold for vascular tissue engineering (Pankajakshan and Agrawal 2010).

Chitosan

Chitosan is a linear polysaccharide composed of β -(1-4)-linked D-glucosamine with

randomly dispersed N-acetyl-D-glycosamine groups, obtained by partially deacetylating chitin, the primary structure of arthropods exoskeletons. Structurally chitosan is similar to the glycosaminoglycans contained in the ECM. Physical and mechanical properties are directly correlated with the molecular weight of the polymer and the degree of deacetylation.

The advantages of using chitosan in tissue engineering are: the antibacterial properties, it is easy to sterilize, it contains nitrogen, it has a low cost, it is bioactive, biocompatible and its degradability can be controlled by changing the level of deacetylation (Huang et al. 2005). This type of material is easily affected by parameters such as pH and temperature. Among its disadvantages we find its poor mechanical properties, however this problem can be overcome by crosslinking with chemical materials (Vieira et al. 2002) or with gelatin (Nair and Thottappillil 2015).

In tissue engineering chitosan is an advantageous biomaterial choice, due to its low cost, ease of production, antimicrobial activity, biocompatibility, biodegradability, and bioactivity (Huang et al. 2005). Chitosan's antibacterial properties and its stimulatory action on leukocytes gives it an enormous potential as a natural polymer for wound-healing applications (Hamedi et al. 2018). On the other hand, it is necessary to consider the poor mechanical properties, which are usually improved by blending it with synthetic polymers and even with gelatin (Nair and Thottappillil 2015).

Chitosan was studied as a vascular scaffold in combination with gelatin by Zhang et al. (2006) who fabricated a two layers tubular chitosan and gelatin scaffold. In order to improve the endothelial cells (ECs) and smooth muscle cells (SMCs) spreading and proliferation, chitosan was modified with dextran sulphate with satisfactory results *in vitro* and *in vivo* (Chupa et al. 2000). To reduce the possibility of clot formation in the vessel, Madhally and Matthew (1999) designed a family of chitosan scaffolds which include heparin-modified porous tubes.

Glycosaminoglycans

Glycosaminoglycans (GAGs) are long unbranched chains composed of disaccharide units containing carboxylic and/or sulphate ester groups. These functional groups bridge and link collagen to form the ECM network.

An example of GAG is hyaluronic acid (HA), present in the mammalian connec-

tive tissue where it acts as a lubricant. HA is an anionic non-sulphated GAG that consists of glucuronic acid and N-acetyl glucosamine (Couet et al. 2007). HA has some remarkable properties such as hydrophilia, non-adhesiveness, biodegradability (Couet et al. 2007; Huang et al. 2004), and the ability of being completely resorbable through multiple metabolic pathways (Bencherif et al. 2008). Another advantage of HA is that its production is easy and controllable in a large scale through microbial fermentation (Pankajakshan and Agrawal 2010), avoiding the risk of animal-derived pathogens. Moreover, HA can bind large amounts of water to form hydrogen bonds with the solvent.

There are studies that evidence that HA is involved in angiogenesis, ECM organization, wound healing, inflammation, and other biological processes (Pankajakshan and Agrawal 2010). The studies on graft based esterified HA show a lower axial strength and higher stiffness compared to normal porcine arteries (Remuzzi et al. 2004). Improvements on the creation of an endothelial monolayer when compressed are achieved through Hyaff-II, a biomaterial obtained from the total esterification of hyaluronan with benzyl alcohol (Pankajakshan and Agrawal 2010). Porcine model implanted with Hyaff-II showed graft occlusion at the end of 3 months, however the graft almost completely degraded while the formation of neo-tissue was complete with endothelium, organized collagen, and elastin (Zavan et al. 2008). This scaffold allows neoangiogenesis and endothelialisation of the luminal surface, it supports elastin synthesis without chemical and cellular preconditioning *in vitro*, for these reasons it is considered a very promising solution (Pankajakshan and Agrawal 2010). HA derivatives are used successfully as scaffold materials for chondrocyte growth (Prestwich 2011), for bone and skin regeneration, for treating vascular diseases due to the biocompatibility and anti-inflammatory properties (Burdick and Prestwich 2011).

Silk Fibroin

Silk fibroin is a protein produced by silkworms, spiders and scorpions, even though it is mainly obtained from *Bombyx mori* silkworm. Its main amino acid composition is 43% glycine, 30% alanine, and 12% serine (Vepari and Kaplan 2007).

It is possible to obtain dissolved silk fibroin by using different kinds of solvents like lithium bromide, formic acid, ionic liquids, and the ternary solvent system $\text{CaCl}_2/$

ethanol/ water. The previous necessary step consists on removing sericin, an antibacterial and UV-resistant protein which glues the silk fibers, using a degumming process via dilute sodium carbonate solution or urea, citric acid, and sodium oleate (Kim et al. 2017). In order to stabilize the film produced with fibrin, silk I and II are combined. Silk I is water soluble, whereas silk II has an antiparallel beta-sheet conformation and is insoluble. Young's modulus, strain and tensile strength are improved when silk I is converted into crystalline silk II through an annealing process (Han et al. 2014).

Because of its excellent mechanical properties, low adverse immune reaction, minimal thrombogenicity, and compatible degradation rates it is employed in vascular tissue engineering (Nair and Thottappillil 2015). Furthermore, it is compatible with a number of manufacturing process, such as electrospinning or gel spun.

Nakazawa et al. performed an *in vivo* study using a rat model, it shows a patency rate of 85% after 12 months, with no thrombosis or aneurysm observed. It was also suggested that the mechanical properties of these scaffolds could be improved to better emulate those of the native vasculature by using fiber alignment techniques during the manufacturing processes (Nakazawa et al. 2011).

Three-dimensional (3D) printing technology employs silk hydrogels with different techniques such as extrusion, lithography and recently digital light process using a grafting methacrylate (Kim et al. 2018). Silk is also combined with other biopolymers, such as gelatin and alginate, to obtain the adequate rheological characteristics for the bioink (Wang et al. 2019).

Gelatin

Gelatin is a natural and low-cost vascular polymer whose properties, such as minimal immunogenicity and appreciable degradability, make it one of the best options for tissue engineering. This polymer is obtained through denaturing the triple helical conformation of collagen; there are two types of gelatin derived from 2 different treatments: gelatin A processed by acids (pH 1–3) and gelatin B processed with alkaline solutions, type A being the most preferable for scaffold building. Gelatin has also been used as a coating agent to enhance cell attachment in vascular tissue regeneration techniques (Nair and Thottappillil 2015).

Gelatin presents gel forming, thickening, emulsifying and foaming proprieties. The

mechanical ones depend on the supramolecular structure (Kozlov and Burdygina 1983).

Synthetization of anionic or cationic gelatin is based on extraction conditions and fundamentally for filling molecules through electrostatic interaction. Since gelatins stability at high temperatures and wide range of pH allows synthetic polymers to be grafted on gelatin backbone. Methods are “grafting from”, polymerisation on the functional surface of the substrate, “grafting to”, grafting end functionalized polymer to the substrate, or “grafting through” (Sadeghi and Heidari 2011).

Methacryloyl group-grafted gelatin, also known as gelatin methacrylate (GelMA) has been used for 3D printing in microfabricated blood vessel. Gelatin electrospun fibers loaded with antibiotic drugs (ciprofloxacin) have a strong antibacterial activity but in this case gelatin has to be reinforced with materials such as graphene oxide and boron nitride to improve poor mechanical proprieties. (Bakhsheshi-Rad et al. 2017; Nagarajan et al. 2016a,b, 2017).

Using electrospinning processes to generate tubular scaffolds allows to obtain a similar morphology to the native ECM structure, gelatin copolymer behaved as a natural cell responsive surface under mechanical stimulation (Thomas and Nair 2012).

Panzavolta et al. (2011) obtained electrospun gelatin nanofibers cross-linked with genipin, a low-toxicity agent, which reduces the extensibility of the electrospun mats, producing appreciable improvements in elastic modulus and breaking stress. Long-term studies on cross-linked electrospun gelatin are still under study to confirm its efficacy as a scaffold material for blood vessel tissue engineering.

Alginate

Alginate is a polysaccharide component of brown algae cell walls and some bacteria capsules (Draget et al. 2005). Its structure is based on two different monomers: b-D-mannuronate (M) and a-L-guluronate (G) organized into blocks. Since G-blocks form ionic bridges, alginates mechanical properties are related with the number and disposition of these blocks (Draget and Taylor 2011). From the biological point of view for medical applications alginate presents nontoxic and noninflammatory properties, *in vivo* degradation does not occur, however cell adhesion is poor and mechanical characteristics are insufficient. Alginate applications were explored in different tissues such as liver, nerve, heart, and cartilage (Brandl et al. 2007).

Polyhydroxy alkanates

Polyhydroxyalkanoate (PHA) and copolymers are polyesters produced by different bacteria which synthesize carbonic chains with different lengths depending on the carbon nutrients limitation. Mechanical properties and degradation rates can be modified according to the length chain of the molecule (Williams et al. 1999).

PHAs remarkable characteristics are its biocompatibility, thermoplasticity, and/or elastomericity, which allows ease of handling during suturing (Valappil et al. 2006). Although PHA vascular grafts sustain cell attachment and proliferation, *in vivo* studies often present an acute immune response. Lipopolysaccharides produced by gram-negative bacteria when PHAs are synthesized appear to be the origin of the problem.

Several studies confirm this theory for vascular conduits made with PHAs. For example, a hybrid tubular scaffold PHA-PGA was implanted using an ovine model and, after 5 months the mechanical properties were similar to the ones of native tissue (Shum-Tim et al. 1999). Another study uses a blood vessel scaffold engineered using PGA coated with poly(4-hydroxybutyrate), combined with fibrin gel and seeded with human myofibroblasts. *In vitro* tests under dynamic strain conditions showed burst pressure results comparable with mammary artery physiological conditions (300 mmHg) after 28 days (Stekelenburg et al. 2009).

1.3.3 Hybrid scaffolds from synthetic and natural polymers

Synthetic and natural polymers can be combined to obtain a hybrid scaffold, so the excellent biological performance of natural polymers with the satisfactory mechanical properties of synthetic materials are combined. With this objective, Table 4 summarizes the relevant studies on TEVGs made using hybrid scaffolds.

Material	Biological <i>in vitro</i> results	Biological <i>in vivo</i> results	Reference
Recombinant human tropoelastin (inner layer) + PCL (outer layer)	SEM and fluorescence microscope (3 days): HUVECs attached and proliferated; platelet attachment: reduced, compared to ePTFE and PCL	Model: rabbit (1 month); maintenance of physical integrity; no evidence of dilatation, anastomotic dehiscence, or seroma; mechanical properties of implanted grafts remained similar to controls	Wise et al. (2011)
PGA + PLLA + collagen type I	Cell culture with NIH/3T3 or HUVEC (3 days); SEM analysis: higher cell number and better adhesion for grafts with collagen	Model: dog (12 months); acellular grafts; 100% patency, no thrombosis or aneurysm; excellent tissue regeneration: complete endothelialization, SMCs, elastin, and collagen fibers; PGA fibers completely absorbed at 2 months, PLLA fibers unabsorbed at 12 months	Yokota et al. (2008)
Blend of PCL + collagen type I	ECs and SMCs from bovine carotid artery; cytotoxicity via direct contact (7 days—MTS assay): no differences in cell viability compared to TCPs; cytocompatibility (7 days—MTS assay): EC and SMC adhesion and proliferation; cell culture on tubular grafts (48 h—SEM and histological analysis): SMCs formed multiple cell layers on the outer region, ECs formed a monolayer on the inner surface	-	Lee et al. (2008)
Blend of PCL + collagen type I	ECs derived from endothelial progenitor cells isolated from live sheep; SMCs isolated from sheep artery explants; dynamic culture using a pulsatile bioreactor under physiologic conditions (9 days); SEM + histological analysis: ECs formed a confluent layer on the inner lumen, SMCs assumed a multilayered configuration on the exterior	Platelet adhesion in a live sheep model for 15 min: no adhesion for seeded grafts, abundant adhesion for unseeded grafts; model: rabbit (1 month); acellular grafts; no aneurysmal degeneration; majority of the grafts remained patent at 1 month; absence of inflammatory infiltrate	Tillman et al. (2009)
PCL/PLA + collagen type I	HCAECs rotationally seeded in the bioreactor for 4 h + static culture (10 days—SEM and histological analysis): HCAECs evenly distributed and well spread on the lumen	Model: rabbit (7 weeks); acellular grafts without collagen coating; no blood leaking; graft structure integrity and patency; foreign body response: no cell infiltration	He et al. (2009)
PLDLA + fibrin	ECs, SMCs, and fibroblasts isolated from ovine carotid arteries; ECs seeding in the inner layer using a rotating chamber; dynamic culture in a bioreactor under physiological pressure conditions for 21–28 days; histological analysis: a dense, homogenous distribution of cells throughout the scaffold thickness, extensive collagen formation, and no evidence of calcification	Model: sheep (6 months); $D \sim 6$ mm; cellular grafts (dynamic culture for 21–28 days); at 3 months 1 graft with a significant stenosis; other grafts: completely patent, no thrombus formation and aneurysm, infection, or calcification; remodeling: confluent endothelium, collagen and other ECM components, and elastin (not assembled in cohesive sheets); fibrin completely degraded after 1 month, sparse PLDLA material remained at 6 months	Koch et al. (2010)

Table 4: TEVGs made using hybrid scaffolds (Catto et al. 2014).

1.4 Decellularized vascular substitutes

The goal of tissue or organ decellularization is to mimic the native tissue and provide a proper environment for cells, through the removal of cells, while preserving the micro and macro architecture of ECM and the niche for cells.

In order to obtain an optimal decellularized matrix, many factors must be considered, which include: the tissue source (the species from which the material has been obtained), the preparation procedures and the efficacy of decellularization. In addition, other factors, such as the use of chemical cross-linking agents or the final sterilization, should be under control because they may also affect the structure of the ECM (Kawecki et al. 2018).

Biological scaffolds are typically allogeneic or xenogeneic in origin, for this reason a maximal decellularization is desirable in order to minimize immunologically induced inflammation (Crapo et al. 2011).

Specific tissue and organ characteristics, such as cell density, matrix density, geometric, tissue thickness and shape, should be considered to process it with the optimal decellularizing method. To preserve the matrix's micro/nano-structure, composition and biological activity properties, the decellularization method should be selected rationally and should be scientifically justified for each kind of matrix or organ (Kawecki et al. 2018). The critical point is not only to use the optimal physical force exposure, but also the choice of non-physiologic chemical and biologic agents such as detergents and enzymes. These aspects will be analyzed below. In the specific case of blood vessels, usually the process consists of mechanical shaking, chemical surfactant treatment and enzymatic digestion. The validation and consolidation of the method effectivity must be guaranteed. The right choice of an optimal decellularization method and its efficacy is crucial for clinical success or failure. Equally important, removal of cell remnants and chemical treatment trace are important to prevent a host response (Crapo et al. 2011).

Focusing on vascular tissue, the preservation of collagen and elastin is crucial to maintain the physiological elasticity necessary to withstand the pulsatile blood flow.

ECM scaffolds present a multifunctional structure with the ability to induce cell

attachment, proliferation, migration, differentiation and maturation, even of stem cells (Guruswamy Damodaran and Vermette 2018), due to cell signaling.

Molecules such as growth factors, glycans, bioactive cryptic peptides and natural proteins like collagen and fibronectin, promote biological activities such as, cell growth, function, differentiation, angiogenesis, anti-angiogenesis, antimicrobial effects and chemotactic effects (Kawecki et al. 2018). Indeed, many studies have demonstrated that proteoglycans from the ECM are involved in these molecular events (Schmidt and Baier 2000; Wight et al. 1992). This specific properties, would present an advantage to using decellularized materials instead of other biological or synthetic materials (Guruswamy Damodaran and Vermette 2018).

Taken all together, there are two main advantages as a rationale for using ECM as a blood vessel scaffold. The first one consists in the fact that after the removal of cells, the decellularized scaffold that constitute the ECM can maintain the mechanical properties of the natural vessels, if correctly treated, to withstand changes in blood pressure (Lin et al. 2018). The second one is the ECM's influence on the cells behavior, mitogenesis and chemotaxis (Bornstein and Sage 2002; Vorotnikova et al. 2010) and direct cell differentiation are verified (Allen et al. 2010; Barkan et al. 2010; Cheng et al. 2009; Cortiella et al. 2010; Ross et al. 2009; Sellaro et al. 2010; Stern et al. 2009). Furthermore, some researchers suggest that after implantation, the biological ECM scaffold induces tissue remodeling and regeneration in the host since they possess immunomodulatory activities (Kawecki et al. 2018; Parekh et al. 2009; Valentin et al. 2010; Xu et al. 2010).

Attending the decellularization characteristics, it is a promising approach to produce small-diameter vascular grafts (Keane et al. 2015; Taylor et al. 2018).

1.4.1 Decellularization agents and techniques

Decellularization protocols have been developed for almost each body tissue. The decellularization method can be different but the aim is always to obtain a balance between the most effective cell removing action and the maximum possible preservation of the native ECM structure (Keane et al. 2015). Since any decellularizing procedure involves the destruction of the ECM, it should be emphasized once more that the

negative impact of cell removal methods is tolerable if the undesirable effects in the mechanical properties will be minimized or completely avoided (Crapo et al. 2011; Guruswamy Damodaran and Vermette 2018).

Different factors such as the amount of cells colonizing the biomaterial (e.g., the liver vs. tendon), the density of ECM structure (e.g., dermis vs. adipose tissue), the fat content (e.g., the brain vs. bladder), and the thickness (e.g., dermis vs. pericardium) affect the chosen decellularization process (Kawecki et al. 2018).

Most decellularization protocols involve a physical treatments such as agitation, sonication, mechanical pressure, or freeze-thawing procedures, in order to disrupt the cell membrane, in combination with extensive washing steps and further chemical processing with ionic solutions and various detergents or/and enzymes (Hinderer et al. 2016).

1.4.2 Physical methods

The main advantage of tissue decellularization by means of physical methods over chemical methods is the lack of introduction of potentially toxic chemicals to the tissue. However, physical methods as cell removal agents require prolonged exposure of the tissues to the agent, which can cause the degradation of the material. For this reason, it is common to include a physical method step in the decellularization protocol (Kawecki et al. 2018).

Physical methods of decellularization include multiple freeze-thaw cycles to disrupt the cellular components, agitation during immersion in chemical solution, and application of pressure or supercritical fluids (Taylor et al. 2018).

Freeze-thaw cycles have a lysis cell effect with no significant alteration on the mechanical properties of the ECM. As all decellularization methods, the tissue micro and nano structure could be modified, therefore this method can be used only if the changes are acceptable. The method limitation is the elimination of cell membranes and intracellular element fragments; therefore, it is common to combine it with chemical methods, reducing the chemical amount required for the lysis step.

In order to increase the methods efficiency, the freezing and thawing cycles are usu-

ally repeated. However, a single cycle may reduce adverse immune reactions, including leukocyte infiltration in vascular ECM scaffolds (Crapo et al. 2011; Keane et al. 2015).

Since these cycles may increase the loss of protein and cause other structural changes (Yang et al. 2010-10), it is suggested to use a cryoprotectant such as 5% trehalose to minimize these adverse effects, without impeding cell lysis.

This method is frequently used for tissues characterized by fine structures such as the bladder, the pericardium, and the amnion (Kawecki et al. 2018). For load-bearing robust tissues, the effect of freeze-thaw processing is minimal from the mechanical properties' point of view (Elder et al. 2010; Jackson et al. 1988).

Another physical decellularization method is sonication. The ultrasounds cause the cell lysis for a cell-free ECM scaffold production.

Freezedrying method has a decellularization effectiveness similar to that of cyclic freezing and thawing, but this method also presents a raised demonstrated effectivity for long-term storage of biological materials. The removal of defaulting cell membranes, nucleic acids, and other cellular organelles can level off at unsatisfactory levels (Kawecki et al. 2018).

Non-thermal irreversible electroporation method (NTIRE) consists in the application of electrical pulses across the tissue, these induce the formation of micropores in the cell membrane due to the destabilization of the electrical potential across the membrane (Lee 2005; Lee and Kolodney 1987).

Usually this technique is used *in vivo*, where the micropores cause loss of cell homeostasis and lead to cell death. *In vivo* experiments in rat carotid arteries demonstrated that the cellular remnants were slowly removed from the tissue over a period of days, leaving an acellular tissue approximately three days after NTIRE treatment (Phillips et al. 2010). The mechanisms for the cellular removal are not clear. By selecting appropriate parameters to reduce heat generation, the integrity and morphology of the remaining ECM appears to be retained, which allows for recellularization by host cells.

The biggest NTIRE limitation is that the decellularization process would need to occur *in vivo* because the cells removal is caused by the organisms' immune system. Furthermore, the probes are relatively small, thereby limiting the size of the tissue that

can be decellularized.

The number of cellular remnants retained within the tissue is to be determined. As discussed previously, ECM scaffolds that have not been thoroughly decellularized promote a very different, less desirable host response than those that have been cleared of cell remnants (Crapo et al. 2011).

1.4.3 Chemical agents

Chemical agents are often used combined with physical methods. According to their chemical properties, the most effective chemical agent combination, for removing cells while preserving the ECM, will be different for each tissue.

Acids and bases cause or catalyze hydrolytic degradation of biomolecules which is important for the decellularization effectiveness but, they have a negative impact on the ECMs mechanical strength and can also denature ECMs components including GAGs, collagen, and growth factors (Keane et al. 2015).

Accordingly, Tsuchiya et al. (2014) confirms that the utilization of acidic or alkaline solutions during decellularization requires a balanced approach to achieve effective decellularization without severe detriment of the ECM constituents. Studies compared the effectiveness of cell and cytoskeletal protein removal with 8 mM CHAPS solutions at different pH values. The cell removals efficiency is higher if the pH value increases however, highly alkaline CHAPS (pH 12) disrupted architecture and resulted in a more fibrotic response compared to that of lungs decellularized in 8 mM CHAPS at pH 8 and pH 10 following subcutaneous implantation. In the same way, Mendoza-Novelo et al. (2011) showed that a calcium oxide treatment results in a dramatic reduction in GAG content and altered the viscoelastic properties of pericardial tissue.

For this reason, it is important to optimize the dose and exposure time when acids are used for decellularization.

Commonly used alkaline bases include ammonium hydroxide, sodium sulfide, sodium hydroxide, and calcium hydroxide and acids frequently used are deoxycholic, acetic and peracetic (Keane et al. 2015). It is important to remark the use of peracetic acid to sterilize decellularized scaffold materials, which is a method approved by the FDA and the

European Union (EU) for medical devices, in addition with its decellularization agent action by removing residual nucleic acids with minimal effect on the ECM composition and structure (Gilbert et al. 2008; Hodde et al. 2007; Hodde and Hiles 2002).

Osmotic pressure solutions affect the cell structure through the lysis of the cellular membrane.

Different kind of solvents can be used such as decellularized agent. In this context, alcohols can diffuse into the cell and replace the intra cellular water, hence, the cells lyse by dehydration. Moreover, the nonpolar carbon chain of alcohols dissolves nonpolar substances such as lipids (Montoya and McFetridge 2009). In fact, alcohols such as isopropanol, ethanol, and methanol are more effective than lipase in removing lipids from tissue and are capable of rendering adipose tissue lipid-free in a relatively brief period of time (Crapo et al. 2011).

Care must be taken in treating tissues with alcohols such as ethanol and methanol due to their use as tissue fixatives in histology, they alter the collagen structure by crosslinking the ECM (Keane et al. 2015).

Another method of removing lipids during decellularization is the use of acetone, but care should be taken when utilizing this solvent because it is a fixative tissue. This can cause damaging in the EMCs structure due to the crosslinks formed by acetone in the EMC, producing a stiffer scaffold (Cole 1984; Jamur and Oliver 2010).

Tributyl phosphate (TBP) is an organic solvent with viricidal properties (Horowitz et al. 1992). Recent studies (Cartmell and Dunn 2000; Deeken et al. 2011; Woods and Gratzner 2005) highlight that TBP appears to be more effective than detergents such as SDS and Triton X-100 to decellularize tendon and ligament tissues. Moreover, collagen matrix, GAGs, and biomechanical properties (including tensile strength and elasticity) were not significantly altered. Although residual cytoskeletal proteins (e.g., vimentin) were not completely removed, TBP is a viable option that warrants further study for other tissue types (Keane et al. 2015).

Triton X-100 as a detergent, solubilizes the cell membrane and dissociates DNA from proteins which is important in order to remove the cell material from the tissue. Nevertheless, the detergent can also disrupt the ECM proteins and this depends on the exposure time (Crapo et al. 2011). Triton X-100 is the most studied non anionic

detergent and it is effectively capable of expelling cell debris from thicker tissues, such as heart valves (Kawecki et al. 2018) on the other hand, some studies demonstrated that Triton X-100 had a poor cell removal capacity for blood vessels decellularization (Keane et al. 2015).

Sodium dodecyl sulfate (SDS), sodium deoxycholate (SDC) and Triton X-200 are the most commonly used ionic detergents. They are used as decellularizing reagents due to their ability to solubilize cytoplasmic membranes, lipids, and DNA (Keane et al. 2015). If compared to Triton X-100, SDS appears more effective in the removal of cell nuclei and acid, while maintaining the mechanical characteristics of the natural tissue/organ in organs including aorta, veins, heart, kidneys and urethra (Guruswamy Damodaran and Vermette 2018). Its use in the decellularization protocol can make a difference between complete and incomplete cell nuclei removal (Crapo et al. 2011).

The use of SDC agent to decellularize is controversial. Some researches demonstrated that SDC treatment obtains an incomplete nuclei removal and its effect can adversely affect the ECM structure and composition (Roosens et al. 2016; Zvarova et al. 2016). By contrast, Gilpin et al. (2014) suggests that SDC may be an effective decellularization factor when applied to tissues and organs that are less dense and have a clear ECM structure, such as the heart valve.

Another detergent proposed for decellularization is 3[(3-cholamidopropyl) dimethylammonio]-1-propanesulfonate (CHAPS) which combines non-ionic and ionic detergent properties, it is considered a zwitterionic detergent.

Blood vessels treated with CHAPS have histologically unaltered collagen and elastin morphologies, and the collagen content remains comparable to that of the native artery (Boccafosci et al. 2017a), due to its net zero electrical charge on the hydrophilic groups. Furthermore, it retains more collagen, GAGs, and elastin than SDS while still removing 95% of nuclear material (O'Neill et al. 2013; Petersen et al. 2012, 2010).

Using enzymes to decellularize materials allows the removal of specific cell components such as cell-cell attachments, cell-ECM attachments, or nucleic acid-ECM attachments, with specific enzymes such as nucleases, collagenases, and proteases (Taylor et al. 2018). For all that, complete cell removal by enzymatic treatment alone is prob-

lematic and enzyme residues may restrain the recellularization or evoke an adverse immune response.

Unremoved nucleic acids may play a role in the immune response after implantation. Hence, reducing the DNA and RNA content in the tissue is essential for a good decellularization result. In this context, nucleases such as DNases and RNases cleave nucleic acid sequences and can be efficient in the removal of nucleotides after cell lysis in tissues (Kawecki et al. 2018). For instance, these, combined with SDS, produced a completely acellular rat aortic valve (Grauss et al. 2005) which highlights the detergent combination steps.

Trypsin is the most common protease used in decellularization protocols. Its function consists in selectively cleaving cell adherent proteins on the carboxyl group of lysine and arginine to detach cells from the tissue surface. Trypsin action, in comparison to that of detergents, presents better preservation of GAG content, but it is more destructive to elastin and collagen structures, this can be associated to changes in mechanical properties. For this reason, concentration and exposure time to trypsin should therefore be set with caution, moreover, to improve the treatment penetration of subsequent decellularization agents, this enzyme should be used as an initial step of the treatment (Crapo et al. 2011). It is known that trypsin does not induce a cytotoxic effect because it is commonly used *in vitro* cell culture, this fact represents an advantage when used in tissue engineering (Kawecki et al. 2018).

Dispase II is a protease used specifically for epithelial cells and its action in the membrane focuses on cleaving fibronectin and collagen IV. Temperature and pH factors compromise its enzymatic activity, which is just effective under physiological conditions. Combination of trypsin and dispase presented a better decellularization effect in comparison to using one of them alone. This results were confirmed for different tissues (Kawecki et al. 2018). Its use is also recommended on the first steps of the decellularization process and it is used in porcine dermis and cornea tissues (Song et al. 2013; Xu et al. 2017) nevertheless, subsequent treatments or use of agents are necessary in order to obtain an adequate decellularization.

Collagenases group is an alternative enzymatic decellularization process used only when the material bioprosthesis does not require the maintenance of the integrity of

the collagen structure for the intended clinical application (Flynn 2010; Perea-Gil et al. 2015).

Ethylenediaminetetraacetic acid (EDTA) and ethylene glycol tetraacetic acid (EGTA) are chelating agents commonly used to dissociate cells from the ECM, these reagents are typically used in combination with trypsin or detergents because chelating agents alone are not sufficient for superficial cell removal even with agitation. In order to minimize the destructive effects on the ECM it is desirable to limit the duration of the exposure to trypsin-EDTA treatments.

An alternative to detergents was individuated on latrunculin B, a marine toxin. This substance allows to preserve the collagen fibrillar ultrastructure largely uncharged even though GAGs were reduced by around 40%. The latrunculin B decellularization efficiency in combination with hypertonic solutions and DNase was demonstrated for skeletal muscle tissue (Keane et al. 2015).

1.4.4 Techniques for agent's application

Agitation and immersion in chemical, detergent, and/or enzymatic solutions are the classical techniques for tissue decellularization when the material is not a natural vasculature used to perfuse the organ. The duration of the protocol depends on the tissues thickness and density, on the detergent used and on the intensity of agitation and it was described for different tissues, including heart valves, blood vessel, skeletal muscle/tendon, peripheral nerve, spinal cord, cartilage/meniscus, trachea, esophagus, dermis, and urinary bladder (Crapo et al. 2011). However, this method may damage the ultrastructure and the integrity of the ECM scaffold and another optimal alternative could exist (Kawecki et al. 2018).

The properties of supercritical fluids, in particular carbon dioxide, such as low viscosity and high transport characteristics for a tissue decellularization allow to obtain simple and short protocols.

The advantages of supercritical gas decellularization include the use of an inert substance for cell removal and minimal alteration of ECM mechanical properties. Furthermore, tissues can be obtained in dry conditions following decellularization and this eliminates the need of lyophilization as a preparatory step for ECM processing and

storage.

Perfusion technique is used for hollow tissues such as vessels and intestine tract to produce a transmural pressure gradient, designated as a convective flow in order to accelerate and improve the efficiency of delivering cell-lysing agents into the tissue and forcing cellular debris out of the tissue (Keane et al. 2015).

Bolland et al. (2007) and Montoya and McFetridge (2009) showed convective flow degraded collagen to a lesser extent than agitation as assessed by hydroxyproline quantification, and collagens I and IV, laminin, and GAG were retained along with some intracellular proteins, and mechanical properties were unaffected by the decellularization process.

Perfusion decellularization, using the natural vasculature, is the best approach for organ decellularization as it can minimize ECM damage due to excessive mechanical forces, while maximizing the delivery of decellularizing solutions to deeper parts of the organ (Taylor et al. 2018).

Table 5 contains the highlights of decellularization agents and techniques.

Agent/technique	Mode of action	Effects on ECM
Physical and miscellaneous agents		
Temperature (freezing and thawing)	Intracellular formation of ice crystals leads to disruption of cell membrane	Ice crystal formation can lead to disruption or fracture of ECM
Sonication	Ultrasound cell lysis	Ultrasound can lead to disruption or fracture of ECM
Freeze-drying		Effective method for long-term storage of biological materials
Electroporation	Pulsed electrical fields disrupt cell membranes	Electrical field oscillation can disrupt ECM
Chemical agents		
Acids and bases	Solubilizes cytoplasmic components of cells, disrupts nucleic acids, tend to denature proteins	May damage collagen, gag, and grow factors
Hypotonic and hypertonic solutions	Cell lysis by osmotic shock, disrupt DNA-protein interactions	Effectively lyses cells, but does not effectively remove cellular residues

Table 5: Summary of the different decellularization agents and techniques (Boccafoschi et al. 2017a; Crapo et al. 2011; Kawecki et al. 2018). *Continued on next page.*

Agent/technique	Mode of action	Effects on ECM
Solvents		
Alcohols	Cell lysis by dehydration, solubilize and remove lipids	Effectively removes cells from dense tissues and inactivates pyrogens, but crosslinks and precipitates proteins, including collagen
Acetone	Cell lysis by dehydration, solubilizes and removes lipids	Effectively removes cells from dense tissues and inactivates pyrogens, but crosslinks and precipitates proteins, including collagen
Tributyl phosphate (TBP)	Forms stable complexes with metals, disrupts protein-protein interactions	Mixed results with efficacy dependent on tissue, dense tissues lost collagen but impact on mechanical properties was minimal
Nonionic detergents	Disrupt DNA-protein interactions, disrupt lipid-lipid and lipid-protein interactions, and, to a lesser degree, protein-protein interactions	
Triton X-100		Mixed results with efficacy dependent on tissue, more effective cell removal from thin tissues, some disruption of ultrastructure and removal of GAG, less effective than SDS
Ionic detergents	Solubilize cell and nucleic membranes, tend to denature proteins	
Sodium dodecyl sulfate (SDS)		Effectively removes nuclear remnants and cytoplasmic proteins from dense tissues, tends to disrupt ultrastructure, removes gag and growth factors and damages collagen
Sodium deoxycholate (SDC)		Mixed results with efficacy dependent on tissue thickness, some disruption of ultrastructure and removal of GAG

Table 5: Summary of the different decellularization agents and techniques (Boccafoschi et al. 2017a; Crapo et al. 2011; Kawecki et al. 2018). *Continued on next page.*

Agent/technique	Mode of action	Effects on ECM
Triton X-200		More effectively removes cells from thin tissues but with greater disruption of ultrastructure compared to other detergents
Zwitterionic detergents	Exhibit properties of non-ionic and ionic detergents	
3-[(3-cholamidopropyl)dimethylammonio]-1-propanesulfonate (CHAPS)		Effectively removes cells with mild disruption of ultrastructure in thin tissues
Sulfobetaine-10 and -16 (sb-10, sb-16)		Effectively removes cells with mild disruption of ultrastructure in thin tissues
Biologic agents, enzymes		
Nucleases	Catalyzes the hydrolysis of ribonucleotide and deoxyribonucleotide chain	Difficult to remove from tissue, could invoke an immune response
Trypsin	Cleaves peptide bonds on the c-side of Arg and Lys	Prolonged exposure can disrupt ECM ultrastructure, removes ECM constituents such as collagen, laminin, fibronectin, elastin, and gag, compared to detergents, as lower gag removal
Dispase	Cleaves specific peptides, mainly fibronectin and collagen iv	Prolonged exposure can disrupt ECM ultra-structure, removes ECM constituents such as fibronectin and collagen IV
Collagenases	Cleaves specific collagen groups	Disruption of ECM structure, removes collagen
Others		
Chelating agents (EDTA, EGTA)	Typically used with enzymatic methods (e.g., trypsin) but can be used with other agents; ineffective when used alone	Chelating agents bind metallic ions, thereby disrupting cell adhesion to ECM
Techniques to apply agents		
Agitation	Can lyse cells, but more commonly used to facilitate chemical exposure and removal of cellular material	Aggressive agitation or sonication can disrupt ECM
Pressure gradient across tissue	Facilitates chemical exposure and removal of cellular material	Pressure gradient can disrupt ECM

Table 5: Summary of the different decellularization agents and techniques (Boccafoschi et al. 2017a; Crapo et al. 2011; Kawecki et al. 2018). *Continued on next page.*

Agent/technique	Mode of action	Effects on ECM
Supercritical fluid	Pressure can burst cells, supercritical fluid facilitates chemical exposure and removal of cellular material	Pressure necessary for supercritical phase can disrupt ECM
Perfusion	Facilitates chemical exposure and removal of cellular material	Pressure associated with perfusion can disrupt ECM

Table 5: Summary of the different decellularization agents and techniques (Boccafoschi et al. 2017a; Crapo et al. 2011; Kawecki et al. 2018)

More specifically, Table 6, summarizes the influences of the different decellularization methods on blood vessel tissue engineering.

Mechanical properties	Decellularization agent	Treated vessel	Effect on mechanical property with respect to native tissue
Compliance	Deoxycholate	Porcine carotid artery, abdominal aorta	No effect (Murase et al. 2006; Pellegata et al. 2013)
	SDS	Ovine carotid artery	Decrease (Mancuso et al. 2014)
	Trion X-100	Ovine carotid	No effect (Mancuso et al. 2014)
Young's modulus	Deoxycholate	Porcine carotid artery, abdominal aorta	No effect (Pellegata et al. 2013)
	Triton X-100	Bovine jugular vein	Decrease (Lü et al. 2009)
	SDS	Human umbilical vein	No effect (Abousleiman et al. 2008)
Stress-strain curves	Triton X-100	Porcine carotid artery	Increase of stiffness (Sheridan et al. 2012)
	SDS+EDTA	Porcine thoracic aorta	No difference (Zou and Zhang 2012)
	Triton X-100 + EDTA	Porcine thoracic aorta	No difference (Zou and Zhang 2012)
	Trypsin + EDTA	Porcine thoracic aorta	No difference (Zou and Zhang 2012)
	SDS + NaN ₃	Canine aortic arch	No difference (Weymann et al. 2014)
Burst pressure	Trypsin + EDTA + SDS	Fetal pig aorta, human saphenous vein, human umbilical artery	No difference (Chen et al. 2013; Liu et al. 2008; Schaner et al. 2004)

Table 6: Influence of different decellularizing methods on blood vessel substitutes mechanical properties (Boccafoschi et al. 2017b).

Even though decellularized matrices have proved to be a very interesting material to use as scaffold for tissue engineering, they present some major flaws given by their poor mechanical properties. To give these materials mechanical properties similar to those of the native tissue some chemical crosslinkers can be used. It is necessary to evaluate that the crosslinker is not toxic and make sure that its use does not adversely affect the bio-tissue's performance. The most commonly used crosslinkers are summarized in Table 7.

Agent	Advantages of Cross-Linking Reaction	Disadvantages of Cross-Linking Reaction
Glutaraldehyde	Amphipathic agent, ECM, stable and resistant to chemical and enzymatic degradation	Polymerization in aqueous solutions, depolymerization in the body of the recipient, untimely calcification, cytotoxicity, immune response, incomplete endothelialization
Formaldehyde	Sterilizing properties, reduction of the immune response	Reversibility of the crosslinking reaction, biomaterials unstable
Glycero diglycidylether	Forms multiple bonds, exhibits low cytotoxicity and reduced calcification	Material less elastic
Hexamethylene diisocyanate (HMDI)	A bifunctional reagent of reduced calcification, low cytotoxicity, high elasticity and scaffold durability	Susceptibility to enzymatic degradation
Acyl azide	High material stability, low cytotoxic effect, thermal resistance	No data
Dimetyloimido-suberynian (DMS)	High bioprosthesis flexibility, no calcification	Cytotoxicity
Genipin	Low biomaterial immunogenicity, low cytotoxicity and calcification, resistance to enzymatic degradation	No data
Tartaric acid	Possible application to the preparation of biomaterials with different stability, low immunogenicity and cytotoxicity	No data
Tanic acid	High stability of biomaterials degrade, low cytotoxicity, biomaterial with morphology very well preserved	No data

Table 7: Selected crosslinking agents and their influence on properties of biomaterials (Kawecki et al. 2018).

1.5 Clinical trials of vascular tissue engineering

Regarding clinical trials for vascular tissue engineering some major concerns must be kept in mind. Firstly, some surgical issues must be evaluated: the type of treatment given before, during and after the surgical procedure, the diameter of the prosthesis which must be identical to that of the native tissue, and the type of prosthesis control used. Secondly, the best results come from animal trials carried out using xenograft prosthesis. Table 8 summarizes the most significant clinical trials.

Author	Tissue Source	Recellularization	Cell Type	Bioreactor	Cell Number or Density	Animal model	Patency Rate (%)	Histology (Endothelialization /Remodeling)
Decellularized Cell-based TEVGs								
Quint (2011)	TEVG from allogenic SMC	Yes	Autologous EPC or EC	15 dynes/cm ² for 24 h	2 x 10 ⁵ /cm ²	Porcine carotid artery (end to side; iv. heparin 100 IU/kg)	100% at 30 days; (control 16,7%)	Less intimal hyperplasia and fewer cell infiltration
Dahl (2011)	Polyglycolic acid with human or canine SMCs	Yes	Canine EC (for small diameter graft)	?	?	Baboon AV shunt (large diameter); Canine peripheral artery (small diameter)	88% up to 3 months in baboon; 83% up to 1 month in dog	No dilatation, calcification and intimal hyperplasia; Endothelialization at both near anastomotic sites and midgraft in both grafts. SMC infiltration by 6 months in baboon model and by 1 month in canine model. No significant collagen degradation; Mechanical robust
Syedain (2014)	TEVG from Ovine fibroplast/Fibrin gel	No	No	No	No	Ovine femoral artery	?	Endothelialization was complete by 24 weeks with elastin deposition evident; No evidence of dilatation or mineralization. Mid-graft lumen diameter was unchanged; Extensive recellularization occurred, with most cells expressing α -SMA
Tondreau (2016)	TEVG from human fibroplast	No	No	No	No	Rat abdominal aorta	83,3% at 6 months	Neointima (ECs) and neomedia (SMCs) at 6 months
Syedain (2017)	TEVG from human fibroplast/fibrin gel	No	No	No	No	Baboon axillary- cephalic; axillary-brachial (antiplatelet)	83% and 60% at 3 and 6 months	No calcifications, loss of burst strength, or outflow stenosis; Developing endothelium at lumen and SMCs
Hybrid decellularized vascular graft								
Hinds (2006)	TSIS / Fibrin / Elastin	No	No	No	No	Porcine carotid artery	?	Significantly longer average patency times than ePTFE; Low thrombogenicity; Cellular repopulation
Row S (2016)	SIS / fibrin gel	Yes	Allogenic EC+SMC	5 rpm	2x10 ⁶ cells / mL, 5 mL / graft	Ovine carotid artery (iv heparin 100 IU/kg)	100% at 3 months (control EC only: 100%)	Cell infiltration at whole layer; Extracellular matrix mature and remodel into functional SMCs; Contractile function+
Gong (2016)	Rat aorta/ Polycaprolactone	No	No	No	No	Rat abdominal aorta (end-to-side; iv. heparin 300 IU/kg)	100% at 6 weeks	No evidence of stenosis and thrombosis; Fiber structure intact; Endothelialization+, SMA+; Reduce extravascular inflammatory cell infiltration
Negishi (2017)	Porcine aorta/ fibrin gel	No	No	No	No	Rat carotid artery	100% at 3 weeks	Cell attachment at luminal surface and cell infiltration at luminal wall

Table 8: Summary of *in vivo* performance of variant decellularized vascular grafts since 2001 (Lin et al. 2018).

1.6 Industrialization process

The scale-up/industrialization process is part of a more complex process of technology transfer from the laboratory to an industrial scale. Scale-up enters into the science of chemical engineering and it attempts the obtaining of a product in the laboratory with the same characteristics and performance as a larger scale production. Also, other processing factors, such as the reproducibility of the process or its control need to be considered. From the normative point of view, in the specific case of the biomedical field, issues such as sterility and the laws that affect these products are important to study throughout the production cycle, from raw materials to the production environment and the chain of material transport. The whole process must be optimized, not only from an engineering point of view but also from an economic point of view, which will be reflected in the economic feasibility study.

In this context, due to the product's origin, it is important to define decellularization, this has been introduced and further explored by Badylak et al. who introduced the criteria which were later introduced in the regulation concerning these kinds of products. These criteria are: (1) complete absence of visible nuclear material upon histological examination (haematoxylin and eosin and 4'-6-diamidino-2phenylindole (DAPI) stains); (2) less than 50 ng of dsDNA per mg ECM dry weight; and (3) remnant DNA molecules shorter than 200 bp (Crapo et al. 2011). In addition to these criteria, others have been added in order to transfer this into an industrialized process, these include: the lack of intracellular membrane compartments (e.g., mitochondria), the lack of cell membrane elements, the presence of unremoved and undamaged ECM elements (collagen, GAG, fibronectin, etc.) the lack of cytotoxicity of the obtained ECM scaffold (Kawecki et al. 2018).

Moreover, in order to be able to produce commercialized products, the medical devices must undergo a sterilization process. In this context, depyrogenation is a mandatory method which eliminates endotoxins, intact viral DNA and bacterial DNA that may be present. For all this, biological security requires a final sterilization of the tissues prior to clinical application and the usual sterilization procedures include ethylene oxide, peracetic acid, slightly acidic electrolyzed water, gamma irradiation, electron beam irradiation, and supercritical CO₂.

Acids and solvents exhibit insufficient penetration through the material and could change the mechanical properties because they have crosslinking tendencies (Gorschewsky et al. 2005; Hodde and Hiles 2002; Matuska and McFetridge 2015-02). Peracetic acid is the most prevalent due to its GAGs preservation, DNA removal efficiency and the ability to maintain collagen's mechanical integrity.

The use of ethylene oxide as a sterilization agent is controversial. Some *in vitro* results show that its use does not affect the cell attachment to ECM or the stimulation of growth factors' secretion by fibroblasts (Hodde et al. 2007). On the other hand, it is classified as a mutagen and as a carcinogen and its elimination is crucial to obtain a secure implantable product. The use of ethylene oxide for terminal sterilization of biologic scaffolds should be considered carefully.

Gamma irradiation exposure is a standard sterilization process, however, dosages lower than 15 kGy increase the strength and modulus of the ECM due to the collagen cross link (this phenomenon occurs even at 5 kGy doses) but, at higher dosages it proportionally changes the tissue properties. Gamma irradiation also causes a negative effect on the ability of cells to attach to the ECM *in vitro* (Matuska and McFetridge 2015-02), the residual lipids to become cytotoxic and it accelerates enzymatic degradation (Moreau et al. 2000-02). Nonetheless, many authors recommend sterilization by gamma radiation or electron beam radiation as an effective and safe sterilization process (Dziedzic-Goclawska et al. 2005; Nguyen et al. 2007).

Supercritical carbon dioxide (SC-CO₂) is already studied as a decellularization method and recently its application in the sterilization phase has obtained satisfactory results in terms of non-toxicity residues and minor changes in mechanical properties when compared with other sterilization methods (Donati et al. 2012; Qiu et al. 2009). However, some works evidence negative impacts on the structure and function of ECM proteins (Wimmer and Zarevúcka 2010).

1.6.1 Clinical products

Now, several clinical products composed of ECM are available in the market. The allogenic or xenogeneic tissue sources are dermis, urinary bladder, small intestine, mesothelium, pericardium, and heart valves, and from several different species. The

applications of these biomaterials include, for example, hernia reconstructive surgery, soft tissue augmentation, breast reconstruction, and wound healing. Table 9 shows available commercial products composed of decellularized tissues. In USA, the FDA classifies these products, such as medical devices, which require to apply the guidelines regarding bacterial load regulated by ISO/DIS 1135-1, ISO/DIS 1137-1 rules (Keane et al. 2015).

Product (Manufacturer)	Tissue Source	Application focus
Cor [™] Patch [®] (Cardiovascular Inc.)	Porcine small intestine	Pericardium, cardiac tissue
Perimount [®] (Edwards Lifesciences LLC)	Bovine pericardium	Valve replacement
Hancock [®] II, Mosaic [®] , Freestyle [®] (Medtronic Inc.)	Porcine heart valve	Valve replacement
Magna Mitral Ease (Edwards Lifesciences LLC)	Porcine heart valve	Valve replacement
Epic [™] , SJM Biocor [®] (St. Jude Medical Inc.)	Porcine heart valve	Valve replacement
Omniflow [®] II (LeMaitre Vascular Inc.) *Not approved for sale in the United States	Cross-linked ovine collagen	Peripheral revascularization, Arteriovenous fistula (AV access)
Organic Arterial Tubular Graft (Braile Biomedica)	Bovine pericardium	Aneurysm reconstruction or aneurysmatic diseases
Artegraft [®] (Artegraft Inc.)	Bovine carotid artery	AV access
CryoGraft [®] (CryoLife Inc.)	Human descending aorta	Aneurysm reconstruction
ProCol [®] (LeMaitre Vascular Inc.)	Bovine mesenteric vein	AV access
CryoArtery [®] (CryoLife Inc.)	Human femoral artery	Peripheral revascularization, AV access
Oasis [®] (Cook Biotech, Inc., Indiana, USA)	Porcine small intestinal submucosa	Management of wounds pressure ulcers, venous ulcers, chronic vascular ulcers, trauma wounds (abrasions, lacerations, second-degree burns, skin tears), draining wounds, surgical wounds

Table 9: Available commercial decellularized products. *Continued on next page.*

Product (Manufacturer)	Tissue Source	Application focus
GraftJacket [®] (Acelity L.P. Inc., Texas, USA)	Acellular human dermis	Repair or replacement of damaged or inadequate integumental tissue
DermACELL [®] (Stryker Global Headquarters 2825 Airview Boulevard Kalamazoo, MI 49002 USA)	Acellular human dermal matrix	Chronic wounds and soft tissue reconstruction
Alloderm [®] (Allergan plc [NYSE: AGN, Dublin, Ireland])	Human dermis	Breast reconstruction post mastectomy
Strattice [™] (Allergan plc [NYSE: AGN, Dublin, Ireland])	Porcine dermis	Abdominal wall repair, damaged soft tissue
AlloSkin [™] AC (AlloSource, Centennial, CO, USA)	Decellularized human dermis	Wound healing
MatriStem [®] (ACell, Columbia, USA)	Porcine Urinary Bladder Matrix	Wound healing and care, surgical repairs
Biodesign [®] (COOK MEDICAL INC., Bloomington, IN, USA)	Porcine small intestine submucosa	Soft tissue, hiatal hernia
Lyoplant [®] (Aesculap, Inc., Center Valley, PA, USA)	Bovine pericardium	Dura mater substitutes in neurosurgery
AlloPatch HD [™] , FlexHD [®] (Musculoskeletal Transplant Foundation)	Human acellular dermis	Tendon, breast
Strattice [™] (Lifecell Corp.)	Porcine dermis	Soft tissue
Zimmer Collagen Repair Patch [™] (Zimmer Inc.)	Porcine dermis	Soft tissue
TissueMend [®] (Stryker Corp.)	Fetal Bovine dermis	Soft tissue, tendon repair surgery
FortaFlex [®] , BioSTAR [®] (Organogenesis Inc.)	Porcine small intestine	Soft tissue and cardiac applications
Meso BioMatrix [™] (Kensey Nash Corp.)	Porcine mesothelium	Soft tissue, wound healing
CopiOs [®] (Zimmer Inc.)	Bovine pericardium	Dentistry, bone healing
Lyoplant [®] (B. Braun Melsungen AG)	Bovine pericardium	Dura mater
Biodesign [®] ; Cook Medical, Bloomington, IN	Porcine small intestine submucosa	Hiatal Hernia

Table 9: Available commercial decellularized products. *Continued on next page.*

Product (Manufacturer)	Tissue Source	Application focus
MIRODERM [®] ; (Miromatrix Medical Inc., Eden Prairie, MN)	Porcine liver	Wound management; venous ulcers, vascular ulcers
MIROMESH [®] (Miromatrix Medical Inc., Eden Prairie, MN)	Vascularized Porcine Liver	Soft tissue repair or reinforcement
SynerGraft [®] (CryoLife Inc.)		Decellularization technology for implantable biological tissues

Table 9: Available commercial decellularized products.

The success of ECM clinical products, confirmed by more than 20 years of commercialization (Guruswamy Damodaran and Vermette 2018), opens the door for developing functional organs to reduce the number of patients awaiting life-saving transplants (Taylor et al. 2018). Some companies, like Miromatrix Medical Inc. (Eden Prairie, Minneapolis) a USA-based biotechnology company or AxoGen Inc. (Alachua, Florida) from USA, are developing decellularized liver, kidney and nerve connectors. Humacyte Inc. (Morrisville, North Carolina), develops acellular grafts to repair vascular damages. Some of their products are under phase III clinical trials (Guruswamy Damodaran and Vermette 2018).

Focusing on currently decellularized vascular grafts on the market, such as Artegraft[®], Solcograaft, ProCol[®], and SynerGraft[®] reported in Table 9, most of them are used for vascular access during hemodialysis or peripheral arterial bypass.

Although already on the market, their performances are not satisfactory due to graft-related thrombosis, infection, and aneurysm. For this reason, currently decellularized xenogeneic grafts offer only non-inferior results compared with alternative synthetic conduits. High cost, when compared with synthetic grafts, and their low performances, entails that they have not been widely used in the clinic (Pashneh-Tala et al. 2016).

For these reasons, there is a continuous pursuit on the application of decellularized ECM in small-diameter vascular tissue engineering. These studies evaluate matrices obtained from human umbilical veins and arteries, porcine’s arteries like the carotid,

the radial, the saphenous, the iliac, the small intestine submucosa and the bovine ureter (Lin et al. 2018).

1.6.2 Regulation aspects

The biological scaffolds commercialized reported on the Table 9 are marketed under the category of 510(K) of the FDA, for the USA market, or under CE medical devices class III category for European market. The EU commission regulation N0 722/2012 of August, 8th, 2012 concerning particular requirements laid down in Council Directives 90/385/EEC and 93/42/EEC with respect to active implantable medical devices and medical devices manufactured utilizing tissues of animal origin, has adopted a regulation based on: the original requirements, and the maintenance of a high level of safety and health protection against the risk of transmitting animal spongiform encephalopathies.

The regulation also considers that the active implantable medical devices and medical devices of class III are subject to the conformity assessment procedures, prior to being placed on the market or put into service, demanding the adoption of more detailed specifications relating to the risk analysis and management.

Regulation establishes requirements in relation to the placing on the market and/or putting into service of medical devices, including active implantable medical devices, manufactured utilizing animal tissue and their derivatives, originating from bovine, ovine and caprine species, deer, elk, mink and cats. In the case of collagen, gelatin and tallow used for the manufacturing of medical devices shall meet at least the requirements as fit for human consumption.

The regulation also establishes that the manufacturer of medical devices or his authorized representative shall carry out the risk analysis and risk management scheme before lodging an application for a conformity assessment.

Conformity assessment procedures for medical devices shall include the evaluation of compliance of the devices with the essential requirements into the current directives and the requirements laid down in this Regulation.

The new two European Health Products Regulations came into force on May, 26th,

2017. The first one, the Regulation (EU) 2017/745 of medical devices, which modifies Directive 2001/83/EC and subsequent derived regulations, repealing Council Directives 90/385/EEC and 93/42/EEC, will be applicable from May, 26th, 2020. The second one, Regulation (EU) 2017/746 of *in vitro* medical devices, which repeals both Directive 98/78/EC and the decision of the commission 2010/227/EU, it will be applicable from May, 26th, 2022.

This is the detail of some of the most important changes and novelties contained in the Sanitary Products Regulation:

- **Transitional period:** Since a transitional period of three years is expected from its entry into force, since May, 26th 2017, and until May, 26th, 2020, both regulatory frameworks may coexist and certificates may be issued in accordance with the provisions of the new Regulation or the old Directives 90/385/EEC and 93/42/EEC. In the latter case, the certificates will have a maximum validity of 5 years and they will be considered invalid as of May, 27th, 2024. In any case, any product introduced on the market in accordance with the requirements of the old Directives can only continue to be marketed or be put into service until May, 27th, 2025.
- **Specification of the definition of health products:** The definition of "health product" is specified and defined. The definition includes clearly computer programs, implants or reagents, and establishes the need that the manufacturer has foreseen a specific medical purpose. In addition, the Regulation clarifies that sanitary products, "control products or support for conception", as well as products specifically intended for cleaning, disinfection or sterilization of medical devices and their accessories are within the scope of this Regulation.
- **Reinforcement of guarantees in all stages:** The pre-commercialization and post-marketing guarantees of medical devices are reinforced. In relation to pre-commercialization guarantees, the role of the European Commission of categorizing and classification of products is increased, and it should no longer be limited to action if a Member State previously requests it, but it must do so *ex officio*. For this purpose, the Member State will count on the help of a Coordination Group of Health Products with European experts.

- Increased transparency and traceability: New measures are introduced aimed at increasing transparency and traceability:
 1. A European Union Global Database (EUDAMED) for medical devices is created, a European portal that is essential for the practical application of the Regulation since it must include the new electronic systems created by the Regulation: the electronic registration system of products, the Unique Product Identification (UDI) database, the electronic system for registering economic agents, the monitoring and post-marketing monitoring system and the electronic market control system. This database must be up and running by March, 25th, 2020.
 2. The Product Registry is created and the Unique Product Identification system (UDI) is established to guarantee the traceability of the products at any time, which obliges manufacturers to assign and maintain an UDI for all their products.
 3. The Registry of economic operators is created in which all manufacturers, authorized representatives and importers must register before introducing a sanitary product on the market.
 4. All manufacturers of implantable products are obliged to accompany the implant card product and information that allow the identification of the product, the warnings or measures that the patient or health professional must take, and the regulation also obligates the Member States for demanding health centers to provide the mentioned card and the required information to patients.
- Definition of obligations of the economic operators: The obligations and responsibilities of each one of the economic agents that were not sufficiently detailed in the previous regulation, are here specified in detail; forcing manufacturers to establish a quality assurance system, a system to obtain and review data after commercialization of products, to establish measures to offer sufficient financial coverage adapted to the type of risk, type of product and size of the company, as well as having a technician responsible for compliance with the regulations, who may be trained in law, medicine, pharmacy, engineering or other scientific

discipline, and one year of professional experience in regulatory matters or in quality management systems related to medical devices.

Taken all together, several aspects are important from the product performances point of view, for example cytotoxicity, sensitization, haemocompatibility (hemolysis, thrombogenicity), pyrogenicity, implantation, genotoxicity, carcinogenicity, reproductive and developmental toxicity, degradation assessments. However, other aspects are crucial for the industrialization process or processability. In particular, low manufacturing costs, availability of large variety of lengths and diameters, stability after sterilization processes, and ease storage are all essential details to obtain a valuable commercial vascular substitute. Government regulations must be considered during all the process. All these parameters were contemplated in this project.

1.7 Thesis outline

The purpose of this thesis was to obtain the prototype of a small caliber vascular prosthesis for its application in damaged vascular tissue substitution. For the *in vitro* performance experiments, specific reactor has been designed, these are meant to recreate physiologically relevant environment condition, optimal for these tests. The characterization will be performed *in vitro*, for both mechanical and biological tests, and the *in vivo* experiments are also presently running. When significant results will be reached the preclinical trial of the product will be complete.

Concerning the industrialization part, an economic estimation will be presented in the BP, this will allow to confirm the availability of the project. Moreover, the pre-engineering of the industrial production reactor, which is based on experimental design parameters, will guarantee the performances of the prototype characterized in the laboratory.

The future perspectives concern the *in vivo* study of the scaffold. The possibility to use the same crosslink technique, increasing the crosslinking agent concentration in the final treatment step, was also evaluated. The goal of this protocol variant is to modify the mechanical properties of the scaffold in order to have a possible application as an arteriovenous fistula in hemodialysis treatment.

2 Materials and methods

2.1 Decellularization process

Porcine femoral and carotid arteries, provided by Life and Device S.r.l. (Turin, Italy), have been decellularized with a three-step protocol. In summary, the vessels have been treated with a 1 M NaCl, 0,8 mM CHAPS and 2,5 mM EDTA solution for 1 hour at 37 °C under stirring. After prolonged PBS rinsing, the matrices have been treated with a second solution of 1 M NaCl, 18 mM SDS and 2,5 mM EDTA for 1 hour at 37 °C under stirring. Finally, in order to completely remove the residual DNA content, samples have been treated with a solution of 6,4 μ M Deoxyribonuclease I from bovine pancreas (Sigma-Aldrich, USA), 0,1 M MgCl₂, and 0,9 M NaCl, and stirred for 16 h at room temperature. The decellularized vessels have been stored at -20 °C before use.

2.1.1 Functionalization of the decellularized biologic tissue (sueGraft[®] process)

Decellularized matrices have been enriched with 1 mg/ml polylysine (Sigma-Aldrich, USA). The process (sueGraft[®]) used was optimized by TissueGraft S.r.l., all details are owned by the company.

To evaluate the efficiency of the enriching process, three different matrices were compared:

1. Native vessel
2. Decellularized matrix
3. Polylysine grafting: decellularized matrix subjected to the enrichment process

2.1.2 Evaluation of the decellularization procedure

In order to verify the efficiency of the decellularization process, several analyses were performed (Wolf et al. 2012), including histology to evaluate the absence of cellular material using 4', 6'-diamidino-2-phenylindole dihydrochloride (DAPI) and hematoxylin and eosin (H&E) staining. For the nuclear staining analysis (DAPI), samples were

fixed in a 4% formaldehyde solution, then rinsed in PBS and soaked in DAPI solution (300 nM for 2 minutes). After an additional PBS rinsing, samples were observed under a fluorescence microscope.

For H&E staining, samples were fixed in 4% formaldehyde solution, dehydrated and paraffin embedded. Samples were then cut into sections of 5 μm , rehydrated and soaked in hematoxylin for 15 minutes. Following this, eosin solution (0,05% eosin in distilled water and acetic acid) was applied for 1 minute. Finally, samples were dehydrated and observed with an optic microscope (Leica DM2500, Leica, Germany). Samples images have been acquired through a Leica DFC7000 T camera (Leica, Germany) and analyzed with Leica Application Suite X software (Leica, Germany).

In addition, the amount of DNA in each sample was also quantified through a DNA quantification assay. Native and decellularized vessel slices (5x5 mm) were lyophilized and digested for 16 h at 55 °C in a buffer solution, containing 100 $\mu\text{g}/\text{ml}$ proteinase K, 75 mM NaCl, 25 mM EDTA, 1% SDS, pH=8. Samples were incubated with a 6 M NaCl solution for 30 minutes and centrifuged at 15.000 rpm; followed by 1 mL of isopropanol. In order to precipitate the DNA after centrifugation, the supernatant was removed, and 70% ethanol added. After evaporation of ethanol, 20 μL of ultrapure water was added and the amount of DNA measured with full-spectrum UV-visible measurements (NanoDrop 2000, Thermo Fisher Scientific, USA).

Finally, agarose gel electrophoresis was used to visualize the DNA fragmentation. Briefly, 50 ng of DNA from native and decellularized samples were mixed with EZ-Vision loading buffer (VWR, Italy), and loaded on a 1% agarose gel. After the electrophoresis, DNA was visualized with ChemiDoc Imaging System (BioRad, Italy).

2.2 Enrichment process assessment and morphological analysis

2.2.1 X-ray Photoelectron Spectroscopy (XPS)

XPS analysis was conducted with a Perkin Elmer PHI 5600 ESCA system. The instrument is supplied with a dual Al (monochromatic) and Mg anode operating at 10 kV and 200 W. The diameter of the analyzed spot was about 500 μm , the sampling

depth was 5–8 nm, and the base pressure 10^{-8} Pa. The angle between the electron analyzer and the sample surface was 45 degrees.

After preliminary evaluation using the monochromated X-ray source, spectra were acquired using the non-monochromated Mg anode, given side-effects due to charging were much lower. Analysis was conducted acquiring wide range survey spectra (0 to 1.000 eV binding energy) and detailed high-resolution peaks of relevant elements.

Quantification of elements was completed using the software and sensitivity factors furnished by the manufacturer.

2.2.2 Attenuated Total Reflectance Infra-red spectroscopy (ATR-IR)

ATR-IR spectra were obtained using a Nicolet iS10 ATR-IR spectrometer with a diamond crystal (Thermo Fisher Scientific, USA). Samples were placed on the crystal and held steady by the specific crimping tool. The experimental set up involved acquisition of 32 scans in the range $500\text{--}4.000\text{ cm}^{-1}$, both of sample and background, at a resolution of 4 cm^{-1} with the sampling depth is approximately $1,6\text{ }\mu\text{m}$. Beside decellularized and polylysine-enriched samples, the ATR-IR spectrum of polylysine (Sigma-Aldrich, USA) was acquired as a reference.

2.2.3 Confocal microscopy

The microscopy visualization of the structures was completed using a Leica TCS SP8 DLS (Digital LightSheet, CLF, Harwell, UK) system with image acquisition technical information as shown in Table 10. The focus of this tool was the observation of the scaffold collagen structures under static conditions. Samples were not stained but fixed in situ with agar to immobilize the sample during the test.

	A	B	C	D
Field of view	1471, 52 μm x 1471, 52 μm	1471, 52 μm x 1471, 52 μm	735, 76 μm x 735, 76 μm	735, 76 μm x 735, 76 μm
Number of spaced steps	127 steps spaced of 6 μm	212 steps spaced of 6 μm	394 steps spaced of 1, 5 μm	342 steps spaced of 1, 5 μm
Illumination laser	405 nm	405 nm	405 nm	405 nm
Laser power	25 μW	25 μW	25 μW	25 μW
Exposure time per plane	600 ms	600 ms	300 ms	600 ms
Bandpass detection filter	504 – 545 nm	504 – 545 nm	504 – 545 nm	504 – 545 nm
Detection objective	HC PL FLUOTAR 5x/0,15 IMM	HC PL FLUOTAR 5x/0,15 IMM	HC APO L 10x/0,30 WATER	HC APO L 10x/0,30 WATER
Illumination objective for light sheet creation	1,6x/0,05 DRY	1,6x/0,05 DRY	HC PL FLUOTAR 2,5x/0,07 DRY	HC PL FLUOTAR 2,5x/0,07 DRY

Table 10: Technical data of confocal images.

2.2.4 Micro Computed Tomography (Micro-CT)

A micro-CT system (High Flux Nikon XTEK Bay, Manchester X-ray Imaging Facility (MXIF)) was used to non-destructively image and visualize the three-dimensional micro-morphology as previously described (Disney et al. 2017; Metscher 2009). Staining method used was 1% (w/v) phosphotungstic acid, $H_3PW_{12}O_{40}$ (PTA) in water for 40 h followed by washing in 70% ethanol and dried for 48 h at room temperature.

Samples were mounted on a stage within the imaging system and subsequently scanned at a voltage of 100 kV and a current of 50–100 mA. Specimens were scanned at a 2 μm resolution with an integration time of 1.000–1.400 ms to produce 3D images. Raw 2D images were thresholded to remove background values (threshold value = 60) and further analyzed using Avizo software (Thermo Fisher Scientific, USA) (Walton et al. 2015).

2.3 Mechanical test

Mechanical properties of native and decellularized enriched matrices were tested. The Young's modulus and tensile strength of the different samples was measured, briefly, Young's moduli were quantified from the stress-strain curve obtained with the Instron 5564 (Instron Corporation, Massachusetts USA). System control and data analyses were performed using Instron[®] Bluehill[™] 3 material-testing software (Instron Corporation, Massachusetts USA). Sample dimensions (length, width and thickness) were measured in order to normalize the mechanical test parameters. Uniaxial tests were performed at room temperature and with a tension rate of 0,5 mm/s.

Burst pressure was also measured. The test was performed using a hydraulic press, a high-precision digital pressure gauge and a PBS solution as a liquid. The sample was stressed by pushing the PBS until bursting, thus detecting the maximum operating pressure in laboratory conditions.

Mechanical properties were also evaluated after simulation of physiological conditions (dynamic condition test). Decellularized and polylysine-enriched vessels have been inserted in a circuit, composed of a peristaltic pump (Masterflex L/S, Cole-Parmer instrument Company, USA), 10 mm diameter tubing (Cole-Parmer instrument Company, USA), and a chamber containing the samples and filled with the PBS. Fluid speed was 15 mL/min and samples were tested for up to 30 days. Samples were weighed before and after the dynamic test in order to evaluate the samples' weight loss after dynamic conditions were applied. Finally, both Instron and burst pressure tests, were performed after dynamic conditions.

2.4 Cell viability assay

Cell viability of human umbilical vein endothelial cells EA.hy926 (ATCC[®] CRL-2922[™]), cultured on decellularized and enriched matrices, was assessed. Cells were cultured with Dulbecco's Modified Eagle's Medium (DMEM – Euroclone, Italy) enriched with 10% fetal bovine serum (FBS), 2 mM glutamine and 100 U/mL penicillin (Euroclone, Italy). Endothelial cells were cultured at $5 \cdot 10^4$ cells/cm². In order to evaluate cell viability, after 1, 3, and 7 days of culture, a MTS assay (CellTiter 96[®]

Aqueous Non-Radioactive Cell Proliferation Assay, Promega, Italy) was performed. Briefly, a 3-(4,5-dimethylthiazol-2-yl)-5-(3-carboxymethoxyphenyl)-2-(4-sulfophenyl)-2H-tetrazolium solution was added to each sample for 3 h. Absorbance was measured by UV-VIS spectrophotometry (V-630 UV-Vis Spectrophotometer, Jasco, USA), at a wavelength of 490 nm. Measures were proportional to cell viability.

In order to evaluate cell adhesion and proliferation, EA.hy926 cells were cultured on decellularized and polylysine enriched matrices for 3 and 7 days. Matrices were then observed through Hematoxylin-eosin staining, as described in Section 2.1.2.

Cell adhesion was evaluated after simulation of physiological conditions (dynamic condition test). In this purpose, a bioreactor was designed and printed in 3D to reproduce conditions as similar as possible to physiological ones, like gravity force and temperature.

EA.hy926 were cultured on the lumen side of decellularized and polylysine-enriched vessels for 24 hours. Afterwards, samples were inserted in a circuit, composed of a peristaltic pump (Masterflex L/S, Cole-Parmer instrument Company, USA), 10 mm diameter tubing (Cole-Parmer instrument Company, USA), and fixed to the bioreactor's structure. The bioreactor allows to create an external and internal flow in the vessel. In this case the external circuit didn't have a flow whereas, the internal vessel's flow was 15 mL/min. The fluid filled was DMEM enriched with 10% FBS and samples were tested for up to 3 days.

2.5 Haemocompatibility

Thromboelastography (TEG) is a technique that measures several parameters relative to blood coagulation by evaluating the viscoelastic properties of blood from the beginning of coagulation to the clot rupture with fibrinolysis. Particularly important parameters are the coagulation formation, its progression, maximum strength, and stability, which provides important information on coagulation, fibrinolysis, and platelet functionality. Blood samples were collected in Vacutainer (BD, USA) containing sodium citrate and tested at 37 °C. Blood was exposed to the control graft (Dacron[®]), the decellularized scaffold and the enriched scaffold for 30 minutes and subsequently analyzed using Thromboelastograph[®] (TEG[®] 5000 Thrombelastograph[®]

Hemostasis Analyzer System) and the Kaolin TEG standard protocol. Briefly, after 30 minutes 1 mL of blood was collected and placed in a vial containing kaolin. After few seconds, 340 μL of blood were sampled in the thrombelastograph with 20 μL of calcium chloride, in order to eliminate the anticoagulant effect of sodium citrate. Coagulation parameters were evaluated through thromboelastogram obtained at the end of the testing time.

2.6 Industrialization

According to the “Manual on Economic Development Projects” from the United Nations Economic Commission, there are several aspects to consider from the economic point of view in order to create the feasibility study of the plant, in particular the compilation of the study market, analysis of the current demand, projection and elasticity of demand, and product price estimation are the main features.

This document also evaluates the basic aspects of the project engineering, such as selection of the production process, specification of operating and assembly equipment, buildings and site and plant layout, supplementary equipment, flexibility of productive capability, work of schedules among others (Nations 1958).

The industrialization part developed for this project is a simplified part of the documents necessary for phase I of the project. It is composed of an economical part, which contains a BP, aiming to make a first assessment on the project feasibility, and an engineering part. In the latter part the installation core’s design, which is the production reactor, has been performed in order to guarantee the same performances of the laboratory’s prototype. Given the type of production process, it was considered necessary to include a table of the reactor’s operation cycles.

2.6.1 Business plan

The business plan is part of the feasibility study, which is important to preview and guarantee the success of the project’s industrial implementation.

The plant’s capacity estimation comes from the document “Vascular Grafts Market 2019 Industry Demand, Share, Global Trend, Industry News, Business Growth, Top

Key Players Update, Business Statistics and Research Methodology by Forecast to 2025” published by the company The Express Wire on May 2019 (Wire 2019).

Capital expenditures (CAPEX) includes the CE certification amount, comprising the preclinical and clinical trials, has been considered in the plant costs. The plant’s construction total cost is based on the following assumptions. The production plant has been inserted in an already existent production plant launching a new product line. This allows to lower the staff’s costs, since some workers can be shared with the already existing installation. In the same way, the aseptic environment production area will also be shared.

The implant can be realized in any EU country, since the legal aspects considered allow to obtain the CE certification and therefore the commercialization of the medical devices in the EU. Moreover, the economical parameters that were fixed to make an economic estimate are based on the Italian legislation, since the product was developed in Italy.

Operating expenses (OPEX) includes the production costs in terms of chemicals, electricity and wastewater production, derived from a balance of materials and energy of the plant.

In the BP the different financial parameters usually used in this kind of studies, like inflation rate, interest rate, and spread were considered over the operative duration time of the plant, which is 10 years.

The taxes considered to obtain the Net Cash Flow were applied in terms of the Italian legislation: Imposta sul reddito delle società (IRES), Imposta regionale sulle attività produttive (IRAP) and imposta municipale unica (IMU).

2.6.2 Reactor design

In order to obtain the design parameters of the reactor some experiments have been performed. The standard batch decellularization protocol used during the arterial scaffold prototype obtainment was taken as a reference, to establish a protocol suitable to produce the same product but on a larger scale.

The important parameters to determine are, not only the volume of liquid in con-

tact to the tissue, but also the different flow inside and outside the vessel. With this purpose a commercial bioreactor was used. To evaluate the efficacy of the different flows of the decellularization solution, cells removal through Hematoxylin-Eosin staining was analyzed. Once the volume to weight ratio has been fixed, a 30% increase was considered as a security factor in the reactor's design.

The parameters obtained were combined to fluid dynamics' basic principles related with adimensional numbers for scale the process. Specifically, for Reynolds (Re) number, a test was performed using a commercial reactor showed in Figure 6 (MiniBreath[®]) in order to determine the optimal flow for each phase of the treatment. The duration and flow have been optimized for each phase, which fixed the adequate conditions for mass transport phenomenon in the system, with the aim to optimize the process and preserve the material.



Figure 6: MiniBreath[®] commercial bioreactor.

The hydraulic circuit configuration is divided in two different circuits, one of them allows only vessel perfusion, while the second one feeds the solutions inside the culture chamber. In the inner path, the solution is drawn from an external reservoir thanks to a Harvard MPII[®] mini-peristaltic pump (Harvard Apparatus), it flows inside the MiniBreath[®] using a Pharmed BTP tubes, 1/16' (1,6 mm) ID, and then into the vessel before it goes back into the reservoir. In the outer path the action of a MasterFlex L/S[®] (Cole Parmer Instrumental Company) pump moves the fluid from the reservoir

to the culture chamber and back into the common reservoir using a Pharmed BTP tubes, 1/8' (3,2 mm) ID.

In this way, each process phase has a different flow rate to modify the Re number and consequently inertial force compared with the viscous one, in order to obtain an efficient treatment across the sample's wall thickness. Maximum inlet flow rate has been fixed using the physiological value to avoid the tissue damage, in this case the flow rate considered using a human popliteal artery, due to its similar characteristics, is 67 mL/min (Holland et al. 1998).

Removing the chemical residues is a very important aspect, due to the immunogenic response they may cause (Struecker et al. 2017), therefore, the reactor's design and production phases must be carefully evaluated, and the washing phase must be standardized and controlled. In this purpose, diffusion phenomenon is predominant in the washing steps in order to guarantee the complete removal of the detergent.

Re number represents the relationship between inertial and viscous forces. Focusing on the flow of the fluid inside a circular section pipe, at low Re (≤ 1.000) the viscous effects dominate, and the flow is laminar. At high Re (≥ 2.000), inertial forces govern the flow dynamic, which becomes turbulent.

Regarding the external circuit, some approximations have been made to calculate Re. Since the reactor chamber has a squared cross section it was approximated to a circular one. In this way, the configuration can be described as the flow of solution inside the annulus given by two coaxial cylinders. The chamber Re was calculated using the hydraulic diameter approximation due to the flow not flowing in a circular pipe.

The largescale production reactor was designed considering all the parameters obtained with the MiniBreath[®]. All the measures and dispositions of the different parts of the reactor will be specified in the attached design belonging to Chapter 3.6.2.

2.7 Ethics

Life and Device company was charged of both providing the porcine native arteries and of performing the *in vivo* studies which are running at the moment. This company

guarantees the compliance of the Directive 2010/63/EU of the European Parliament and of the Council of September, 22th, 2010 and the Decreto Legislativo March, 4th, 2014, n. 26 according with the Italian legislation.

3 Results

3.1 Decellularization process efficiency

In order to evaluate the efficiency of the decellularization protocol, DAPI staining was performed on native and decellularized tissue. Figure 7 shows the native tissue and the presence of cellular nuclei in native tissues while, after the decellularization treatment, however, no nuclei were present. H&E histology results confirmed the preservation of the ECM microstructure within the decellularized samples. No cellular nuclei could be detected in the decellularized tissue samples.

DNA quantification on native and decellularized tissues strengthened the previous results, indicating a successful DNA removal from the matrix. In contrast to native tissue, which contained 860 ± 300 ng DNA per mg wet weight ($n = 3$), decellularized tissues showed a significant decrease of DNA content to 15 ± 11 ng DNA per mg wet weight ($n = 3$). Agarose gel showed that no DNA strands longer than 100 bp were available on decellularized samples, while in native samples the DNA presence was verified.

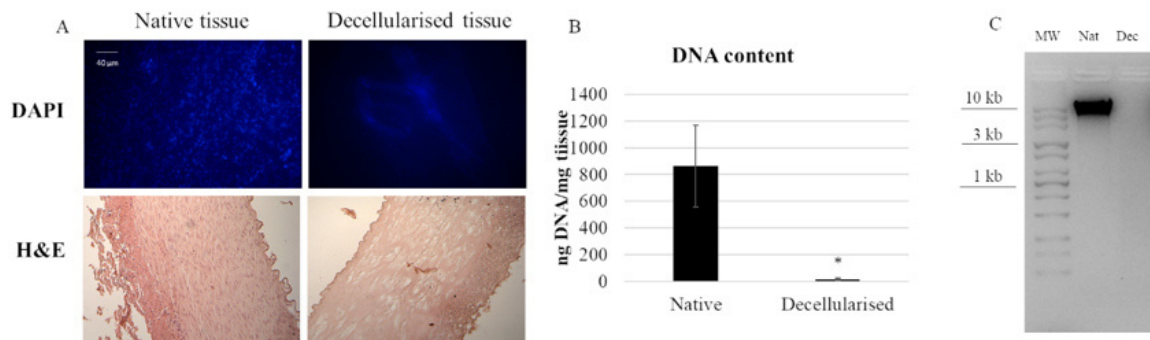


Figure 7: Decellularization of porcine artery showing A) DAPI and H&E histology before and after decellularization process. B) Quantitative determination of DNA in a native and decellularized matrix. Data are expressed as mean values \pm SD. ($n = 3$, $* = p \leq 0,05$). C) Agarose gel electrophoresis of DNA derived from native and decellularized matrices. The image is representative of three different analyses.

3.2 Enrichment process assesment and morphological analysis

Samples were analyzed, as shown in Figure 8 A and B, the survey spectra of decellularized and polylysine-enriched samples show differences, with the obtained surface composition reported in Table 11. Decellularized scaffolds showed peaks due to carbon, oxygen and silicon, and just a very weak signal from nitrogen. XPS tests just the outermost molecular layers of materials (the sampling depth is about 5–8 nm), and the obtained data likely reflects surface side-effects due to processing. Silicone is a common contaminant of surfaces and the peak of Si is a common finding in surface analysis of biological samples. There was also a lower than expected N/C and N/O ratio, which was probably due to processing aids (see also discussion of ATR-IR results) remaining on or combined with the sample surface. In contrast, the XPS spectrum of polylysine-enriched samples showed a strong peak due to nitrogen. Hence, the sample surface showed being enriched with a nitrogen-containing compound, clearly supporting the presence of polylysine. Further information was provided by ATR-IR analysis, as reported in the next section.

Sample	O	N	C	Si
Decellularized	17,1 ± 0,3	1,4 ± 0,1	68,4 ± 0,3	13,1 ± 0,5
Polylysine	16,7 ± 0,2	11,3 ± 0,4	72,0 ± 0,4	–

Table 11: Surface composition (atomic %) of tested samples ($n = 3$).

ATR-IR analysis of decellularized (red), polylysine-enriched (blue) and reference polylysine (green) was analyzed in the amide band region of the IR spectrum (Figure 8 C). The sampling depth of ATR-IR, using a diamond crystal, is around 1,6 μm , that is this technique is less surface-sensitive than XPS. All samples show the typical spectral features due to amide bonds, as expected. Concerning differences between tested samples, the Amide II band at about 1.550 cm^{-1} shifts towards lower wavenumbers from decellularized to polylysine-enriched (arrow), centering close to the Amide II band of the polylysine reference. Also, around 1.400 cm^{-1} the shape of the band (arrow) changes from decellularized to polylysine. Taken together, XPS and ATR-IR results strongly suggest that successful enrichment with polylysine of the decellularized sample is obtained through this process.

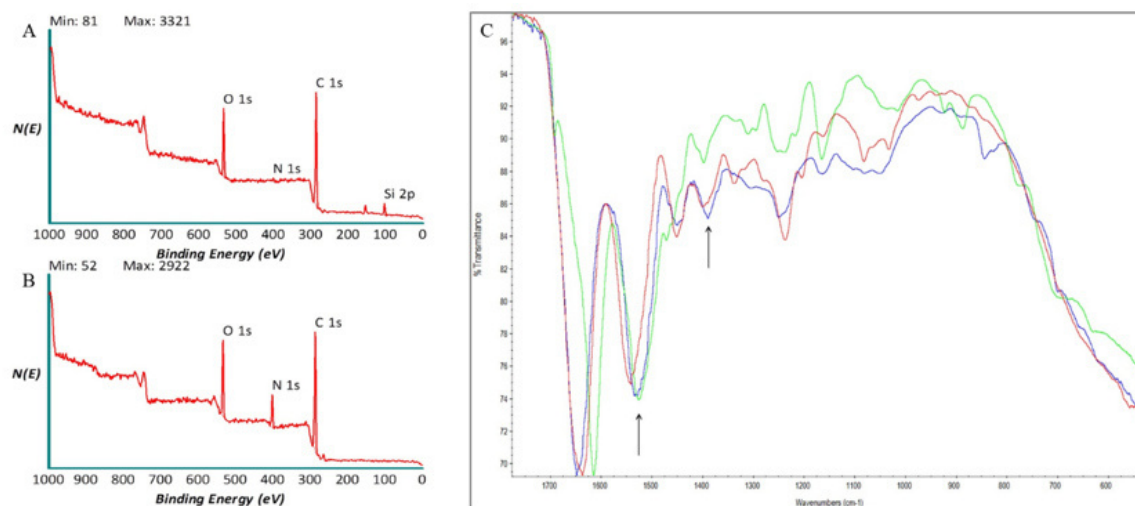


Figure 8: XPS spectra of A) decellularized and B) polylysine enriched matrices. C) AT-IR spectra of decellularized (red), polylysine enriched matrices (blue) and Polylysine as a control (green).

In Figure 9 A the structure of decellularized and polylysine-enriched matrices are shown through confocal microscopy. The polylysine-enriched sample shows a structure of fractures better defined than in the decellularized sample, and the roughness is narrower than the latter. In general, the enriched sample shows more vertical oriented fractures, while in decellularized the lines are not so straight composing soft curves. The images suggest that the enrichment treatment changes the micro and macro collagen structure, orientating and bridging collagen fibers, as can be seen in Figure 9 B, which confirms the data obtained from confocal microscopy. Indeed, decellularized sample's tissue seems thinner and hollower with respect to both native and polylysine enriched matrix. The thickness and the wall microfiber structure of polylysine enriched matrix seems adequately similar, suggesting that the fiber reorganizing after enrichment process leads to a structure comparable to native sample.

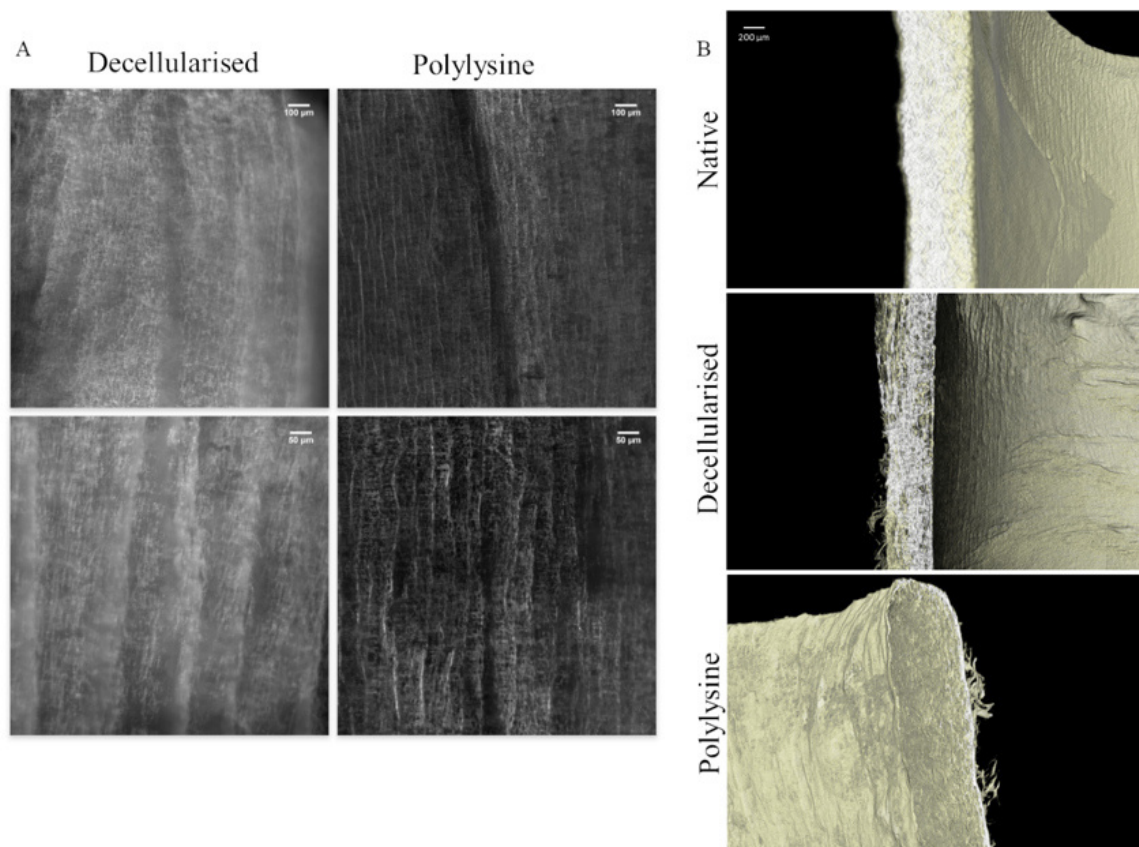


Figure 9: A) Confocal microscopy of decellularized and polylysine-enriched vessels. B) Micro-CT analysis of native vessel, decellularized and polylysine-enriched matrices.

3.3 Mechanical test

3.3.1 Young's modulus, tensile strength and burst pressure results: static conditions

To characterize the mechanical properties (Figure 10 A and B) specimens were tested, using an Instron instrument, and strained until specimen failure.

The Young's modulus is directly related to the compliance of the material. Decellularized samples present a significant Young's modulus decrease when compared with native and polylysine sample values. On the other hand, the tensile strength of the polylysine enriched matrix is increased, compared to the native vessel, while the same parameter between the decellularized matrix is lower with respect to the other samples.

The figure shows that, with respect to the native control, elasticity is not affected. The Young's modulus of the enriched matrix is shown to be not significantly different

to the native vessel. The scaffold wall is strengthened after enrichment.

3.3.2 Young's modulus, tensile strength and burst pressure results: dynamic conditions

Samples were tested for up to 30 days under dynamic flow conditions, perfusing the vessel lumen. After performing dynamic tests, matrix degradation was measured. All the samples reveal a weight loss: native samples' mass decreases of 60%, while decellularized samples roughly 55%. Nevertheless, the polylysine samples present only a 28% weight loss, with an evident matrix preservation compared to other samples (Figure 10 C).

Burst pressure was measured before and after applying dynamic conditions. Native artery pressure is 1,3 bar, while with polylysine treatment, the value is considerably increased, rising to 3,2 bar.

After 30 days, the maximum pressure value supported by the samples decreases by 40% in the native sample and only a 13% in the sample treated with polylysine.

The successful performances of polylysine enriched matrices are confirmed by the evaluation of matrix degradation in terms of tensile strength loss. Indeed, after 10 days polylysine enriched matrices lose only 5% of tensile strength while, decellularized matrix is 17% weaker than the static control. The differences are more evident after 20 days where decellularized matrices lose 26% of tensile strength, while treated decellularized vessels showed similar performances with respect to 10 day samples.

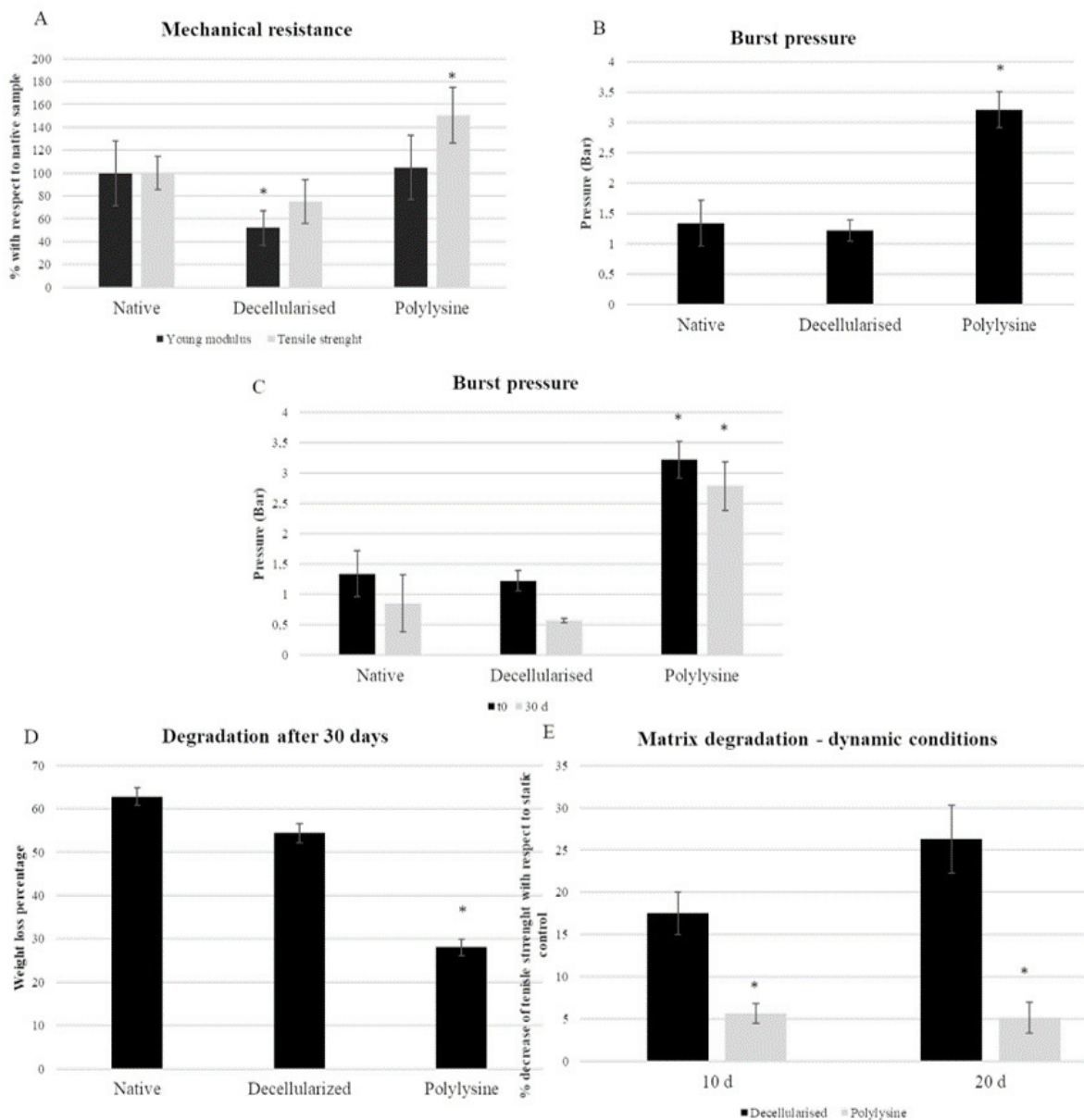


Figure 10: Mechanical testing results under static conditions: (A, left panel) Young's modulus and tensile strength representation for native, decellularized and polylysine grafting. Data are expressed normalized with a native vessel. The data origin is the stress-strain curves. Data are expressed as mean values \pm SD. ($n = 3, * = p \leq 0,05$). B) Burst pressure data for native, decellularized and polylysine grafting. Data are expressed as mean values \pm SD. ($n = 3, * = p \leq 0,05$). Mechanical testing results under dynamic conditions: C) Burst pressure data for native, decellularized, and polylysine grafting for static and dynamic conditions. Data are expressed as mean values \pm SD. ($n = 3, * = p \leq 0,05$). D) Degradation assays in terms of weight loss. Data are expressed as mean values \pm SD. ($n = 3, * = p \leq 0,05$). E) Degradation assays in terms of tensile strength loss. Data are expressed as mean values \pm SD. ($n = 3, * = p \leq 0,05$).

3.4 Cell viability assay: static and dynamic conditions

Endothelial cells were seeded in the vessels lumen and cell proliferation rate was measured after 1, 3 and 7 days. Figure 12 A shows comparable cell proliferation rates for decellularized and polylysine-enriched samples after 7 days. Endothelial cells' adhesion and proliferation were also evaluated, using hematoxylin-eosin and DAPI staining. Results show that after 3 days, cells adhered on both decellularized and polylysine-enriched samples, while after 7 days of culture cells formed an almost continuous monolayer only on polylysine-enriched surfaces (Figure 12 B). Finally, cell adhesion was evaluated after 3 days of dynamic conditions. In this purpose, as showed in Figure 11, a bioreactor was designed and printed in 3D.

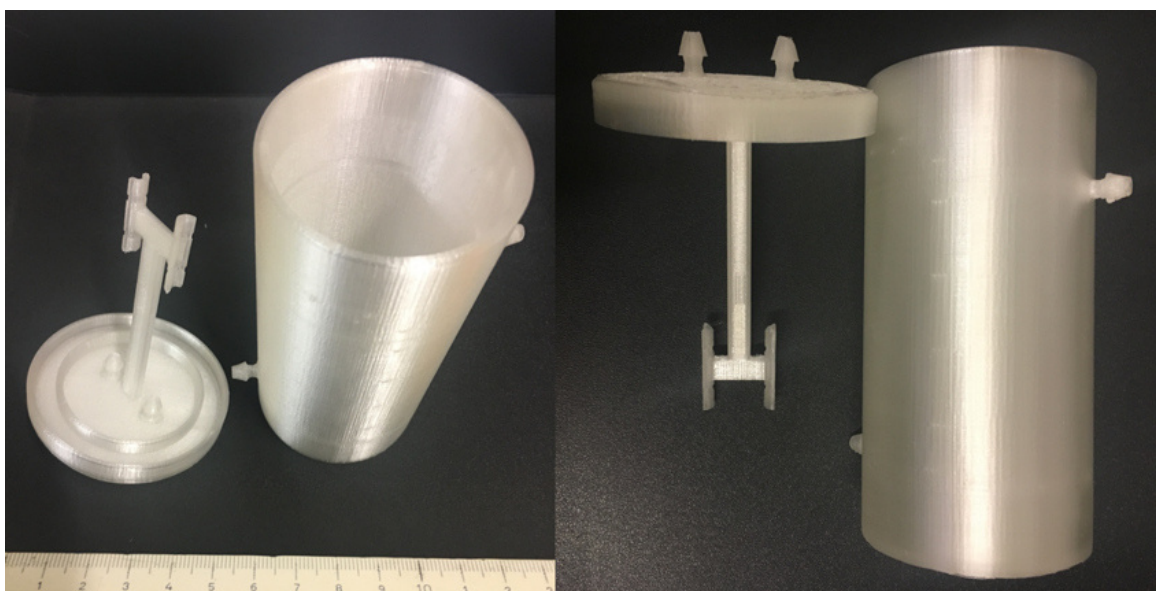


Figure 11: Photographs of the 3D printed bioreactor.

In Appendix A, sections and 3D pictures are reported.

In Figure 12 C DAPI staining shows almost no cell nuclei on decellularized samples, indicating that cells do not remain adherent to the matrix. On the other hand, polylysine-enriched samples show cell nuclei almost forming a continuous monolayer throughout the full length of the vessel, suggesting that cell adhesion is optimized on enriched matrices.

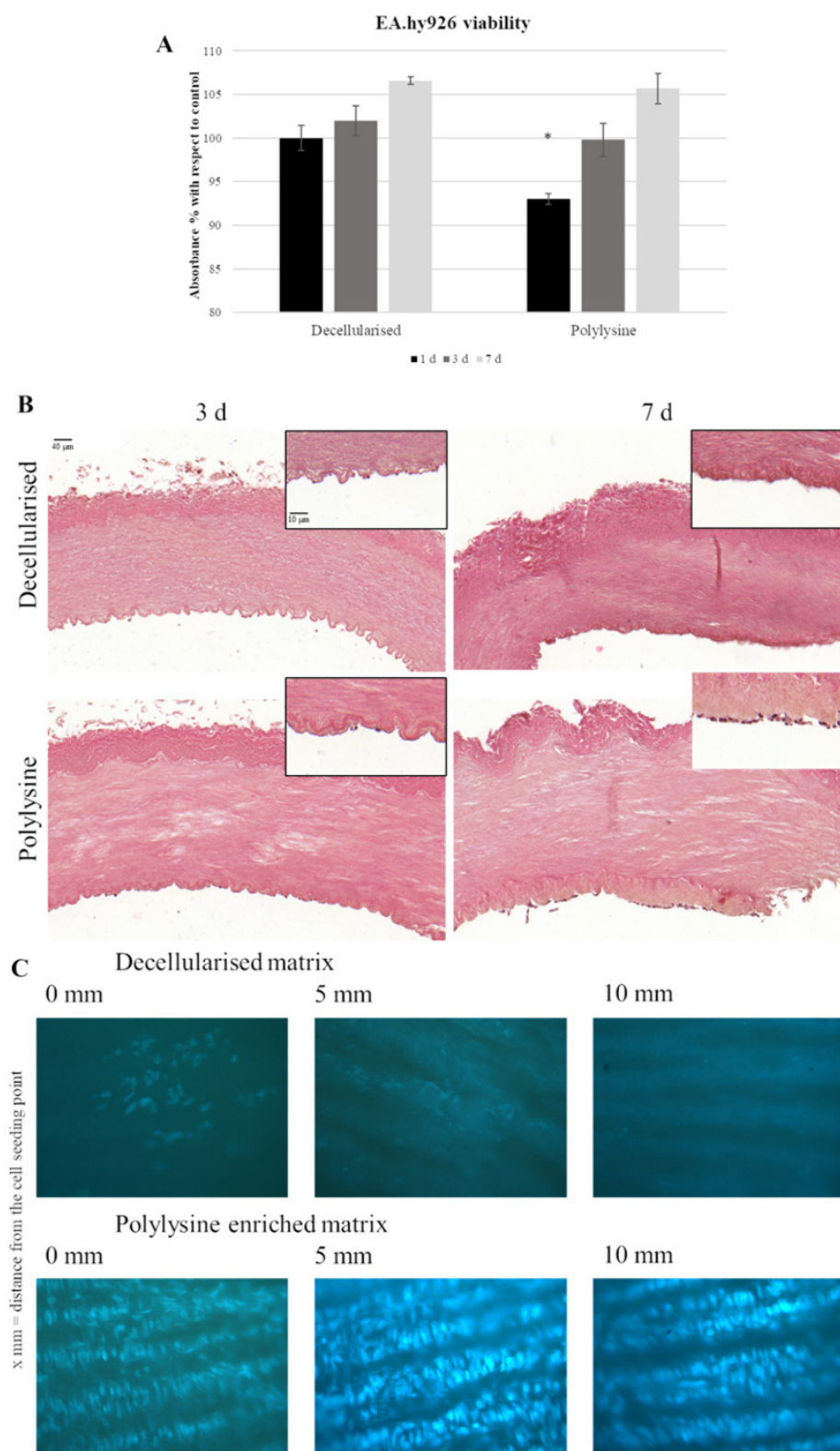


Figure 12: A) Endothelial cells viability assays. MTS test was performed after 1, 3, and 7 days. Data are expressed as mean values \pm SD. ($n = 3, * = p \leq 0,05$). B) Hematoxylin-Eosin staining of decellularized and polylysine enriched matrices with cells cultured for 3 and 7 days. C) DAPI staining of decellularized and polylysine enriched matrices after dynamic conditions.

3.5 Haemocompatibility test

The material's haemocompatibility was evaluated using thromboelastography (TEG). Among the coagulation parameters, reaction time (R) indicates the time required to induce the clot formation. The matrices treated with polylysine have a significantly increased R-value with respect to Dacron[®] and decellularized matrices. Fibrinogenic activity is rather decreased on enriched matrices, as a result the clot strength is lower than both matrices used as reference. The coagulation time parameter is directly correlated with the required time for the clot formation, in order to reach the maximum strength value before starting the dissolution process. This value increases in the samples treated with polylysine reflecting a benefit in terms of functionality. In addition, platelet aggregation confirms the lower rate in the clot formation process (Figure 13). These results clearly indicate a favorable influence on coagulation parameters in the presence of polylysine enrichment in terms of haemocompatibility.

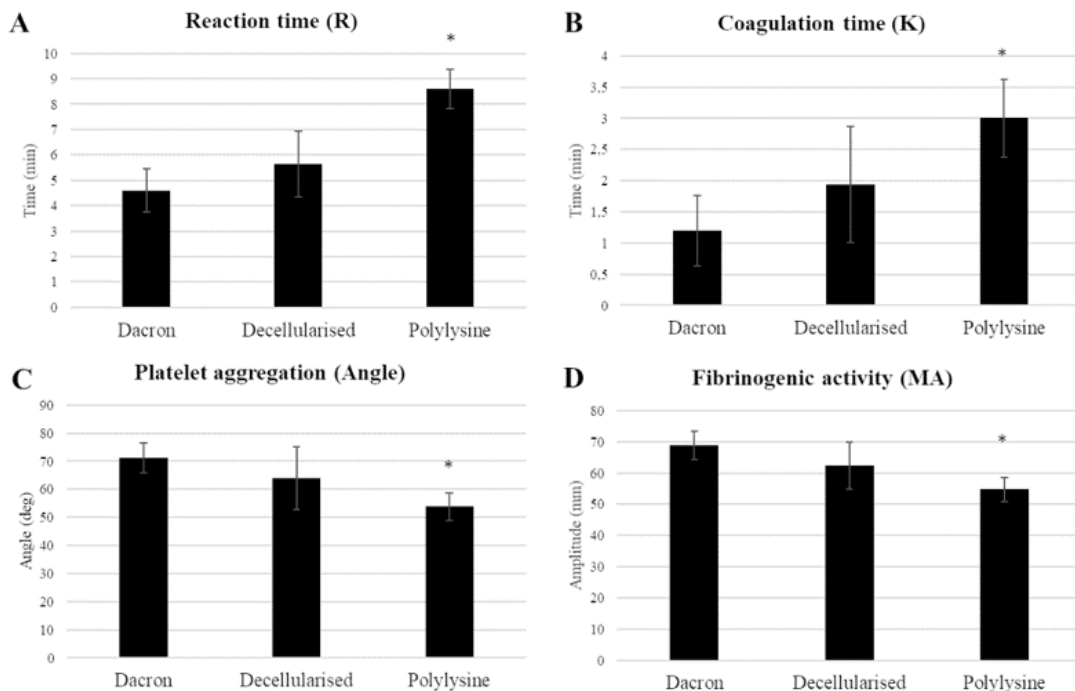


Figure 13: Haemocompatibility test. Coagulation parameters (A: reaction time; B: coagulation time; C: platelet aggregation; D: fibrinogenic activity) were evaluated on synthetic vascular substitutes (Dacron[®]) and treated matrices. Data are expressed as mean values \pm SD. ($n = 3$ from different healthy donors, $* = p \leq 0,05$).

3.6 Industrialization

3.6.1 Business plan

The plant's capacity was fixed in 50.000 vessels each year, although the market study consulted estimates the European market close to 600.000 vessels each year. This consideration allows to approach the investment in a conservative way and allows to take it as a constant during all the period with a low risk.

In order to fix the product price, similar competitor's prices were consulted and, as an average price, 1.500 € was obtained for each vessel prosthesis. To take a position as an aggressive competitor in the market, the sell product price was fixed in 800 €/vessel.

Considering the price and the amount of product the total revenue is 40 M€ each year which will be actualized using an inflation rate during the 10 years of the business plan period.

Total operating cost considered includes raw materials, chemicals, quality control and routine analysis, maintenances, administration and finance cost, work staff, electrical energy, insurance, delivery, wastewater treatment, amortization, and contingency. In the Appendix B all the costs are summarized. Among them, the heist cost corresponding to raw materials and chemicals. Femoral and carotid arteries are used as a raw material and the cost was fixed in 1.000 € including the animal and extraction cost. Chemicals cost is an incisive cost in the business plan due to DNase and polylysine have a 5.290 €/g and 2.540 €/g respectively.

Sales have been considered constant throughout the business plan period to simplify the estimate and due to the lack of predictive tools at the moment. This consideration is motivated by two aspects, the first concern that the vessel prosthesis production line is integrated into an existing plant operating into the medical devices field. This will allow to benefit from the distribution network and contacts already used by the company. Secondly, the production capacity considered is around the 10% of the total market demand so, although some occasionally fluctuations in sales occur, on average all production will be absorbed by the market. As a result of these two considerations and the lower price compared with the competitors, the consideration made can be assumed as reasonable.

OPEX, CAPEX, taxes and its amounts are summarized in Appendix B as well as the equity and the financed amount for the investment.

As a result of the business plan study internal rate of return (IRR) and return of the investment (ROI) indicators were obtained. They confirm the economic viability of the investment at this phase of the project.

3.6.2 Reactor design

Different tests were performed to obtain the ratio volume of solution to length of vessel treated. Figure 14 summarizes decellularization protocol for the first, second and third experiment and its H&E staining histology. From these three results it is important to underline the material's behavior, because constant flows inside and outside cannot guarantee the vessel's decellularization.

Step	Q _{in} (ml/min)	Re _{in}	Q _{out} (ml/min)	Re _{out}	Time (min)
Phase 1	13	126	17	26	60
Wash	13	126	17	26	45
Phase 2	13	126	17	26	60
Wash	13	126	17	26	45
Phase 3	13	126	17	26	overnight
Wash	13	126	17	26	45

Step	Q _{in} (ml/min)	Re _{in}	Q _{out} (ml/min)	Re _{out}	Time (min)
Phase 1	2	19	2	3	60
Wash	2	19	2	3	45
Phase 2	2	19	2	3	60
Wash	2	19	2	3	45
Phase 3	2	19	2	3	overnight
Wash	2	19	2	3	45

Step	Q _{in} (ml/min)	Re _{in}	Q _{out} (ml/min)	Re _{out}	Time (min)
Phase 1	6	62	80	26	60
Wash	6	62	80	26	45
Phase 2	6	62	40	26	60
Wash	6	62	40	26	45
Phase 3	6	62	60	26	overnight
Wash	6	62	60	26	45

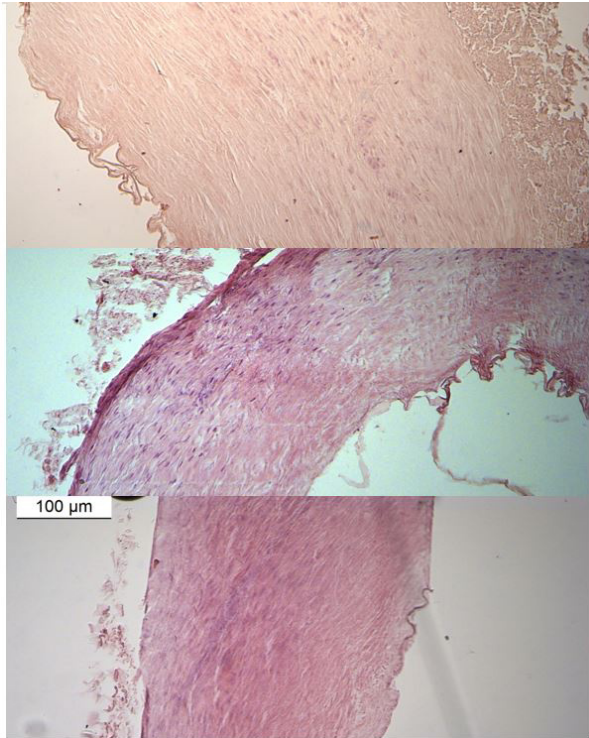


Figure 14: Hydraulic conditions and their H&E staining results for the three different settings of the dynamic decellularization test.

Flow parameters reported on Table 12, obtained the best performance in terms of decellularization, volume and time consuming. Figure 15 shows the matrix preservation and the absence of cell's nuclei.

	Q_{in} (ml/min)	Re_{in}	Q_{out} (ml/min)	Re_{out}	Time (h)
Phase 1	7	107	48	107	1
1 st PBS wash	9	133	60	134	0,5
2 nd PBS wash	2	32	15	33	1
3 rd PBS wash	5	83	37	83	1
Phase 2	7	107	48	107	1
1 st PBS wash	9	133	60	134	0,5
2 nd PBS wash	2	32	15	33	1
3 rd PBS wash	5	83	37	83	1
Phase 3	4	59	25	107	15
Wash in H ₂ O	7	107	48	107	2

Table 12: Final decellularization protocol selected for the three treating and washing phases. For each inner and outer solution are reported volumetric flow rates, Re and time.

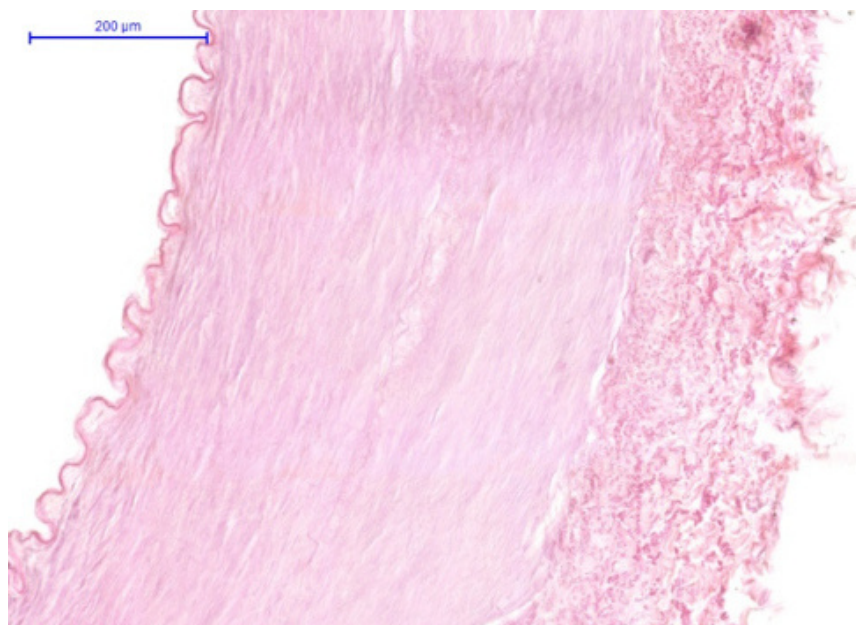


Figure 15: H&E histology of the blood vessel obtained using the selected protocol.

Re number representation during the time (Figure 16) reflects the intervention of the inertial forces compared to the viscous forces during the first steps of washing due to the high flow. Instead, an opposite situation occurs by significantly decreasing the flow, as in the second washing phase, in which the action of the viscous forces is stronger. Concerning the final washing step, an intermediate flow rate has been established, between the previous two, thus balancing the action of inertial and viscous forces. Finally, regarding the 3rd step solution, an even smaller flow rate has been chosen, in order to facilitate the diffusive transport across the membrane and favors the enzyme action.

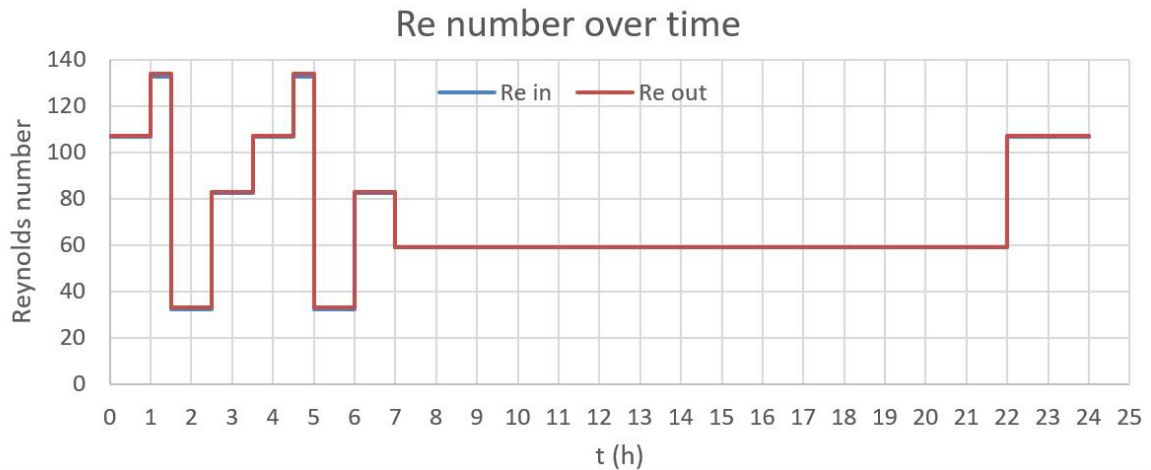


Figure 16: Schematic representation of Re for the inner (Re_{in}) and outer (Re_{out}) perfusion circuits over time on the optimized MiniBreath[®] protocol.

According with the 3 ml/cm of treated vessel and the fixed plant capacity, it is necessary to use 4 reactors.

The design of the production reactor is of cylindrical shape with 23 L of volume. Internally, it contains a structure formed by 265 hollow tubes of 2 mm of external diameter and 1,5 mm of internal diameter, which will be introduced in the native vessel. These tubes have perforations of 0,25 mm diameter following a helicoidal path, with an 5° angle in respect to the longitudinal axis, in order to facilitate the fluids' movement. The space around each tube guarantees the material to be in contact with the right solution volume.

The fluid will be forced to move inside and outside the vessel with opposite flow direction, which increases the effectiveness of the material's treatment. Because of this, the reactor will have perforations on the external chamber's base, which will be connected to tubes and controlled by automatic valves which fix the fluid's flow in the filling, emptying and recirculation phase.

Given the dimensions and configuration of the tubes that make up the reactor, the most suitable material for its realization is steel. This implies that the rest of the reactor must be constructed in ANSI 316 steel, in order to weld the parts to the structure and to avoid weak points in the structure, that would be created using other materials such as the plexiglass. The welds used in its construction phase must be as flat as possible,

to minimize undesirable material deposition. Seal welds are important to guarantee the sterility of the process even though the environment will be controlled. The costs of the material and the construction of the reactor have been considered acceptable within the BP study.

All the quota's and configuration details are included in Appendix C.

4 Discussion

Although autologous arterial and venous grafts are the gold standard as bypass graft material, they are not available in roughly 40% of patients, due to their insufficient length or quality of native vessels (Moroni and Mirabella 2014).

Synthetic grafts, including Dacron[®] and ePTFE, which efficiently work for large-diameter vascular grafts, have shown disappointing clinical results in small-diameter artery reconstruction, due to thrombotic complications, when compared to venous bypasses (Klinkert et al. 2004). For these reasons, decellularized scaffolds were introduced. The ECM is an optimal substrate in terms of biological performances, because it is able to drive cell adhesion, proliferation, and differentiation (Barnes et al. 2011); in this way, unlike synthetic materials, decellularized substitutes are able to solve a problem as complex as the repopulation with different cell types, as showed by Pellegata et al. (2013). On the other hand, decellularized matrices progressively lose the suitable mechanical properties needed for tissue replacement (Williams et al. 2009; Xiong et al. 2013). In the present study, we exploited the properties of the decellularized matrices, strengthened with polylysine enrichment, to prevent wall weakening (Gu et al. 2018). Polylysine is a polymer that has been widely used in tissue engineering, as a promoter of cell adhesion, because of its strong positive charge (Wang et al. 2018; Zhang et al. 2019) and as a biomaterial strengthener (Collin et al. 2004; Wang et al. 2016).

The evaluation on the effectiveness of the decellularization process showed that no cell nuclei are present in decellularized matrices, and that the DNA quantity is significantly lower than the native vessel, as well as also being lower than the gold standard defined by literature (Crapo et al. 2011). However, it is unclear if the DNA left in decellularized matrices could elicit a biological response from the host (Keane et al. 2012). Several commercial products derived from decellularized matrices with positive clinical outcomes contain DNA fragments, for this reason the probability that residual DNA could induce a host response is low (Gu et al. 2018; Pellegata et al. 2013).

In order to predict the possible outcome of a vascular substitution, mechanical properties are a crucial parameter to evaluate. In particular, graft failure occurs when the substitute's compliance is different from the native vessel (Xue and Greisler 2003). Although Young's modulus and failure strength of these substitutes are not signifi-

cantly different from native vessels, the compliance was not taken into account as a key factor (Bergmeister et al. 2005; Ketchedjian et al. 2005; Mahara et al. 2015). On the contrary, Xue and Greisler (2003) showed that, in human patients graft failure occurs when the substitute's compliance is different from the native vessel. For this reason, in this study the differences in compliance between polylysine-enriched substitute and the native vessel were evaluated. As known from literature, compliance is also related to wall stiffness (Baltgaile 2012), which can be evaluated by Young's modulus. Mechanical characterization of the matrices in static conditions showed that polylysine enriched matrix showed increased wall strength, while the Young's modulus is similar to that of native vessels. The assessment of mechanical properties shows that, given the similarities in stiffness between native vessel and polylysine enriched matrices, the compliance is comparable.

In order to assess the durability of the enrichment and the behavior of the substitute under dynamic conditions, degradation rates were also evaluated, as weight loss and tensile strength loss. In both cases, polylysine enriched vessels showed the best behavior, retaining matrix and mechanical properties, while all the other matrices considered lost their properties after 30 days. The importance of mechanical properties evaluation is underlined in Williams et al. (2009), who studied the differences in stiffness between fresh and decellularized rabbit carotid arteries; also Mahara et al. (2015) focused on difference in the stress strain curve between original tissue and peptide-enriched decellularized ostrich carotid artery graft; finally, López-Ruiz et al. (2017) evaluated tensile strength, maximum load and burst pressure of native, decellularized and coated porcine carotid arteries.

Treated matrix cytocompatibility showed to be adequate compared to decellularized matrices, indicating a favorable environment for efficient repopulation by the host's vascular cells. The adequacy of modified decellularized matrices was also demonstrated by Mahara et al. (2015) who indicated adequate cell repopulation of peptide-enriched decellularized grafts in porcine model; also Boerboom et al. (2002) confirmed good recellularization of a decellularized carotid artery implant; finally Hilbert et al. (2004) further highlights successful repopulation of decellularized carotid goat graft. Moreover, haemocompatibility tests displayed that polylysine enriched matrices develop blood clots slower and with less strength with respect to both decellularized matrices

and Dacron[®], a synthetic polymer widely used in vascular substitution. Furthermore, coagulation assays indicate that polylysine enriched matrices could help to avoid thrombosis, another drawback of synthetic substitute (Fukunishi et al. 2016).

Given the positive results obtained by these *in vitro* experiments, these polylysine enriched substitutes are under preclinical evaluation using ovine models.

Overall, our tests confirm the efficiency of both decellularization and enrichment methods, as well as the ability of polylysine enriched matrices to maintain adequate mechanical properties, while allowing cell adhesion and proliferation. Thus, the enriched biological substitutes could represent an innovative engineering approach for application in vascular tissue engineering.

Further *in vitro* studies, using primary endothelial cells and fibroblast, may be integrated in the scaffold characterization to foresee the scaffold repopulation of all the cell types that are present in the native tissue.

Vessel prototype's future perspectives are evolving in two different directions. On one hand, *in vivo* test is now carried on using a sheep model (Figure 17) in order to complete the preclinical phase of this product.

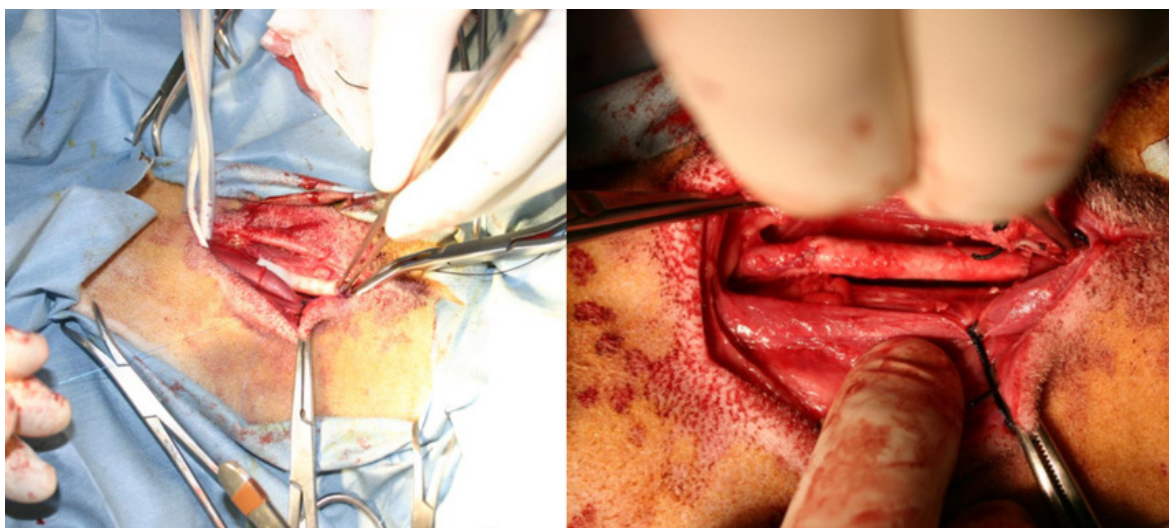


Figure 17: Photograph of the surgical intervention to implant the vascular polylysine graft in the left carotid artery.

On the other hand, the last grafting step using polylysine presents a promising approach to obtain a new derivate product, a hemodialysis arteriovenous fistula. This

new application must be resistant enough to support the frequent puncture necessary for the hemodialysis treatment. In this purpose, a preliminary test was performed, different polylysine concentration vessels underwent uniaxial mechanical test in order to evaluate its Young's modulus and tensile strength.

Further advances in transversal techniques may be implemented in this vascular graft. Human-iPSCs decellularised scaffolds could avoid the intake of immunosuppressive drugs required after organ transplantation and, in combination with the new performed amplification cells techniques, the product can be further upgraded. Bioreactors must be developed from sterility and control point of view to guarantee the recellularization step. Taken all together, production time and high cost of manufacturing must be optimized to implement these new approaches.

From the engineering point of view, the heterogeneity of the raw material is an aspect to be aware so, extra quality controls can avoid further problems.

Regarding the new traceability requirements established in the Directive 98/87/EC, UDI code must be included for each product in order to be registered in the EU-DAMED. Implantable decellularization products cannot allow an ink traceability mark so, a traditional database is the available alternative. New alternatives are already studied in the food industry field and could be implemented to satisfy the EU requirements of UDI products (Aung and Chang 2014; Karlsen et al. 2013; Markiewicz-Keszzycka et al. 2019).

Among the available post-sterilization methods, CO₂-SC was chosen, since it is characterized by the mechanical properties' preservation of the treated material. This technique offers some versatility by changing the pressure and temperature conditions during the process, which will offer a different degree of product sterility. These conditions must be established in successive phases of the project. Even so, it has been considered as a valid alternative, since other companies NovaSterilis or Biobank use it such as a part of the sterilization process technology in the treatment of human autologous implants.

The packaging and the stocking of both the raw materials and the final product must be deepened in successive phases of the project. In this first phase, the stocking of raw materials is not considered a problem, since it can be frozen at $-20\text{ }^{\circ}\text{C}$, it offers

some flexibility before its use. The distribution of products is usually a problematic issue in this type of device because the properties of the product can be affected by environmental changes, which their control can be difficult when it is necessary to cover large distances or small delivery times. In this case, since the prosthesis will be produced in Europe and for the European market, it is expected that the distribution will be carried out by road where the environmental conditions can be easily controlled.

The sensors implementation in the production process control, in addition to increasing the quality and precision of the production, will allow the access to state economic incentives that currently encourage the implementation of Industry 4.0. A new generation of sensors, called “Smart Sensors”, allow an easy communication directly with the user or transferring the data wirelessly (Durrezi 2016). The goal of the Industry 4.0 is not just getting data, but collect data and converting it into useful, understandable information that optimizes the control of the process and the business properly. This is the reason why Artificial Intelligence (AI) technologies plays a key role in the fourth industry revolution, offering a more sophisticated use of machine learning, digitization, and informed decision making from top to bottom in an organization (Javaid and Haleem 2019).

Until now, process optimization had been carried out using software such as SixSigma, AI is revolutionizing the field of industrial processes optimization, because of its very wide range of applications from process control to logistics, storage, industrial distribution and even plant maintenance prediction.

The benefits of AI implementation in the new industry generation are potentially huge, thus the designed plant will be equipped with the necessary sensors in order to obtain the complete control of the important variables for the process involved in the fully and smart plant control.

References

- Abousleiman, R. I., Reyes, Y., McFetridge, P., and Sikavitsas, V. 2008, *Artificial Organs*, 32, 735
- Achilli, M., Lagueux, J., and Mantovani, D. 2010, *Macromolecular Bioscience*, 10, 307
- Akowuah, E. F., Sheridan, P. J., Cooper, G. J., and Newman, C. 2003, *The Annals of Thoracic Surgery*, 76, 959
- Allen, R. A., Seltz, L. M., Jiang, H., et al. 2010, *Tissue Engineering. Part A*, 16, 3363
- Athanasίου, T., Saso, S., Rao, C., et al. 2011, *European Journal of Cardio-Thoracic Surgery*, 40, 208
- Aung, M. M., and Chang, Y. S. 2014, *Food Control*, 39, 172
- Bakhsheshi-Rad, H., Hadisi, Z., Hamzah, E., et al. 2017, *Materials Letters*, 207, 179
- Baltgaile, G. 2012, *Perspectives in Medicine*, 1, 146
- Barkan, D., Green, J. E., and Chambers, A. F. 2010, *European Journal of Cancer* (Oxford, England: 1990), 46, 1181
- Barnes, C. A., Brison, J., Michel, R., et al. 2011, *Biomaterials*, 32, 137
- Bencherif, S. A., Srinivasan, A., Horkay, F., et al. 2008, *Biomaterials*, 29, 1739
- Bennett, J. E., Stevens, G. A., Mathers, C. D., et al. 2018, *The Lancet*, 392, 1072
- Bergmeister, H., Boeck, P., Kasimir, M.-T., et al. 2005, *Journal of Biomedical Materials Research Part B: Applied Biomaterials*, 74B, 495
- Bobryshev, Y. V. 2005, *Atherosclerosis*, 180, 293
- Boccafoschi, F., Botta, M., Fusaro, L., et al. 2017a, *Journal of Tissue Engineering and Regenerative Medicine*, 11, 1648
- Boccafoschi, F., Ramella, M., Fusaro, L., Catoira, M. C., and Casella, F. 2017b, in *Reference Module in Biomedical Sciences* (Elsevier)
- Boerboom, L. E., Barillo, D. J., Coleman, C. L., et al. 2002, *Cell Preservation Technology*, 1, 53
- Boland, E. D., Matthews, J. A., Pawlowski, K. J., et al. 2004, *Frontiers in Bioscience: A Journal and Virtual Library*, 9, 1422
- Bolland, F., Korossis, S., Wilshaw, S.-P., et al. 2007, *Biomaterials*, 28, 1061

- Bornstein, P., and Sage, E. H. 2002, *Current Opinion in Cell Biology*, 14, 608
- Brandl, F., Sommer, F., and Goepferich, A. 2007, *Biomaterials*, 28, 134
- Buijtenhuijs, P., Buttafoco, L., Poot, A. A., et al. 2004, *Biotechnology and applied biochemistry*, 39, 141
- Burdick, J. A., and Prestwich, G. D. 2011, *Advanced Materials*, 23, H41
- Cartmell, J. S., and Dunn, M. G. 2000, *Journal of Biomedical Materials Research*, 49, 134
- Catto, V., Farè, S., Freddi, G., and Tanzi, M. C. 2014, *ISRN Vascular Medicine*, 2014, 1
- Chen, G., Ushida, T., and Tateishi, T. 2002, *Macromolecular Bioscience*, 2, 67
- Chen, S., Li, J., and Dong, P. 2013, *Acta Cardiologica Sinica*, 29, 451
- Cheng, N.-C., Estes, B. T., Awad, H. A., and Guilak, F. 2009, *Tissue Engineering. Part A*, 15, 231
- Chew, D. K., Owens, C. D., Belkin, M., et al. 2002, *Journal of Vascular Surgery*, 35, 1085
- Cho, K. R., Kim, J.-S., Choi, J.-S., and Kim, K.-B. 2006, *European Journal of Cardio-Thoracic Surgery*, 29, 511
- Chupa, J. M., Foster, A. M., Sumner, S. R., Madihally, S. V., and Matthew, H. W. 2000, *Biomaterials*, 21, 2315
- Cole, M. B. 1984, *Journal of Microscopy*, 133, 129
- Collin, D., Lavalle, P., Garza, J. M., et al. 2004, *Macromolecules*, 37, 10195
- Conte, M. S. 2013, *Journal of Vascular Surgery*, 57, 8S
- Cortiella, J., Niles, J., Cantu, A., et al. 2010, *Tissue Engineering. Part A*, 16, 2565
- Couet, F., Rajan, N., and Mantovani, D. 2007, *Macromolecular Bioscience*, 7, 701
- Crapo, P. M., Gilbert, T. W., and Badylak, S. F. 2011, *Biomaterials*, 32, 3233
- Daamen, W., Hafmans, T., Veerkamp, J., and van Kuppevelt, T. 2001, *Biomaterials*, 22, 1997
- Dardik, H., Ibrahim, I. M., and Dardik, I. I. 1979, *Annals of surgery*, 189, 189
- Deeken, C. R., White, A. K., Bachman, S. L., et al. 2011, *Journal of Biomedical Materials Research. Part B, Applied Biomaterials*, 96, 199

- Desai, N. D., Cohen, E. A., Naylor, C. D., and Femes, S. E. 2004, *New England Journal of Medicine*, 351, 2302
- Disney, C. M., Madi, K., Bodey, A. J., et al. 2017, *Scientific Reports*, 7, doi:10.1038/s41598-017-16354-w
- Donati, I., Benincasa, M., Foulc, M.-P., et al. 2012, *Biomacromolecules*, 13, 1152
- Draget, K. I., Smidsrød, O., and Skjåk-Bræk, G. 2005, in *Biopolymers Online*, ed. A. Steinbüchel (Wiley-VCH Verlag GmbH & Co. KGaA), bpol6008
- Draget, K. I., and Taylor, C. 2011, *Food Hydrocolloids*, 25, 251
- Duresi, M. 2016, in *Comprehensive Analytical Chemistry*, Vol. 74 (Elsevier), 389–413
- Dziedzic-Goclawska, A., Kaminski, A., Uhrynowska-Tyszkiewicz, I., and Stachowicz, W. 2005, *Cell and Tissue Banking*, 6, 201
- Elder, B. D., Kim, D. H., and Athanasiou, K. A. 2010, *Neurosurgery*, 66, 722
- Eskandari, M. K. 2015, *CURRENT VASCULAR SURGERY: 40TH ANNIVERSARY OF THE NORTHWESTERN VASCULAR SYMPOSIUM (PMPH-USA)*
- Flynn, L. 2010, *Biomaterials*, 31, 4715
- Fukunishi, T., Best, C. A., Sugiura, T., et al. 2016, *PLOS ONE*, 11, e0158555
- Gilbert, T. W., Wognum, S., Joyce, E. M., et al. 2008, *Biomaterials*, 29, 4775
- Gilpin, S. E., Guyette, J. P., Gonzalez, G., et al. 2014, *The Journal of Heart and Lung Transplantation*, 33, 298
- Goldman, S., Zadina, K., Moritz, T., et al. 2004, *Journal of the American College of Cardiology*, 44, 2149
- Gorschewsky, O., Puetz, A., Riechert, K., Klakow, A., and Becker, R. 2005, *Bio-Medical Materials and Engineering*, 15, 403
- Goyannes, D. 1906, *J. El. Siglo Medico*, 53, 546
- Grassl, E. D., Oegema, T. R., and Tranquillo, R. T. 2002, *Journal of Biomedical Materials Research*, 60, 607
- Grauss, R., Hazekamp, M., Oppenhuizen, F., et al. 2005, *European Journal of Cardio-Thoracic Surgery*, 27, 566
- Gross, R. E., Hurwitt, E. S., Bill Jr, A. H., and Peirce 2nd, E. C. 1948, *New England Journal of Medicine*, 239, 578

- Gu, Y., Wang, F., Wang, R., et al. 2018, *Cell and Tissue Banking*, 19, 311
- Guruswamy Damodaran, R., and Vermette, P. 2018, *Biotechnology Progress*, doi:10.1002/btpr.2699
- Haisch, A., Loch, A., David, J., et al. 2000, *Medical & Biological Engineering & Computing*, 38, 686
- Hamedi, H., Moradi, S., Hudson, S. M., and Tonelli, A. E. 2018, *Carbohydrate Polymers*, 199, 445
- Han, F., Liu, S., Liu, X., et al. 2014, *Acta Biomaterialia*, 10, 921
- Harskamp, R. E., Lopes, R. D., Baisden, C. E., de Winter, R. J., and Alexander, J. H. 2013, *Annals of Surgery*, 257, 824
- He, W., Ma, Z., Teo, W. E., et al. 2009, *Journal of Biomedical Materials Research Part A*, 90A, 205
- Higgins, S. P., Solan, A. K., and Niklason, L. E. 2003, *Journal of Biomedical Materials Research*, 67A, 295
- Hilbert, S. L., Boerboom, L. E., Livesey, S. A., and Ferrans, V. J. 2004, *Journal of Biomedical Materials Research*, 69A, 197
- Hinderer, S., Layland, S. L., and Schenke-Layland, K. 2016, *Advanced Drug Delivery Reviews*, 97, 260
- Hinds, M. T., Rowe, R. C., Ren, Z., et al. 2006, *Journal of Biomedical Materials Research Part A*, 77A, 458
- Hodde, J., and Hiles, M. 2002, *Biotechnology and Bioengineering*, 79, 211
- Hodde, J., Janis, A., Ernst, D., et al. 2007, *Journal of Materials Science. Materials in Medicine*, 18, 537
- Holland, C. K., Brown, J. M., Scutt, L. M., and Taylor, K. J. 1998, *Ultrasound in Medicine & Biology*, 24, 1079
- Horowitz, B., Bonomo, R., Prince, A. M., et al. 1992, *Blood*, 79, 826
- Huang, Y., Onyeri, S., Siewe, M., Moshfeghian, A., and Madihally, S. V. 2005, *Biomaterials*, 26, 7616
- Huang, Z.-M., Zhang, Y., Ramakrishna, S., and Lim, C. 2004, *Polymer*, 45, 5361
- Jaboulay, M., Briau, E., et al. 1896, *Lyon méd*, 81, 97

- Jackson, D. W., Grood, E. S., Wilcox, P., et al. 1988, *The American Journal of Sports Medicine*, 16, 101
- Jamur, M. C., and Oliver, C. 2010, *Methods in Molecular Biology* (Clifton, N.J.), 588, 55
- Javid, M., and Haleem, A. 2019, *Current Medicine Research and Practice*, 9, 102
- Kannan, R. Y., Salacinski, H. J., Butler, P. E., Hamilton, G., and Seifalian, A. M. 2005, *Journal of Biomedical Materials Research Part B: Applied Biomaterials*, 74B, 570
- Karlsen, K. M., Dreyer, B., Olsen, P., and Elvevoll, E. O. 2013, *Food Control*, 32, 409
- Kawecki, M., Labus, W., Klama-Baryla, A., et al. 2018, *Journal of biomedical materials research. Part B, Applied biomaterials.*, 106, 909
- Keane, T. J., Londono, R., Turner, N. J., and Badylak, S. F. 2012, *Biomaterials*, 33, 1771
- Keane, T. J., Swinehart, I. T., and Badylak, S. F. 2015, *Methods*, 84, 25
- Ketchedjian, A., Jones, A. L., Krueger, P., et al. 2005, *The Annals of Thoracic Surgery*, 79, 888
- Khavandgar, Z., Roman, H., Li, J., et al. 2014-02, *Journal of Bone and Mineral Research*, 29, 327
- Kim, H. J., Kim, M. K., Lee, K. H., et al. 2017, *International Journal of Biological Macromolecules*, 104, 294
- Kim, S. H., Yeon, Y. K., Lee, J. M., et al. 2018, *Nature Communications*, 9, 1620
- Klinkert, P., Post, P., Breslau, P., and van Bockel, J. 2004, *European Journal of Vascular and Endovascular Surgery*, 27, 357
- Koch, S., Flanagan, T. C., Sachweh, J. S., et al. 2010, *Biomaterials*, 31, 4731
- Kottke-Marchant, K., and Larsen, C. 2006, in *Encyclopedia of Medical Devices and Instrumentation*, ed. J. G. Webster (John Wiley & Sons, Inc.)
- Kozlov, P., and Burdygina, G. 1983, *Polymer*, 24, 651
- Lee, R. C. 2005, *Annals of the New York Academy of Sciences*, 1066, 85
- Lee, R. C., and Kolodney, M. S. 1987, *Plastic and Reconstructive Surgery*, 80, 672
- Lee, S. J., Liu, J., Oh, S. H., et al. 2008, *Biomaterials*, 29, 2891

- Lemson, M., Tordoir, J., Daemen, M., and Kitslaar, P. 2000, *European Journal of Vascular and Endovascular Surgery*, 19, 336
- Li, M., Mondrinos, M. J., Chen, X., et al. 2006, *Journal of Biomedical Materials Research Part A*, 79A, 963
- Lin, C.-H., Hsia, K., Ma, H., Lee, H., and Lu, J.-H. 2018, *International Journal of Molecular Sciences*, 19, 2101
- Liu, G.-F., He, Z.-J., Yang, D.-P., et al. 2008, *Chinese Medical Journal*, 121, 1398
- Liu, X., Zheng, C., Luo, X., Wang, X., and Jiang, H. 2019, *Materials Science and Engineering: C*, 99, 1509
- López-Ruiz, E., Venkateswaran, S., Perán, M., et al. 2017, *Scientific Reports*, 7, 407
- Lü, W.-D., Zhang, M., Wu, Z.-S., and Hu, T.-H. 2009, *Interactive CardioVascular and Thoracic Surgery*, 8, 301
- Madhally, S. V., and Matthew, H. W. 1999, *Biomaterials*, 20, 1133
- Mahara, A., Somekawa, S., Kobayashi, N., et al. 2015, *Biomaterials*, 58, 54
- Mancuso, L., Gualerzi, A., Boschetti, F., Loy, F., and Cao, G. 2014, *Biomedical Materials*, 9, 045011
- Marelli, B., Achilli, M., Alessandrino, A., et al. 2012, *Macromolecular Bioscience*, 12, 1566
- Markiewicz-Keszycka, M., Cama-Moncunill, R., Pietat Casado-Gavaldà, M., Sullivan, C., and Cullen, P. J. 2019, *Current Opinion in Food Science*, 28, 96
- Masden, D. L., Seruya, M., and Higgins, J. P. 2012, *The Journal of Hand Surgery*, 37, 2362
- Mathers, C. D., and Loncar, D. 2006, *PLoS Medicine*, 3, e442
- Matuska, A. M., and McFetridge, P. S. 2015-02, *Journal of Biomedical Materials Research Part B: Applied Biomaterials*, 103, 397
- Mendoza-Novelo, B., Avila, E. E., Cauich-Rodríguez, J. V., et al. 2011, *Acta Biomaterialia*, 7, 1241
- Metscher, B. D. 2009, *BMC Physiology*, 9, 11
- Meyer, U., Meyer, T., Handschel, J., and Wiesmann, H. P. 2009, *Fundamentals of Tissue Engineering and Regenerative Medicine* (Springer Science & Business Media),

- google-Books-ID: aytt2V19hfIC
- Montoya, C. V., and McFetridge, P. S. 2009, *Tissue Engineering. Part C, Methods*, 15, 191
- Moreau, M. F., Gallois, Y., Baslé, M.-F., and Chappard, D. 2000-02, *Biomaterials*, 21, 369
- Moroni, F., and Mirabella, T. 2014, *American Journal of Stem Cells*, 3, 1
- Murase, Y., Narita, Y., Kagami, H., et al. 2006, *ASAIO Journal*, 52, 450
- Nagarajan, S., Pochat-Bohatier, C., Teyssier, C., et al. 2016a, *RSC Advances*, 6, doi:10.1039/C6RA23986B
- Nagarajan, S., Soussan, L., Bechelany, M., et al. 2016b, *Journal of Materials Chemistry B*, 4, 1134
- Nagarajan, S., Belaid, H., Pochat-Bohatier, C., et al. 2017, *ACS Applied Materials & Interfaces*, 9, 33695
- Nair, P., and Thottappillil, N. 2015, *Vascular Health and Risk Management*, 79
- Nakazawa, Y., Sato, M., Takahashi, R., et al. 2011, *Journal of Biomaterials Science, Polymer Edition*, 22, 195
- Nations, U. 1958, *Manual on economic development projects*. (Publisher not identified)
- Nguyen, H., Morgan, D. A. F., and Forwood, M. R. 2007, *Cell and Tissue Banking*, 8, 81
- Olin, J. W., White, C. J., Armstrong, E. J., Kadian-Dodov, D., and Hiatt, W. R. 2016, *Journal of the American College of Cardiology*, 67, 1338
- O'Neill, J. D., Anfang, R., Anandappa, A., et al. 2013, *The Annals of Thoracic Surgery*, 96, 1046
- Owens, C. D., Wake, N., Conte, M. S., Gerhard-Herman, M., and Beckman, J. A. 2009, *Journal of Vascular Surgery*, 50, 1063
- Pai, A., Leaf, E. M., El-Abbadi, M., and Giachelli, C. M. 2011-02, *The American Journal of Pathology*, 178, 764
- Pankajakshan, D., and Agrawal, D. K. 2010, *Canadian Journal of Physiology and Pharmacology*, 88, 855
- Panzavolta, S., Gioffrè, M., Focarete, M. L., et al. 2011, *Acta Biomaterialia*, 7, 1702

- Parekh, A., Mantle, B., Banks, J., et al. 2009, *The Laryngoscope*, 119, 1206
- Pashneh-Tala, S., MacNeil, S., and Claeysens, F. 2016, *Tissue Engineering Part B: Reviews*, 22, 68
- Pellegata, A. F., Asnaghi, M. A., Stefani, I., et al. 2013, *BioMed Research International*, 2013, 1
- Perea-Gil, I., Uriarte, J. J., Prat-Vidal, C., et al. 2015, *American Journal of Translational Research*, 7, 558
- Petersen, T. H., Calle, E. A., Colehour, M. B., and Niklason, L. E. 2012, *Cells Tissues Organs*, 195, 222
- Petersen, T. H., Calle, E. A., Zhao, L., et al. 2010, *Science*, 329, 538
- Phillips, M., Maor, E., and Rubinsky, B. 2010, *Journal of Biomechanical Engineering*, 132, 091003
- Prestwich, G. D. 2011, *Journal of Controlled Release*, 155, 193
- Qiu, Q.-Q., Leamy, P., Brittingham, J., et al. 2009, *Journal of Biomedical Materials Research Part B: Applied Biomaterials*, 91B, 572
- Rajan, N., Lagueux, J., Couet, F., et al. 2008, *Biotechnology Progress*, 24, 884
- Remuzzi, A., Mantero, S., Colombo, M., et al. 2004, *Tissue Engineering*, 10, 699
- Rodrigues, I. C. P., Kaasi, A., Maciel Filho, R., Jardini, A. L., and Gabriel, L. P. 2018, *Einstein (Sao Paulo, Brazil)*, 16, eRB4538
- Roosens, A., Somers, P., De Somer, F., et al. 2016, *Annals of Biomedical Engineering*, 44, 2827
- Ross, E. A., Williams, M. J., Hamazaki, T., et al. 2009, *Journal of the American Society of Nephrology: JASN*, 20, 2338
- Ruoslahti, E., and Engvall, E. 1997, *The Journal of Clinical Investigation*, 100, S53
- Sadeghi, M., and Heidari, B. 2011, *Materials*, 4, 543
- Sahni, A., and Francis, C. W. 2000, *Blood, The Journal of the American Society of Hematology*, 96, 3772
- Santhosh Kumar, T., and Krishnan, L. K. 2002, *Tissue engineering*, 8, 763
- Schaner, P. J., Martin, N. D., Tulenko, T. N., et al. 2004, *Journal of Vascular Surgery*, 40, 146

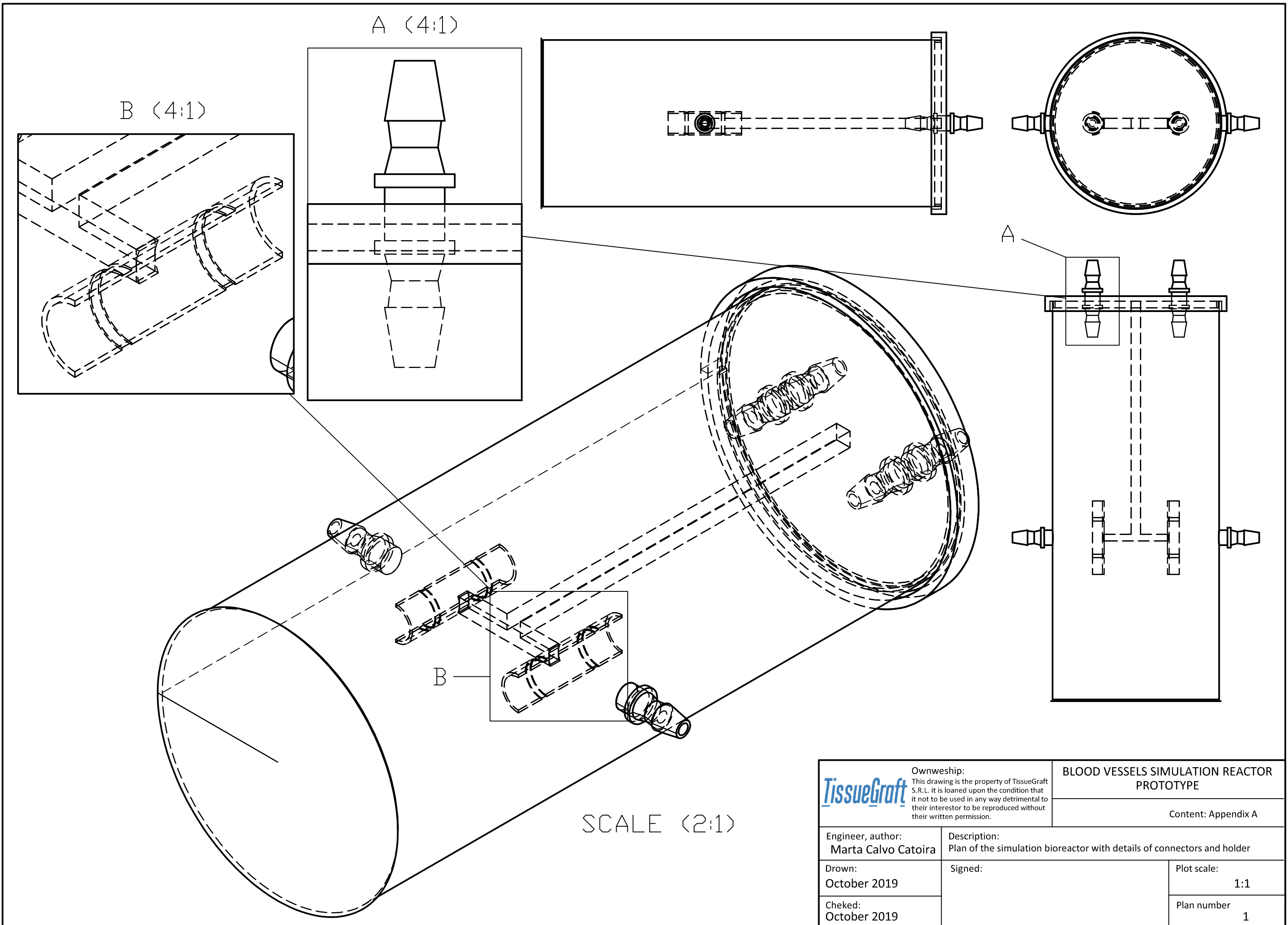
- Schmidt, C. E., and Baier, J. M. 2000, *Biomaterials*, 21, 2215
- Schmitto, J. D., Rajab, T. K., and Cohn, L. H. 2010, *Current Opinion in Cardiology*, 25, 609
- Seifu, D. G., Purnama, A., Mequanint, K., and Mantovani, D. 2013, *Nature Reviews Cardiology*, 10, 410
- Sellaro, T. L., Ranade, A., Faulk, D. M., et al. 2010, *Tissue Engineering. Part A*, 16, 1075
- Settembrini, P., Bonardelli, S., and Settembrini, A. M. 2017, *Vascular surgery: why, when, how : a reasoned approach to decision making through experience (Minerva medica)*, OCLC: 1045967385
- Sheridan, W., Duffy, G., and Murphy, B. 2012, *Journal of the Mechanical Behavior of Biomedical Materials*, 8, 58
- Shum-Tim, D., Stock, U., Hrkach, J., et al. 1999, *The Annals of Thoracic Surgery*, 68, 2298
- Song, J. J., Guyette, J. P., Gilpin, S. E., et al. 2013, *Nature Medicine*, 19, 646
- Stekelenburg, M., Rutten, M. C., Snoeckx, L. H., and Baaijens, F. P. 2009, *Tissue Engineering Part A*, 15, 1081
- Stern, M. M., Myers, R. L., Hammam, N., et al. 2009, *Biomaterials*, 30, 2393
- Stitzel, J., Liu, J., Lee, S. J., et al. 2006, *Biomaterials*, 27, 1088
- Struecker, B., Butter, A., Hillebrandt, K., et al. 2017, *Journal of Tissue Engineering and Regenerative Medicine*, 11, 531
- Tara, S., Rocco, K. A., Hibino, N., et al. 2014, *Circulation Journal*, 12
- Taylor, D. A., Sampaio, L. C., Ferdous, Z., Gobin, A. S., and Taite, L. J. 2018, *Acta Biomaterialia*, 74, 74
- Taylor, L. M., Edwards, J. M., Brant, B., Phinney, E. S., and Porter, J. M. 1987, *The American Journal of Surgery*, 153, 505
- Thomas, L. V., and Nair, P. D. 2012, *Journal of Biomaterials Science, Polymer Edition*, ahead-of-print, 1
- Tillman, B. W., Yazdani, S. K., Lee, S. J., et al. 2009, *Biomaterials*, 30, 583
- Tsuchiya, T., Balestrini, J. L., Mendez, J., et al. 2014, *Tissue Engineering Part C:*

- Methods, 20, 1028
- Tucker, W. D., and Mahajan, K. 2019, in StatPearls (StatPearls Publishing)
- Valappil, S. P., Boccaccini, A. R., Bucke, C., and Roy, I. 2006, *Antonie van Leeuwenhoek*, 91, 1
- Valentin, J. E., Turner, N. J., Gilbert, T. W., and Badylak, S. F. 2010, *Biomaterials*, 31, 7475
- van Eldijk, M. B., McGann, C. L., Kiick, K. L., and van Hest, J. C. 2012, *Topics in current chemistry*, 310, 71
- Vepari, C., and Kaplan, D. L. 2007, *Progress in Polymer Science*, 32, 991
- Vieira, S., da Silva Moraes, A., Silva-Correia, J., Oliveira, J. M., and Reis, R. L. 2002, *Encyclopedia of Polymer Science and Technology*, 1
- Voorhees, A. B., Jaretzki, A., and Blakemore, A. H. 1952, *Annals of Surgery*, 135, 332
- Vorotnikova, E., McIntosh, D., Dewilde, A., et al. 2010, *Matrix Biology: Journal of the International Society for Matrix Biology*, 29, 690
- Wagenseil, J. E., and Mecham, R. P. 2009, *Physiological Reviews*, 89, 957
- Walton, L. A., Bradley, R. S., Withers, P. J., et al. 2015, *Scientific Reports*, 5, doi:10.1038/srep10074
- Wang, J., Tian, L., Chen, N., Ramakrishna, S., and Mo, X. 2018, *Materials Science and Engineering: C*, 91, 715
- Wang, Q., Han, G., Yan, S., and Zhang, Q. 2019, *Materials*, 12, 504
- Wang, R., Zhou, B., Xu, D.-l., et al. 2016, *Journal of Bioactive and Compatible Polymers*, 31, 242
- Wang, W., Liu, Y., Wang, J., et al. 2009, *Tissue Engineering Part A*, 15, 65
- Weymann, A., Radovits, T., Schmack, B., et al. 2014, *PLoS ONE*, 9, e103588
- Wight, T. N., Kinsella, M. G., and Qwarnström, E. E. 1992, *Current Opinion in Cell Biology*, 4, 793
- Williams, C., Liao, J., Joyce, E., et al. 2009, *Acta Biomaterialia*, 5, 993
- Williams, S. F., Martin, D. P., Horowitz, D. M., and Peoples, O. P. 1999, *International Journal of Biological Macromolecules*, 25, 111
- Wimmer, Z., and Zarevúcka, M. 2010, *International Journal of Molecular Sciences*, 11,

- Wire, T. E. 2019, Vascular Grafts Market 2019 Industry Demand, Share, Global Trend, Industry News, Business Growth, Top Key Players Update, Business Statistics and Research Methodology by Forecast to 2025
- Wise, S. G., Byrom, M. J., Waterhouse, A., et al. 2011, *Acta Biomaterialia*, 7, 295
- Wolf, M. T., Daly, K. A., Reing, J. E., and Badylak, S. F. 2012, *Biomaterials*, 33, 2916
- Woods, T., and Gratzer, P. F. 2005, *Biomaterials*, 26, 7339
- Xiong, Y., Chan, W. Y., Chua, A. W., et al. 2013, *Artificial Organs*, 37, E74
- Xu, C. C., Chan, R. W., Weinberger, D. G., Efuno, G., and Pawlowski, K. S. 2010, *Journal of Biomedical Materials Research. Part A*, 92, 18
- Xu, J., and Shi, G.-P. 2014, *Biochimica et Biophysica Acta (BBA) - Molecular Basis of Disease*, 1842, 2106
- Xu, K., Kuntz, L. A., Foehr, P., et al. 2017, *PLOS ONE*, 12, e0171577
- Xue, L., and Greisler, H. P. 2003, *Journal of Vascular Surgery*, 37, 472
- Yang, Y., Jia, Z., Li, Q., et al. 2010-10, *IEEE Transactions on Dielectrics and Electrical Insulation*, 17, 1592
- Yokota, T., Ichikawa, H., Matsumiya, G., et al. 2008, *The Journal of Thoracic and Cardiovascular Surgery*, 136, 900
- Zarge, J. I., Huang, P., Husak, V., et al. 1997, *Journal of vascular surgery*, 25, 840
- Zavan, B., Vindigni, V., Lepidi, S., et al. 2008, *The FASEB Journal*, 22, 2853
- Zhang, H., Zhou, Y., Yu, N., et al. 2019, *Acta Biomaterialia*, 91, 82
- Zhang, L., Ao, Q., Wang, A., et al. 2006, *Journal of Biomedical Materials Research. Part A*, 77, 277
- Zou, Y., and Zhang, Y. 2012, *Journal of Surgical Research*, 175, 359
- Zvarova, B., Uhl, F. E., Uriarte, J. J., et al. 2016, *Tissue Engineering. Part C, Methods*, 22, 418

Appendixes

Appendix A: Blood vessel simulation reactor prototype




A (4:1)

B (4:1)

A

B

SCALE (2:1)

 <p>Ownweship: This drawing is the property of TissueGraft S.R.L. it is loaned upon the condition that it not to be used in any way detrimental to their interestor to be reproduced without their written permission.</p>		<p>BLOOD VESSELS SIMULATION REACTOR PROTOTYPE</p>	
		<p>Content: Appendix A</p>	
<p>Engineer, author: Marta Calvo Catoira</p>		<p>Description: Plan of the simulation bioreactor with details of connectors and holder</p>	
<p>Drawn: October 2019</p>		<p>Signed:</p>	
<p>Choked: October 2019</p>		<p>Plot scale: 1:1</p>	
		<p>Plan number 1</p>	

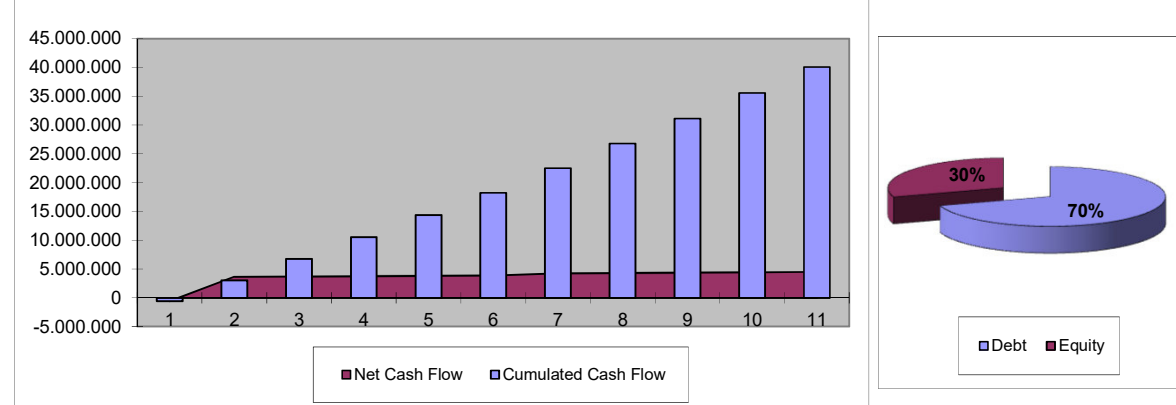
Appendix B: Business plan

Appendix B

1. DSCR minimo	29,40	DSCR OK
2. DSCR average	32,61	Coverage not required

Production	50.000	vessel/year
Inflation	1,40%	
Turn key	2.000.000	€
Other cost	0	€
Total investment	2.000.000,0	€
Equity	30%	
Equity outflow	600.000	
Euribor base rate (3 months)	0,30%	www.euribor.it/
Spread	4,00%	
Interest rate	4,30%	
Reid of return	10,00%	
Financial period	180	month

Installment	-128.573	€
Ires	24,00%	
Irap	1,90%	
IMU	0,20%	



	0	1	2	3	4	5	6	7	8	9	10	Total
		2021	2022	2023	2024	2025	2026	2027	2028	2029	2030	
Inflation rate		1,00	1,01	1,03	1,04	1,06	1,07	1,09	1,10	1,12	1,13	
Vessel production (d=5mm; L=10cm)	50.000	vessel/year	50.000	50.000	50.000	50.000	50.000	50.000	50.000	50.000	50.000	500.000
Vessel revenue	800	€/vessel	€	40.000.000	40.560.000	41.127.840	41.703.630	42.287.481	42.879.505	43.479.818	44.088.536	426.164.241
Revenues		€	€	40.000.000	40.560.000	41.127.840	41.703.630	42.287.481	42.879.505	43.479.818	44.088.536	426.164.241

Raw material	12.500.000	€/year	€	12.500.000	12.675.000	12.852.450	13.032.384	13.214.838	13.399.845	13.587.443	13.777.667	13.970.555	14.166.143	133.176.325
Chemicals	20.900.000	€/year	€	20.900.000	21.192.600	21.489.296	21.790.147	22.095.209	22.404.542	22.718.205	23.036.260	23.358.768	23.685.790	222.670.816
Quality control & rutine analysis	30.000	€/year	€	30.000	30.420	30.846	31.278	31.716	32.160	32.610	33.066	33.529	33.999	319.623
Maintenance plant	50.000	€/year	€	50.000	50.700	51.410	52.130	52.859	53.599	54.350	55.111	55.882	56.665	532.705
Administration & Finance cost	10.000	€/year	€	10.000	10.140	10.282	10.426	10.572	10.720	10.870	11.022	11.176	11.333	106.541
Work staff	500.000	€/year	€	500.000	507.000	514.098	521.295	528.594	535.994	543.498	551.107	558.822	566.646	5.327.053
Electrical energy	10.000	€/year	€	10.000	10.140	10.282	10.426	10.572	10.720	10.870	11.022	11.176	11.333	106.541
Insurance	200.000	€/year	€	200.000	202.800	205.639	208.518	211.437	214.398	217.399	220.443	223.529	226.658	2.130.821
Delivery	30.000	€/year	€	30.000	30.420	30.846	31.278	31.716	32.160	32.610	33.066	33.529	33.999	319.623
Wastewater treatment (23,907 t/a 18euro/t))	10.000	€/year	€	10.000	10.140	10.282	10.426	10.572	10.720	10.870	11.022	11.176	11.333	106.541
Amortization	5	year	€	400.000	400.000	400.000	400.000	400.000	0	0	0	0	0	2.000.000
Contingency	15,0%		€	300.000	304.200	308.459	312.777	317.156	321.596	326.099	330.664	335.293	339.987	3.196.232
Total costs	34.240.005		€	34.940.000	35.423.560	35.913.890	36.411.084	36.915.239	37.026.453	37.544.823	38.070.451	38.603.437	39.143.885	369.992.822

Operating Cash Flow		€	5.060.000	5.136.440	5.213.950	5.292.545	5.372.241	5.853.052	5.934.995	6.018.085	6.102.338	6.187.771	56.171.419
---------------------	--	---	-----------	-----------	-----------	-----------	-----------	-----------	-----------	-----------	-----------	-----------	------------

Installment		€	(128.573)	(128.573)	(128.573)	(128.573)	(128.573)	(128.573)	(128.573)	(128.573)	(128.573)	(128.573)	(1.285.732)
Loan redemption		€											0

Renewal		€	4.931.427	5.007.867	5.085.377	5.163.972	5.243.668	5.724.479	5.806.422	5.889.512	5.973.765	6.059.198	54.885.687
---------	--	---	-----------	-----------	-----------	-----------	-----------	-----------	-----------	-----------	-----------	-----------	------------

Ires		€	1.183.542	1.201.888	1.220.490	1.239.353	1.258.480	1.373.875	1.393.541	1.413.483	1.433.704	1.454.207	13.172.565
Irap		€	93.697	95.149	96.622	98.115	99.630	108.765	110.322	111.901	113.502	115.125	1.042.828
IMU	0,2%	3080	€	3.080	3.080	3.080	3.080	3.080	3.080	3.080	3.080	3.080	30.800

Net Cash Flow			-600.000	3.651.107	3.707.749	3.765.184	3.823.423	3.882.478	4.238.759	4.299.479	4.361.048	4.423.480	4.486.786	40.039.494
Cumulated Cash Flow			-600.000	3.051.107	6.758.857	10.524.041	14.347.464	18.229.942	22.468.702	26.768.180	31.129.229	35.552.709	40.039.494	

DSCR			29,40	29,84	30,28	30,74	31,20	33,97	34,44	34,92	35,40	35,90
------	--	--	-------	-------	-------	-------	-------	-------	-------	-------	-------	-------

3. NPV	€ 21.703.387
--------	--------------

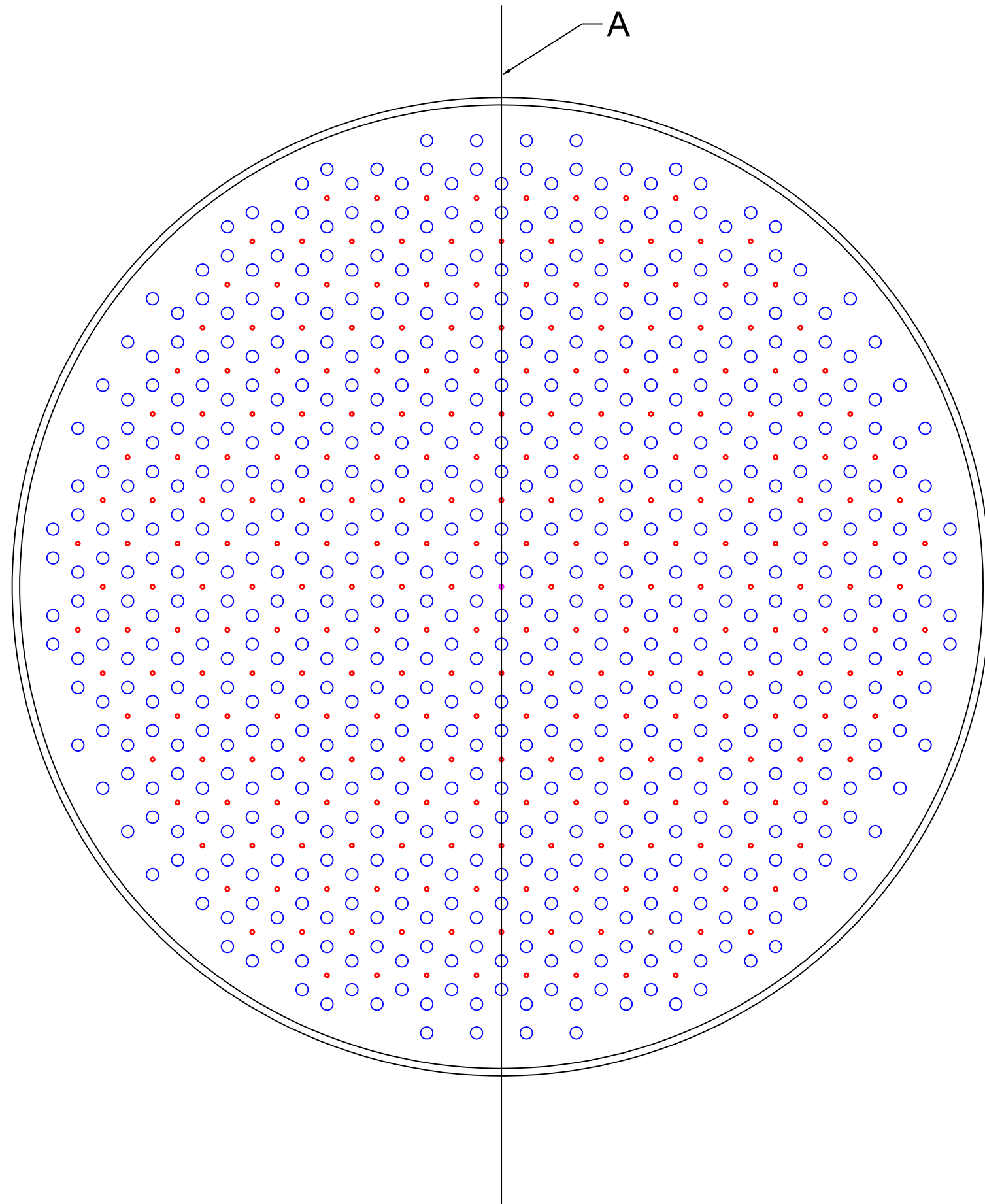
4. IRR	610,07%
--------	---------

5. ROI 1st year	253,00%
-----------------	---------

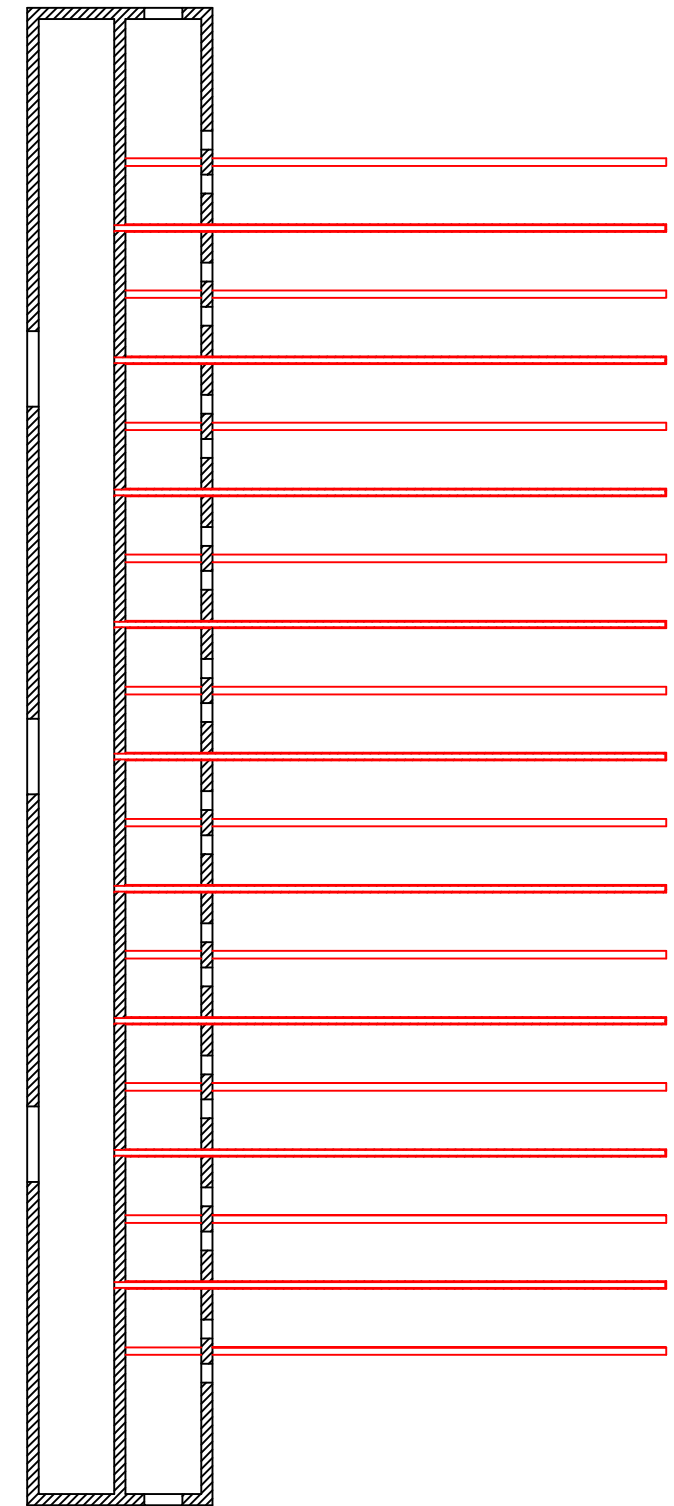
6. ROE 1st year	608,52%
-----------------	---------


1. DSCR min: Min Debt Service Coverage Ratio
2. DSCR average: average Debt Service Coverage Ratio
3. NPV: Net Present Value
4. IRR: Internal Rate of Return
5. ROI: Return of Investment
6. ROE: Return of Equity

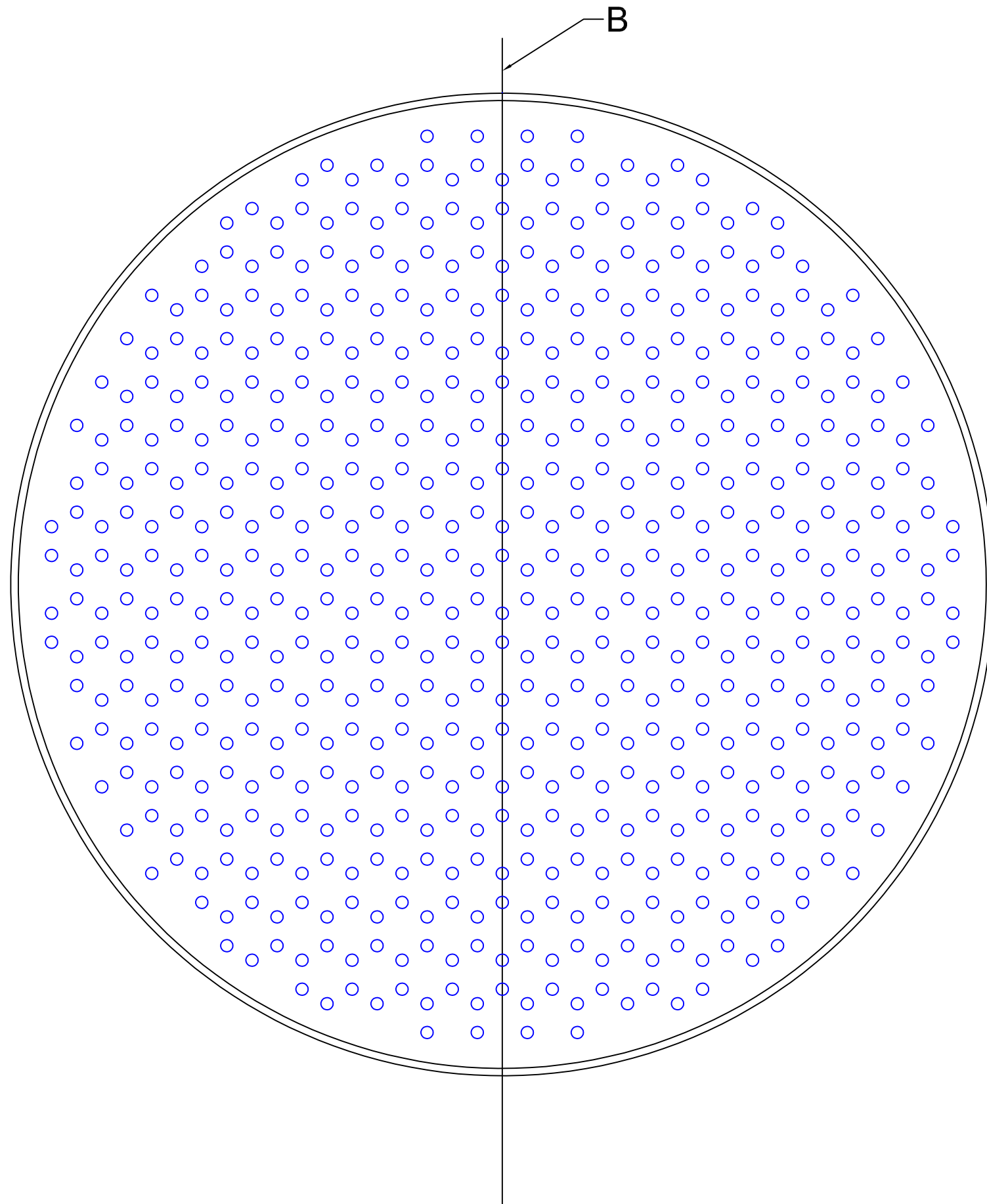
Appendix C: Blood vessel decellularization reactor prototype



Section A




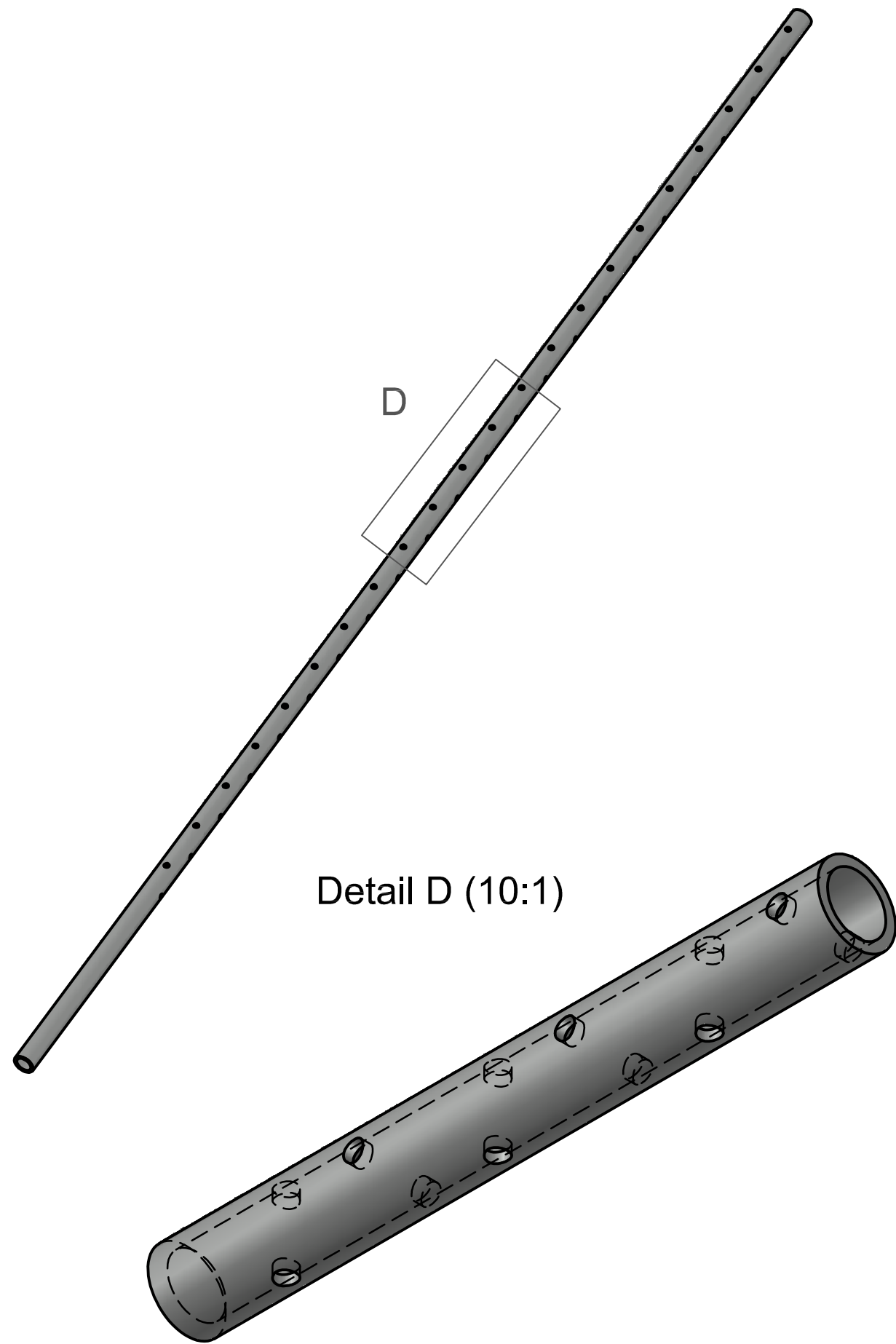
 <p>Ownweship: This drawing is the property of TissueGraft S.R.L. it is loaned upon the condition that it not to be used in any way detrimental to their interestor to be reproduced without their written permission.</p>		BLOOD VESSELS DECELLULARIZATION REACTOR PROTOTYPE	
		Content: Appendix C	
Engineer, author: Marta Calvo Catoira	Description: Closing element of the decellularization reactor (section A)		
Drown: October 2019	Signed:		Plot scale: 1:2
Cheked: October 2019			Plan number 1



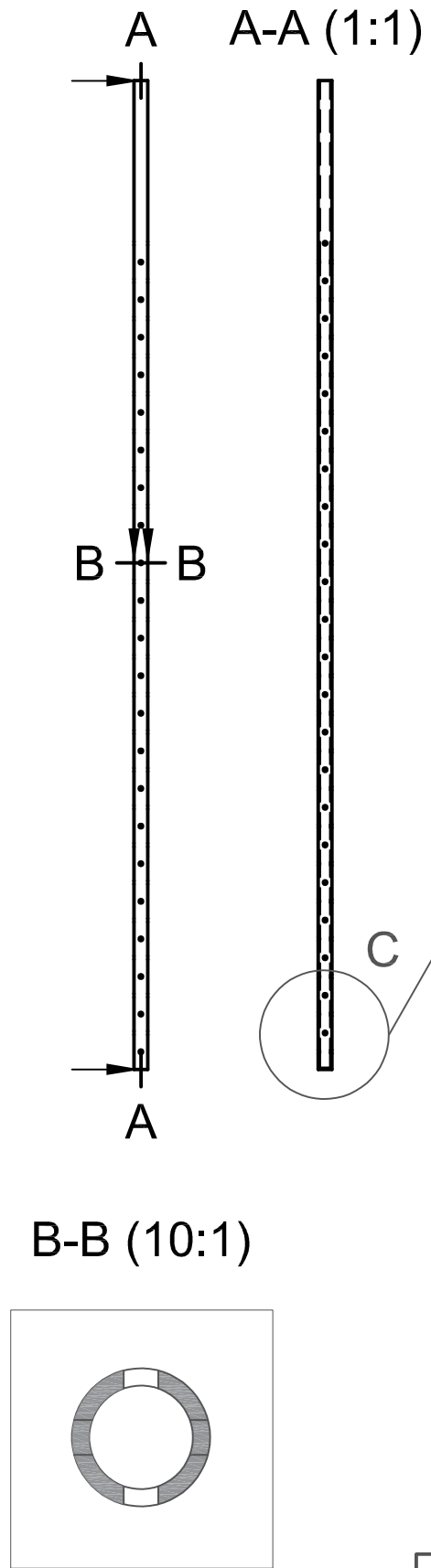
Section B



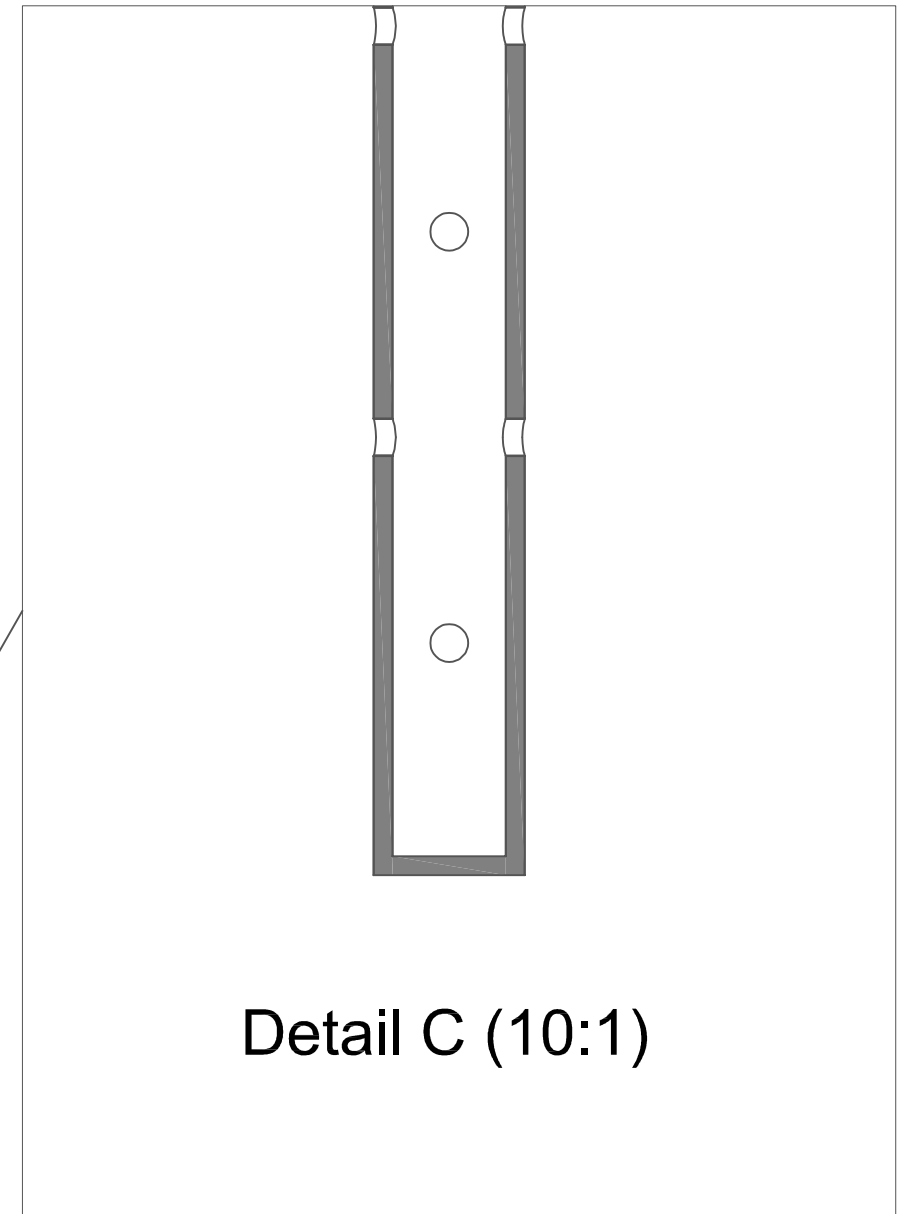
 <p>Ownweship: This drawing is the property of TissueGraft S.R.L. it is loaned upon the condition that it not to be used in any way detrimental to their interestor to be reproduced without their written permission.</p>		<p>BLOOD VESSELS DECELLULARIZATION REACTOR PROTOTYPE</p>	
		<p>Content: Appendix C</p>	
<p>Engineer, author: Marta Calvo Catoira</p>	<p>Description: Cylindrical chamber of the decellularization reactor (section B)</p>		
<p>Drawn: October 2019</p>	<p>Signed:</p>		<p>Plot scale: 1:2</p>
<p>Cheked: October 2019</p>			<p>Plan number 2</p>




Detail D (10:1)



B-B (10:1)



Detail C (10:1)

	Ownwship: This drawing is the property of TissueGraft S.R.L. it is loaned upon the condition that it not to be used in any way detrimental to their interestor to be reproduced without their written permission.		BLOOD VESSELS DECELLULARIZATION REACTOR PROTOTYPE	
			Content: Appendix C	
Engineer, author: Marta Calvo Catoira	Description: Reactor's tube configuration and detail			
Drown: October 2019	Signed:		Plot scale: 1:2	
Cheked: October 2019			Plan number 3	